NOVEL UNCERTAINTY QUANTIFICATION METHOD FOR COMPUTATIONAL REACTOR DESIGN ANALYSIS OF NUCLEAR THERMAL PROPULSION CORES

A Dissertation

by

VISHAL K. PATEL

Submitted to the Office of Graduate and Professional Studies of
Texas A&M University
in partial fulfillment of the requirements for the degree of

DOCTOR OF PHILOSOPHY

Chair of Committee,	Pavel V. Tsvetkov
Committee Members,	Sunil S. Chirayath
	Karen Vierow Kirkland
	Michael B. Pate
Head of Department,	Michael Nastasi

December 2019

Major Subject: Nuclear Engineering

ABSTRACT

Nuclear thermal propulsion (NTP) designs include large margins for manufacturing, thermal, and neutronic uncertainties. In the past these uncertainties could be better understood through rapid design and experimental measurements. In the current socio-political climate, rapid prototyping is not possible and work has shifted to computational designs. Larger computing power is now available such that uncertainties can be quantified using computational means. New NTP designs use Monte-Carlo (MC) analysis where well established deterministic uncertainty quantification techniques are not valid. This research develops a new method by extending the MC based Total Monte Carlo (TMC) and GRS uncertainty propagation methods such that they can be used for full-core design efforts that include calculating uncertainties in local quantities such as reaction rates and energy dependent flux and propagating uncertainties to the thermal hydraulics domain. mcACE is a software created in this research to implement the new method for practical applications using V&V'd codes, particularly MCNP. mcACE allows for sampling of any part of an MCNP input from random distributions to determine output uncertainties based on those inputs. Burn-up uncertainty propagation is achieved by coupling MCNP with ORIGEN (version in SCALE 6.1+) while using predictor/corrector methods with sub-steps for time-stepping. Manufacturing uncertainties are captured by sampling MCNP inputs through mcACE based on densities and geometry. Nuclear data uncertainties are captured by sampling continuous nuclear data cross-sections using ASAPy. ASAPy is a software created in this research to sample ACE data files using ENDF covariance information. Sensitivity analysis via variance decomposition for correlated inputs is used to create new insights on correlated sampling for MC neutronics. Calculating traditional sensitivity profiles proved to be out of reach for the selected uncertainty propagation methods though uncertainties

can still be readily calculated. To verify uncertainty calculations and sampling methods, eigenvalue uncertainties are compared with iterated fission probability method. The MC uncertainty quantification is extended to the thermal domain by calculating uncertainties in power profiles and reaction rates from uncertain input sources. These uncertain power profiles are used in a hot-channel analysis to calculate performance uncertainties. The developed method is applied to two NTP cores, SNRE, a heritage HEU graphite fueled design and SCCTE, an LEU tungsten-cermet design are analyzed at the unit-cell and full core levels. Burn-up with uncertainty propagation is demonstrated on a typical NTP operation cycle.

DEDICATION

Dedicating to just the cats is probably a bad move, but here we are.

ACKNOWLEDGMENTS

I would like to thank my advisor, Pavel Tsvetkov, who taught me to think as a researcher, Steve Howe who broadened my research interests to include space nuclear systems, Will Windes and Jorge Navarro who enabled me to conduct research into uncertainty quantification methods, my friends who encouraged me to do big things, and my family who have supported me with their love and understanding.

Finally, I would like to thank you, who took your time to read this.

CONTRIBUTORS AND FUNDING SOURCES

Contributors

This work was supported by a dissertation committee consisting of Professor Pavel Tsvetkov (Advisor) of the Department of Nuclear Engineering and Sunil S. Chirayath (NE), Karen K. Vierow (NE) and Michael B. Pate (ME).

All work conducted for this dissertation was completed by the student independently.

Funding Sources

This was was partially supported by the U.S. Department of Energy (DOE) under Battelle Energy Alliance, LLC Contract No. DE-AC07-05ID14517, particularly the ATR related results and MCNP input generator and output parser. Other parts of this dissertation were self funded.

TABLE OF CONTENTS

Page

LIST OF FIGURES

FIGURE Page

LIST OF TABLES

TABLE Page

1. INTRODUCTION

Interest in Nuclear Thermal Propulsion (NTP) design was renewed when NASA [4] suggested NTP as a good choice for a Mars the mission (and beyond). Historically the Rover/Nerva [5] and the SNRE [6] have been well funded programs to build NTP engines. NERVA has had 22 fueled engine tests but never flew a rocket. Cancellation of programs were politically, not technically motivated. Important data was gathered in these tests and studies that may enable the construction of an NTP engine in the near future. However, increased regulations and loss of manufacturing capability along with new materials in designs may reduce the impact of historical data, forcing more computational based designs to be used. New manufacturing techniques and simulation tools can enable a new NTP design using lessons learned from past programs. This NTP can be tailored for specific missions sets and created to be extendible to other missions. This approach to NTP can allow for new reactor designs that were not possible or thought of in past programs.

Heritage NTP designs relied on engineering approximations that could be validated with many experiments. Many of the tools used to create historical NTP designs are either outdated or unavailable. It is often not clear how the approximations made in historic analyses were created. Next generation modeling tools can be used to determine the validity of historical analysis to guide the creation of new experiments. For any new reactor design, experiments to test understanding of physics must be created before a license for construction can be granted. Experiments requiring nuclear materials tend to be very expensive and difficult to create due to many regulatory and safety concerns. This has lead to the creation of predictive computer codes that are validated by experiments whenever possible.

These predictive codes tend to do a good job in the code's area of interest, but never are

exactly correct. Uncertainty and sensitivity analysis is used with these codes to quantify the uncertainty of predicted values. A drawback of performing these uncertainty analysis is that they are not always well defined or they take too long to perform for practical applications. This is especially true for coupled neutronic and thermal calculations. Recent methods [7] have addressed how to perform uncertainty quantification using Monte-Carlo based neutron trasport tools, but these methods are generally only applied to benchmark and nuclear data evaluations.

The work performed in this dissertations is to address modeling uncertainties in the NTP design process that describes how nuclear, material, and geometric uncertainties impact performance and safety metrics.

1.1 Nuclear Thermal Propulsion

NASA has a history of working on NTP concepts off and on over the past 50 years. The original program demonstrated NTP concepts and was in the process of delivering flight ready hardware when the program was canceled to to political reasons. In recent years, a new effort has been initiated by NASA-Marshall with the Space Capable Cryogenic Thermal Engine program, which uses a low enriched uranium tungsten-cermet fuel. The DOE has expressed interest in pursing heritage graphite composite fuels as a main option and cermet fuel type as a second option, both having highly enriched uranium. No matter the reactor chosen, tools must exist to analyze the selected design both from experimental design and safety points of view. Many tools have been developed over time, however their availability and validity are in general questionable due to the lack of quality assurance documentation, verification and validation documentation, and uncertainly quantification.

1.1.1 Design Process

The initial design process for terrestrial power reactors is well known, albeit quite complex. The product of an initial design study is usually a critical core with enough heat

transfer area to cool the core, and enough excess reactivity to created heat for a certain time. After an initial design is created, deeper studies are performed where optimizations will take place to reduce reactivity swings and flatten core power profiles for more even heat transfer. The product of the deeper study is usually a core with large engineering margins that can achieve high burnup with minimal fuel management, and proper heat transfer to the balance of plant. The next steps involve accident and regulatory analysis with practically every other engineering discipline mixed in.

The initial design process for an NTP is similar to power reactors however the optimization targets are different. For example, far from optimal critical geometries are acceptable in order to allow for coolable cores. Designs usually do not have simple flow geometries either so hot channel analyses must be posed differently than power reactors, and less accurate approximations must be made. A hot channel in an NTP core consists of a fuel element and a tie-tube (or moderator) element. There is a downward supply H2 channel and an upward return H2 channel within a tie-tube, and there are several coolant channels within the fuel element. This makes for a difficult geometry to solve flow and heat equations over because heat is conducting out of the fuel into the coolant and into the tie-tube, while coolant is picking up heat in the tie-tube and the fuel with a turbine between the two. Approximations are typically made to make the problem tractable without invoking multi-dimensional mesh based analyses.

1.2 Motivation for Monte-Carlo Uncertainty Quantification

Uncertainty quantification in neutronics is a well studied area, particularly in deterministic transport problems and for criticality safety calculations. A recent trend in reactor design has shifted focus from deterministic calculations to monte-carlo (MC) methods. Monte-carlo methods allow for exact descriptions of reactor geometry and continuous angle and energy treatment of neutrons as well as ease of software usage compared to

deterministic methods that often require a deep understanding of transport theory. An unfortunate consequence of this MC design trend is the loss of rich deterministic UQ/SA theory that is not directly applicable to MC methods. Uncertainty quantification at the conceptual design phase for new reactor concepts can help find gaps in knowledge and guide future research directions.

To facilitate performing UQ, two codes were written to enable rapid analysis in a tractable form. mcACE was created to edit MCNP input files, randomly sample input files, track material data, implement coupling with ORIGEN (SCALE 6.1+) for time-stepping, parse MCNP and ORIGEN outputs, and calculate UQ statistics; a block diagram of this is shown in Fig. 1.1. ASAPy was created to sample nuclear data according to nuclear data covariances for use in MCNP calculations; a block diagram of this is shown in Fig. 1.2.

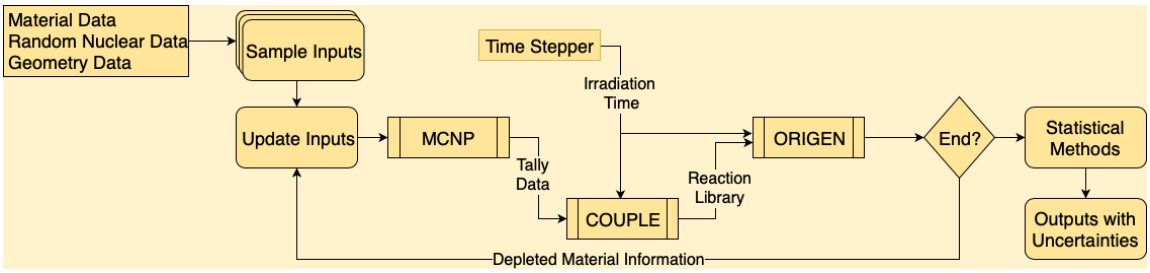

Figure 1.1: mcACE UQ Process

1.3 Dissertation Objectives

The objective of this dissertation is to create a method to incorporate uncertainty quantification in the nuclear thermal propulsion design process. The contribution of this dissertation is to calculate uncertainties of local reactor quantities such as energy dependent flux and reaction rates and using these calculations to propagate uncertainty to other physics domains. This contribution is achieved by creating sampling tools to sample MCNP inputs

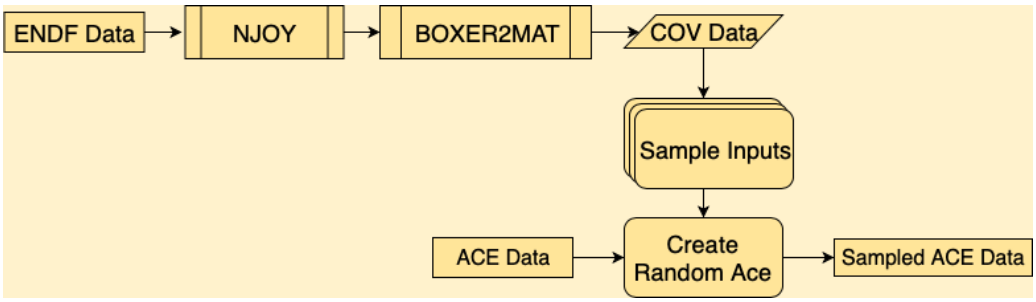

Figure 1.2: ASAPy Nuclear Data Sampling Process

in a generic manner, sample nuclear data based on covariance data, and perform statistical analysis based on input uncertainties to quantify relevant outputs such at peak temperatures and power levels. This will substantially increase the fidelity of computational reactor designs, specifically for nuclear thermal propulsion designs. The significance of this contribution is a better understand how the uncertainties in an unproven design can be quantified to make sound engineering judgement. NTP reactors are prime candidates for this analysis method because of the need for coupled neutronic and thermal analysis as well as the lack of experimental data leading to large uncertainties in expected designs. By better quantifying the uncertainty of results for design analyses, safety factors and design margins can be reduced. A list of contributions follows:

- Implementation of uncertainty tool for Monte Carlo calculations to support UQ with industry tools.
- Extension of neutronic UQ methods to spectrum and reaction rate calculations.
- Creation of a new nuclear data sampling tool.
- Verification of fast UQ statistical methods for large complex reactor systems by comparing to long running, traditional methods

- Application of methods to the heritage NERVA designs as well as cutting edge designs

1.4 Structure of Dissertation

This dissertation is organized into several chapters. Following this chapter, Chapter 2: *BACKGROUND* describes neutronic UQ/SA methods and their applicable ranges to motivate the need for a new analysis pathway and describes NTP operations and a historical review. Chapter 3: *CREATING MCACE AND ASAPY FOR UNCERTAINTY QUANTIFICATION* describes implementation details of the data sampling procedure and selected UQ methods. Chapter 4: *VERIFICATION AND VALIDATION STUDIES* describes the verification of the implemented UQ methods with code-to-code verification and method-to-method verification. Chapter 5: *APPLICATION TO NUCLEAR THERMAL PROPULSION REACTOR DESIGNS* describes the UQ analysis performed on the SNRE and SCCTE NTP reactors. Chapter 6: *CONCLUSIONS* summarizes the dissertation and work performed.

2. BACKGROUND

Models are used to predict real-life physics. The utility of the model depends on how well it can predict the quantity of interest. Several fields of interest are connected to determining how well a model behaves. The broad groups are verification and validation of models and uncertainty quantification and sensitivity analysis of model inputs and outputs. Verification deals with the process of ensuring the model being used is correctly implemented and validation deals with ensuring the model being used is able to predict the quantities of interest. These two fields are extremely important and once completed, uncertainty quantification (UQ) sensitivity analysis (SA) can be performed. Usually the UQ/SA steps are performed at the same time as verification and validation of models.

Often uncertainty quantification and sensitivity analysis are used interchangeably, though they are in fact separate terms. Sensitivity analysis is used to quantify the effects of parameter variations on calculated results as well as determining what input source uncertainties caused the output uncertainties (ranking). Uncertainty quantification is used to determine the effects of parameter uncertainties on the uncertainties in calculated results [8]. For example, one would perform an sensitivity analysis to determine the effect of uncertain temperatures on a criticality calculation, compared to performing a sensitivity analysis to determine how much a changing temperature effects the criticality. More specifically, a small change in temperature could lead to a small change in reactivity showing temperature has a small sensitivity, however a large uncertainty in the temperature could still mean a large uncertainty in the criticality calculation, even though the calculations are not sensitivity to temperature.

Within the scope of reactor design and analysis, monte-carlo based analyses are often used. These calculations tend to not have any uncertainty in the result beyond the numeri-

cal monte-carlo statistical uncertainty. The uncertainty quantification solution developed is the culmination of many different areas of research, namely UQ of solutions to the Boltzman neutron transport equation and the Bateman transmutation equations, coupling of the transport and transmutation equations, and generation of uncertain nuclear data. This section describes previous works of those research areas. The focus of this dissertation is to develop UQ/SA of the neutron transport equation and Bateman transmutation equations as well as the coupling of the two.

2.1 Deterministic Sensitivity and Uncertainty Quantification

Every model accepts inputs and produces outputs. All inputs in reality have some amount of uncertainty associated with them. These uncertainties stem from inherent randomness (aleatoric variability) or from measurement or modeling issues (epistemic uncertainty). An example of aleatoric variability is a neutron interaction cross-section measurement. Due to the variability of states of a material at a specific temperature (e.g., random vibrations), the neutron cross-section cannot be known exactly. An example of an epistemic uncertainty is a measurement of a control rod in a core. The rod may have a position transducer that is accurate to 1 cm, meaning there is a 1 cm uncertainty in the rod position. Aleatoric variability cannot be eliminated because it is inherent to the process. This type of uncertainty will not be discussed in detail. Epistemic uncertainty that is present can be quantified and modeled.

Within the framework of probability and statistics, the value associated with a random variable is the mean the variable takes. The spread of the values the random variable may take is described by the standard deviation. The square of the standard deviation is the variance of the variable. Formally, given a continuous random variable (X), the

probability (P) of the variable X being between a lower (l) and upper (u) limit is

$$P[l \leq X \leq u] = \int_l^u f_X(x)dx, \tag{2.1}$$

where f_X is the probability density function. The expectation value (or mean value) of the random variable X ($\mathbf{E}[X]$) is

$$\mathbf{E}[X] = \int_{-\infty}^{\infty} x f_X(x)dx. \tag{2.2}$$

Given the mean values is described as $\mu = \mathbf{E}[X]$, the variance can be written as

$$\mathrm{Var}(X) = \mathbf{E}[(X - \mu)^2], \tag{2.3}$$

where $\mathrm{Var}(\cdot)$ is the variance operator. It is useful to expand the quantity in the expectation operator by using properties of expectations (linearity and the expectation of a constant is the constant itself),

$$\begin{aligned} \mathrm{Var}(x) &= \mathbf{E}[X^2 - 2X\mu + \mu^2] \\ &= \mathbf{E}[X^2] - 2\mu\mathbf{E}[X] + \mu^2] \\ &= \mathbf{E}[X^2] - \mu^2. \end{aligned} \tag{2.4}$$

The variance is the square of the standard deviation (σ): ($\mathrm{Var}(X) = \sigma^2$).

The goal of a model is to provide an expression for the expectation value of some output variable given a set of input variables. If the input variables have associated uncertainties (which they assuredly do), then the output variables should take those input uncertainties into account. This process specifically is uncertainty quantification. Many methods for uncertainty quantification exist, relevant methods will be discussed.

The first developments of UQ/SA occurred with respect to the transport equation under the diffusion approximation [9]. Other developments have occurred in other fields but are not completely relevant in the nuclear field. However, the original UQ/SA worked developed in the field has been generalized under the Adjoint Sensitivity Analysis Procedure (ASAP) [8]. The ASAP has the advantage of only needing a single adjoint calculation per response and does not depend on the input variations. Though very well formally established, the ASAP is still difficult to implement when non-approximate transport equation solutions are desired. ASAP is very efficient in calculated first order local effects but it's efficiency drops when higher order effects are desired due to the need of solving an adjoint system for each input parameter variation. Furthermore, for continuous energy calculations, the response (energy dependent flux) has many outputs thus making the ASAP and other deterministic UQ/SA procedures difficult to calculate.

Within a multi-group framework, UQ/SA has been performed and implemented in production tools. Specifically, the adjoint multi-group transport equation can be solved with small changes in the physics kernels in both deterministic and Monte-Carlo solutions. For continuous energy adjoint calculations the situation is different. Group to group scattering cross-sections cannot be easily inverted because cross-sections are represented as relations and not discrete points. By representing the scattering matrix as discrete points, the computer memory requirements for calculations grows to unfeasible amounts.

2.2 Stochastically Uncertainty Quantification

Many nuclear engineering related problems use stochastic methods to solve problems. Specifically, the neutron transport equation and probabilistic risk assessment (PRA) problems are the leading candidates for stochastic solutions. These solutions tend to be used because they are easy to implement, even in complex cases. For example, stochastic solutions to the transport equation can allow for removal of two very broad approximations

that are generally used: homogenization in energy and space, instead allowing for exact geometry modeling and continuous energy representations of cross-sections. In PRA, stochastic solutions allow for efficiently sampling event trees.

The biggest drawback to stochastic solutions is the time to solution is generally much longer than deterministic approaches due to the large number of samples required to obtain good stochastic statistics. This means uncertainty quantification through sampling methods is prohibitively difficult due to the large number of runs required to obtain good statistics. However, computing power has increased substantially in the past few decades such that sampling based UQ is possible in some cases. During the years where sampling techniques could not be utilized, other methods were also developed. In the nuclear field, these solutions generally supported criticality safety calculations.

2.2.1 Monte Carlo Techniques

The Monte Carlo (MC) method is a method to solve integrals using stochastic, rather than deterministic approaches [10]. The method has it roots in nuclear engineering to solve the neutron transport equation. Originally, the transport equation was solved using deterministic methods, but often these approaches failed to solve problems due to the many approximations used. The approximations generally homogenized geometry, and averaged complex nuclear data. The MC method could relax many of these approximations, particularly able to represent geometries more realistically, and use more energy groups.

The ability to solve complex problems with MC comes from the easy methods of implementation and understanding. For example, the question 'what is the value of Pi (or the area of a unit circle)?' can be solved using MC means. The simplest approach uses a so called darts game where one throws darts at a board shaped like a unit square. Each dart (x, y) position is noted in order to make a set of random numbers. Given two sets of random variables, $\hat{X}_k, \hat{Y}_k$, and k samples, the area of the circle can be determined by

counting the number of dart hits that had $x_k^2 + y_k^2 \leq 1$, e.g., hit within the unit circle. Dividing this by the total number of dart hits gives the area of the circle, which is 1/4 of pi. A mathematical approach of this same problem is to solve the integral,

$$A = \int_0^1 \sqrt{1 - x^2} dx, \tag{2.5}$$

where the integrand is a parametrized arc, and A is the final area. Taking N samples uniformly chosen on the unit interval, the area can be approximated as

$$A \approx \frac{1}{N} \sum_{k=1}^{N} \sqrt{1 - x_k^2}. \tag{2.6}$$

These two approaches are equivalent and allow for both physical and mathematical interpretations of the MC method. More information on solving the neutron transport equation using MC methods can be found in literature [10].

For MC methods, determining the mean value of a quantity can be performed easily. However, due to the random nature of the solution, each mean value is accompanied with variance that describes the uncertainty of the output. For example, only throwing 10 darts in the circle area problem would lead to a poor estimate of the mean, resulting in a large variance. Throwing 10,000 darts would allow for a good estimate with small variance. Determining how many 'darts' a given problem needs apriori is difficult, and even if a converged mean is found, the variance of the solution can still be large.

Estimates for the variance exist within the MC framework. Given a set of N random samples, X_N, the mean value is

$$\bar{x} = \frac{1}{N} \sum_{i=1}^{N} x_i, \tag{2.7}$$

with variance of the samples as in Eq. (2.4),

$$\sigma^2 = \frac{1}{N}\sum_{i=1}^{N} x_i^2 - \bar{x}^2, \tag{2.8}$$

with σ as the standard deviation. The variance of the mean is $\frac{\sigma^2}{N}$, or

$$\sigma_{\bar{x}} = \frac{1}{\sqrt{N-1}}\sqrt{\frac{1}{N}\sum_{i=1}^{N} x_i^2 - \bar{x}^2}. \tag{2.9}$$

A common problem with MC methods is that often many random samples must be made to get a reasonably well resolved mean value, e.g., relative standard deviation $\ll 10\%$. This representation for the standard deviations allows for ideas on how to reduce the standard deviation: increase, N, the number of random samples. Other variance reduction methods exist that rely on changing the sampling method without changing the expected mean value, however those methods are problem dependent.

In the context of sensitivity and uncertainty quantification, the difficulty in finding well converged mean values for outputs is immense. When computers were not as powerful, any random input style uncertainty quantification was prohibitive due to the vast amount of computer time required. Fortunately, in the recent decade, large enough computers have been built to allow for sampling based MC UQ/SA. Based on the currently available UQ/SA methods, this is the approach that will be taken in this research.

2.2.2 Perturbation Based Techniques

Effects of perturbations can be directly calculated from forward Monte-Carlo calculations, e.g., no need to run parametric studies for small perturbations. In general, the perturbed parameters are nuclear data related and the response function is the criticality eigenvalue. These calculations are sensitivity calculations and output uncertainties can be

determined from multiplying the magnitude of uncertainties with sensitivities.

The differential operator sampling method [11] assumes the effect of the perturbation being made (usually nuclear data) can be represented by a Taylor series expansion around the mean value, generally using a 1st or 2nd order expression. The derivative involved in the series expansion can be calculated using Monte-Carlo means. The original developments did not include all the required steps to get generally correct answers. The fission source was not perturbed during sampling such that a bias was introduced [12]. The methodology without the fission source perturbation will tend to disagree with similar perturbation calculations [13].

The adjoint flux can in principle be calculated using monte-carlo methods, though efficient methods have not been implemented to do so for continuous in energy problems. In general to solve the problem would require an inverse random walk from the end of the calculation to the beginning, e.g., a backwards calculation. Recently, the iterated fission probability method [14] has been used to determine the adjoint flux from forward monte calculations. This method relies on the physical interpretation of the adjoint flux as an importance weighting[9]; it is the affect of a neutron introduced somewhere in phase space of a critical system. This means during power source iterations, keeping track of what a neutron produced in some iteration i does in a later iteration asymptotic generation n can allow for a creation of the adjoint flux. This adjoint can then be used in typical deterministic manners using the sandwich rule to determine sensitivities. Furthermore, it has been shown [15] that this method of adjoint calculation is equivalent to the differential operator sampling method with fission source perturbations. A drawback of this method is that a large computer memory is required due to storing of many histories as well as their original birth conditions. The memory requirement is proportional to the number of particles kept track of in each generation and the number of latent generations used to establish an asymptotic case.

Contribution-Linked eigenvalue sensitivity/Uncertainty estimation via Tracklength importance CHaracterization (CLUTCH) [16] is a similar to the integrated fission probability method was recently implemented in SCALE. This method avoids some pitfalls of the IFP method in that computer memory requirements do not scale directly with the number of particle histories. This is accomplished by following particle histories directly from birth to death and computing relevant MC integrals once a particle dies. The methodology agrees with well multi-group MC methods as well as the IFP [16].

The DOS, IFP, and CLUTCH methods are good at S/U calculations for system wide (integral quantities) such as k_{eff}, and kinetics parameters but has difficulties determining specific tallies like dosimeter calculations because of the large amount of memory required to track all neutrons through generations. The CLUTCH method has the potential to reduce memory requirements and perform sensitivity calculations though has not been completely implemented in any production tool. The work developed in this dissertation allow for uncertainty quantification of these important outputs as well as the system wide quantities.

2.2.3 General Sampling

Many methods to perform UQ/SA exist, such as differential analysis, response surface methodology, variance decompositions, and Monte Carlo sampling. These methods excel in certain areas and are used when relevant. The Monte Carlo approach [17] is relevant in this study due to the large number of input variables. This approach is based on random sampling of inputs to a system followed by statistical analysis of the outputs. Questions that can be answered by this approach is what is the uncertainty of an output given the uncertainty of an input, and how important are uncertainties in an input relative to other inputs in causing the uncertainty in the output, e.g., UQ and SA.

Various aspects of the Monte Carlo approach to UQ/SA can be explored. The generation of inputs involves choosing statistical distributions to sample from and evaluating

correlations in inputs. Often times, uncertainties in inputs are not known and must be estimated using expert opinion, or the number of inputs is so vast that expert opinion must be used to reduce the input size by pinning certain parameters to a best estimate value. Once the inputs have been made, simulations must be carried out. Much of the time, simulations are expensive to run (computer time), such that surrogate models must be used. These models are reduced order models that should be fast to run without compromising input/output relationships. These are difficult to create and validate, but can enable UQ/SA. After simulations are completed with the generated inputs, uncertainties and sensitivities must be calculated. Uncertainties can generally be calculated in straight-forward methods such as simply taking the variance of the outputs. Sensitivity analysis is trickier since the effects of individual inputs must be explored and sometimes the structure of the model explored. Regression analysis, rank transformations, correlations, and other statistical tools can be used to determine sensitivity.

The creation of inputs based on distributions such as uniform, normal, log-normal, and beta are well known. Sampling methods such as latin-hyper cube allow for more efficient exploration of input space. These can be applied to the analysis at hand in providing dimensional and number density uncertainties, for example, control drum angle uncertainty of boron loading uncertainty. The model at hand is the 3D continuous energy neutron transport equation. Though simplified models exist, the use of the full model is important due to intricacies in material reactor operations and geometries. However, within the input/model framework, very interesting UQ methods exist such that the total calculation times can be dramatically reduced for a given UQ case. These methods are discussed next.

2.2.4 Total Monte Carlo

The Total Monte Carlo (TMC) method, first introduced to propagate nuclear data uncertainty through reactor physics calculations [18] is a method to propagate uncertainties

with deterministic and MC methods. It is in essence a general sampling method that uses a brute-force approach. Many random inputs to a MC code are created, ran for a long time to get good MC statistics, then uncertainties on outputs from input changes can be found by observing the output distribution and subtracting MC uncertainties. It is an excellent method to propagate input uncertainties through MC calculations, but takes a very long time to perform, needing at least 500 calculations with random inputs, e.g., 500 times longer than a single run. This method will be described in more detail in Sec. 3.1.5.

2.2.5 GRS Method

The GRS method [19] is similar to TMC where simulations are run many times with inputs randomly selected and outputs stored for statistical analysis to determine uncertainties. However, this method does not have the drawback of needing to run each simulations for a long time. Rather, N simulations with different inputs are run for a short time with a single random number seed, then each N simulation is reran with a different random number seed (totaling about twice the runtime of a single long calculation). The two different random number seed simulations have identical MC (aleatoric) uncertainty distributions. The covariance of the output sets is the epistemic uncertainty of the varying inputs [19] because the MC uncertainty is almost eliminated (goes to zero as MC sample batch sizes increases). This method will be described in more detail in Sec. 3.1.6.

2.2.6 Fast Total Monte Carlo

The Fast Total Monte Carlo (FTMC) method [20] follows the development of the GRS method but uses the basis of TMC to propagate uncertainties. Instead of running many long running calculations to get good MC statistics. Only a single long run is performed and the statistics found from that run are used for the statistics that would be found for the other random runs. This requires the random runs not deviate too much from the long run, but that is generally the case. FTMC excels at fast computation of uncertainties

in integral quantities but tends to take similarly as long as TMC for local quantities like energy dependent flux. This method will be described in more detail in Sec. 3.1.7.

2.3 SCALE Based Uncertainty Quantification Tools

The study of UQ of the time dependent neutron transport equations is not a new concept. Many tools have been developed to solve this problem with varying levels of approximations. These tools have performed well within criticality safety applications as well as supporting of licensing activities. A brief overview of current UQ tools is described in this section. This is not a full list, and tends to skew towards tools that are available to the public.

SCALE [21] is a suite of codes that solves individual nuclear problems in reactor physics. SCALE acts as a wrapper around these tools to facilitate data transfer such that user intervention between codes is minimal. SCALE solves problems including transport (deterministic, Monte-Carlo) using vary approximations (diffusion, multi-group, continuous energy, 1D, 3D), activation and depletion calculations, shielding, cross-section processing, and sensitivity analysis and uncertainty quantification. Several tool-chains within SCALE have potential of solving the current dosimetry problem, however none meet all requirements.

2.3.1 TSUNAMI

The TSUNAMI (Tools for Sensitivity and UNcertainty Analysis Methodology Implementation) tools have widely been used for criticality safety calculations. First order perturbation theory was applied to the 1D and 3D multi-group transport equations based on cross-section uncertainty. Sensitivities based on cross-sections can be calculated then combined with built-in cross-section covariances to determine uncertainties in k-eigenvalue. The limitation to MG-MC is prohibitive such that this is not an appropriate method for the current dosimetry calculations because fine core details cannot be resolved.

2.3.2 SAMPLER

The SAMPLER [21] super-sequence in SCALE has recently been implemented to propagate any input uncertainty through SCALE calculations from start to end. It accomplishes this by sampling inputs from defined PDFs as well as use pre-prepared random nuclear data for transport and inventory calculations. Currently, continuous energy cross-sections for Monte-Carlo calculations cannot be handled by SAMPLER. Furthermore, only multi-group data with covariances can be sampled, though there is no restrictions for sampling model input variables.

The SAMPLER sequence has much potential for UQ/SA within the SCALE framework, however there is no pathway to use the sequence with external transport solvers since SCALE solvers are currently required. If functionality to use SAMPLER with standalone ORIGEN calculations was implemented, this would provide a good pathway for transmutation UQ/SA. The general philosophy of sampling inputs is used in the tools developed in this dissertation.

2.3.3 GEAR-MC

The GEneralized Adjoint Responses in Monte Carlo (GEAR-MC) method has recently (version 6.2) been implemented in SCALE. This method allows for continuous energy Monte-Carlo sensitivity calculations using CLUTCH and IFP. The IFP and CLUTCH were discussed in Sec. 2.2.2. The IFP large memory requirements still exist, however CLUTCH allows for parallel calculations with low memory footprint. However, this is still a developing implementation such that only one response can be defined. In the dosimetry calculations that are required in this study, many responses are needed so this approach is currently not viable.

2.4 MCNP Based Uncertainty Quantification Tools

The Monte-Carlo-N-Particle transport code [22] is a code to simulate the neutron transport equation with an MC approach using a general geometry and continuos energy. It has proven itself to be a workhorse of the industry, supporting safety calculations and often used to create numerical experiment benchmarks. It comes equipped with UQ/SA methods, though they are not general enough for use with any calculation.

2.4.1 Differential and Adjoints (Whisper)

The differential operator sampling method described in Sec. 2.2.2 is implemented [13] in MCNP to determine sensitivities from material densities, compositions, and reaction cross sections on outputs (tallies and eigenvalue). The fission source perturbations are not considered such that the differential approach should only be used in fixed source calculations. Furthermore, all outputs are stored in memory, one output for each perturbation. This becomes very memory intensive such that only a few perturbations and outputs should be made. The problem at hand requires many tallies due to burnup and focuses on using the eigenvalue mode of MCNP.

Adjoint based methods also exist within MCNP. The adjoint-weighted perturbation methodology finds changes in the eigenvalue based on material substitutions. This UQ method can be used to perform SA, however it is meant only for material substitution calculations. The iterated fission probability (IFP) method can also be used to determine the adjoint in terms of the eigenvalue. Cross-section perturbations can than be used to determine sensitivity of the eigenvalue based on cross-section perturbations. This method is useful for benchmarking but is not extended to region dependent sensitivities, or any other parameter other than the eigenvalue. The uncertainties of material irradiations are the focus of this research. This method is implemented within the Whisper [23] tool of MCNP.

2.4.2 P-STUDY

MCNP also provides a sampling based methodology to determine uncertainties. MCNP-PSTUDY [24] allows the user to mark inputs as random given some distribution in order to create many random inputs to run. The tool then collects outputs and returns uncertainties and mean values. This is the basis of almost every sampling based tool and is quite relevant in the context of this research. The tool performs excellently in created random inputs, however, more flexibility is required to implement the relevant UQ procedures for this research.

2.5 Nuclear Data Sampling

A main sources of uncertainty for transport and depletion calculations are within nuclear data. In general, nuclear data is created from experimental means [25], however to resolve the quickly varying portions of cross-sections as well as temperature dependence, evaluators create evaluations [26]. Cross-sections can also be created from a theoretical basis and corrected with experimental results [7]. Uncertainties in cross-sections are complex because of correlations between different reaction channels as well as variances in channels themselves. These uncertainties are stored in nuclear data evaluations as covariance matrices. Recently, there has been an effort to perturb nuclear data directly through sampling. These created nuclear data are then used in the transport calculation of choice to propagate the nuclear data uncertainty. Within Monte-Carlo calculations, the previously described TMC, FTMC, and GRS methods can be used with the uncertain data to determine uncertainties. It should be noted that processing evaluating nuclear data files is not a trivial process with many codes [27, 28, 29] dedicated to the task.

Perturbation theory offers similar calculations with multi-group nuclear data and has been historically the tool of choice for sensitivity and uncertainty quantification, for example SCALE's TSUNAMI [21] uses this method. The nuclear data sampling described is

based on Monte-Carlo approaches, thus allowing the data to be used with any transport approximation instead of just multi-group calculations. An unfortunate aspect of the nuclear data sampling tools are they are either proprietary or in-house implementations, thus not easily available. Open source tools [30] to manipulate nuclear data exist, however concise, reliable APIs to use the methods developed are not yet available. The TENDL-2012 [31] nuclear data library published many iterations of randomly created data and is the largest source of openly available random nuclear data.

2.5.1 Continuous Energy Covariance Based

Evaluated nuclear data comes with multi-group covariance matrices to describe cross-section uncertainties. Tools have been developed to use these covariances to sample nuclear data. Nuclear Data Uncertainty Analysis (NUDANA) [32] and KIWI [33] are two such tools. A drawback of using nuclear data covariances is that covariances are not available for all nuclide and are not all available for all reaction channels. Nonetheless, the available covariances can be used to sample nuclear data.

2.5.2 Multi-Group Covariance Based

Often reactor physics codes use the multi-group approximation to make problems tractable. Continuous data can be collapsed into suitable energy bins by various means to create multi-group nuclear data. Nuclear data covariances can then be used to adjust the multi-group data after collapse. The Cross Section Uncertainty and Sensitivity Analysis (XSUSA) [34] tool implements this method of cross-section sampling. It's built to be create nuclear data with the SCALE covariance matrices for use with the TSUNAMI sequence.

2.5.3 Theoretical Model Based

The TALYS Evaluated Nuclear Data Library (TENDL) [7] is a complete nuclear data library based on theoretical calculations along with specific evaluated data. The use of theoretical calculations allows for evaluations of cross sections that have not been measured and the creation of covariance matrices that have not been measured. The library is created to agree with benchmarked data as much as possible. It features many isotopes of interests and many, many more covariances than typical libraries that rely more on experimental data. Due to the computational nature of library creation, random nuclear data evaluations can be made using inputs to the theoretical model rather than relying on provided nuclear data covariances. The model inputs are varied until many sets of cross sections are made that are not rejected (e.g., agree with experimental data).

2.5.4 ACE Data Based

A more direct method of sampling is to use vary the ACE (A Compact ENDF) data format that MCNP uses. ACE data stores nuclear data in a point-wise manner such that linear interpolations can be made between points to create 'continuous' data. The Nuclear data Uncertainty Stochastic Sampling (NUSS) tool [35] directly perturbs the pointwise data based on multi-group nuclear data covariances. This eliminates the need to manipulate very complex ENDF data, but requires confidence in inputted covariance matrices. A comparison of NUSS and theoretical model based nuclear data perturbations was performed previously [36]. The two methods agreed well for benchmark criticality cases. However, there are cases where the theoretical model produced nuclear data with a non-zero skewness, which are not represented in ENDF data. These skewed data leads to skewed uncertainties which could be important in some safety calculations. The NUSS tool was also extended with better statistical methods to perform global sensitivity analysis based on the group-wise covariances and sampled made. The new method uses a

relatively complicated sampling scheme that assumes normal distributions that would not scale well to sampling other non-nuclear data quantities of interest due to having different probability distributions.

2.5.5 Generalized Sampling

In general, when sampling based techniques are implemented, or even parametric studies are performed, a method to create many inputs and analyze outputs is required. A naive approach would be to perform the required tasks by hand. For very small applications this is appropriate, however, very quickly a programmatic solution should be created.

The SCALE Sampler super-sequence was described in Sec. 2.3.2, and MCNP P-STUDY was described in Sec. 2.4.2. Both of these approaches changes the inputs using a set of pre-described keys

Sensitivities and Uncertainties in Criticality Inventory and Source Term Tool (SUnCISTT) [37] is a tool to generically couple the GRS statistics package SUSA to various nuclear MC codes such as the criticality control sequences within SCALE 6.1 and the eigenvalue mode fo MCNP5 (though no publications show these results). In essence, the statistics tool generates variable samples and SUnCISTT manipulates input files given some set of keywords to replace the generated variables, executes the inputs and parses the outputs to give back to the statistics tool for analysis. The tools are not available publicly, with most analyses focusing on criticality safety. If upgraded with the fast statistical approaches mentioned previously, along with a standalone SCALE's ORIGEN, this tool would be very functional.

The approach taken within this analysis is not very different than previous approaches of sampling inputs, running them, parsing outputs then performing statistics. The differences arise from the goal of the calculations (reactor design calculations), and the specific codes being couple (MCNP with thermal analysis tools).

2.5.6 Applications to Data Adjustment

The tools described thus far have had much success in application to benchmark problems, nuclear data adjustment as well as more complex problems.

An important sanity check to pass with cross-section adjustment methods is the ability to agree with nuclear data benchmark problems. These problems are well crafted, well documented experiments generally created for criticality safety. Often these experiments are used to determine bias in calculations tools. Many of the nuclear data sampling methods described have been used to successfully agree with computational [38, 34] and experimental benchmarks [39]. The UQ/SA performed could be used to perform cross section adjustments of evaluated data.

The most studied use of cross-section perturbation UQ/SA is to evaluate nuclear data files. Adjustment procedures [40] have been proposed such that many random nuclear data files are created then ran on many benchmark problems. The nuclear data files that best matches all of the benchmark problems should be the data file that is accepted. This method can be applied from experimentally evaluated cross-sections or those from theoretical calculations [41]. Interesting results have been presented that adjust ^{239}Pu [42] and H_2O thermal scattering [43] data. Potential pitfalls of this adjustment procedure is that the nuclear physics calculation tool is assumed to be perfect and that benchmark experiments are assumed to be all equivalently performed.

Benchmark problems, although extremely important in verification and validation, and US/SA, are generally not as complex as typical nuclear systems like power, propulsion, and research reactors. Applying UQ/SA techniques to these complex problems proves very difficult due to the large number of physics involved as well as the total number of inputs and outputs involved that can only be known with certain precision and accuracy. Nonetheless, the objective of UQ/SA is to tackle these difficult problems.

An example of a difficult problem is the Martin-Hoogenboom benchmark problem. The problem was envisioned to be a complex problem unsolvable at the time (2003), to be something to strive to. It consists of a PWR core with 241 fuel assemblies, each with 264 fuel pins. The goal was to resolve (within a reasonable time) pin power to 1% statistical uncertainty as well as about 100 nuclide reaction rates, which requires about 6.3 million tallies. This is both a memory and cpu intensive problem. The fast GRS and the fast TMC statistics methods were applied to this problem [44]. Though each calculation does not conform to the 1% uncertainties prescribed in the benchmark, input uncertainties based on nuclear data can be calculated. This ability to tackle complex problems is the main reason to use these methods within the analysis at hand.

2.6 Nuclear Thermal Propulsion Background

2.6.1 NTP Operations

Nuclear thermal propulsion works on the same principle as chemical rockets: propellant is heated up and sent through a nozzle to to create thrust. NTP can use lighter working fluids than chemical rockets such as H_2, which allows for high exhaust velocities, almost increasing the impulse produced by a factor of 2. The extra impulse can be used to carry more payload, or decrease transit time on a mission. Thrust is the force delivered by the rocket, and impulse is a function of the force per unit propellant mass. Impulse can be considered rocket efficiency and can be maximized by increasing the propellant velocity and decreasing the propellant mass.

Figure 2.1 shows impulse and thrust of different propulsion vehicles. A large thrust and impulse is ideal, but no proven vehicle with these specifications exists, though with this metric NTP is the best. A low thrust, high impulse vehicle has the attributes of large payloads but long transit times. The highest impulses come from drives using ions as the working fluid.

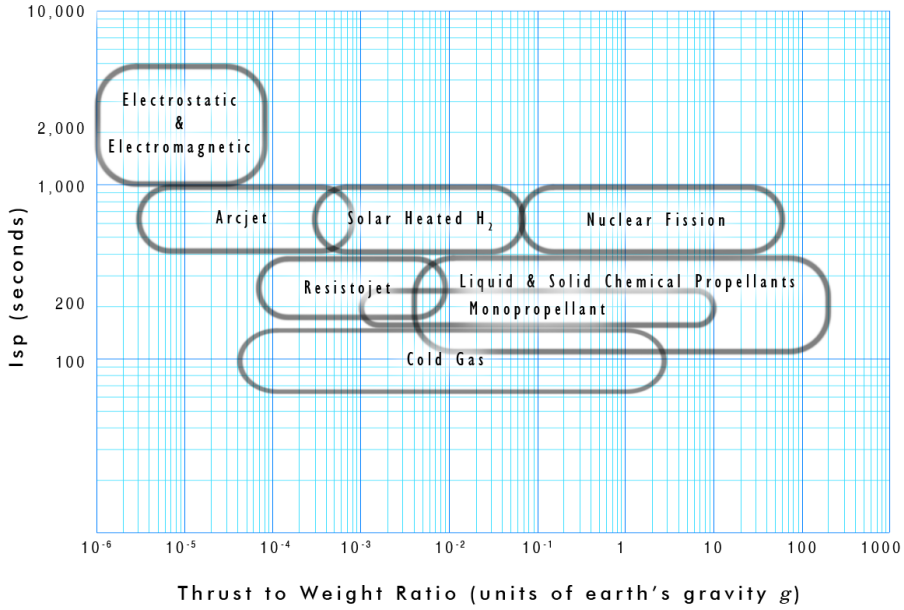

Figure 2.1: Impulse and Thrust of Various Propulsion Vehicles. Reprinted from [1]

Nuclear propulsion works by pumping hydrogen stored at cryogenic conditions to high pressures (5-20 MPa), splitting the flow, on path cooling the nozzle and reflector and the other path cooling the moderator containing tie-tubes. The energy transfered to the hydrogen is then used to drive a turbine which exhausts into the nuclear fuel to gain additional energy. The hydrogen is finally expanded through a converging-diverging nozzle to produce thrust. Figure 2.2 shows a schematic diagram of this flow passage.

2.6.2 Neutronic Analysis Methods

NTP cores have unique geometries that are not easily analyzed correctly by deterministic methods due to a highly heterogenous core with streaming paths and short neutron mean free paths. Monte-Carlo methods allow for fast iteration on dimensions and materials. It also allows for easier treatment of cores where the fuel to moderator ratio changes. Figure 2.3 shows the detailed fuel and tie-tube geometries. The fuel is in hexagon forms

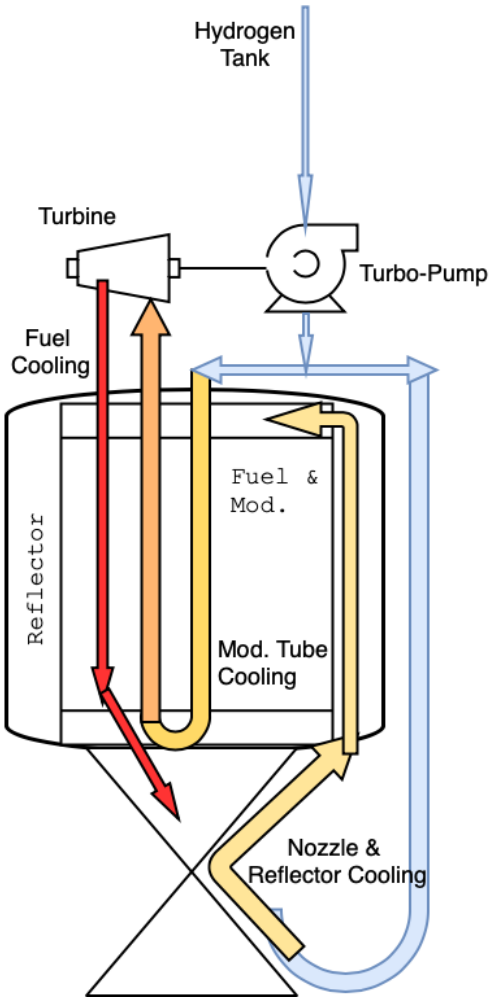

Figure 2.2: NTP Flow Schematic

with coolant channels through them. The tie-tube in some designs acts as the support structure and contains insulator to reduce heat transfer and have two cooling pathways that connect at the lower part of the core. The active cooling of the moderator is required to keep the ZrH cool.

2.6.3 Program History: Project Rover / NERVA

The Rover/NERVA nuclear rocket program ran from 1955 to 1973 with the goal of transporting humans to Mars and to probe the outer planets. The program had a budget of

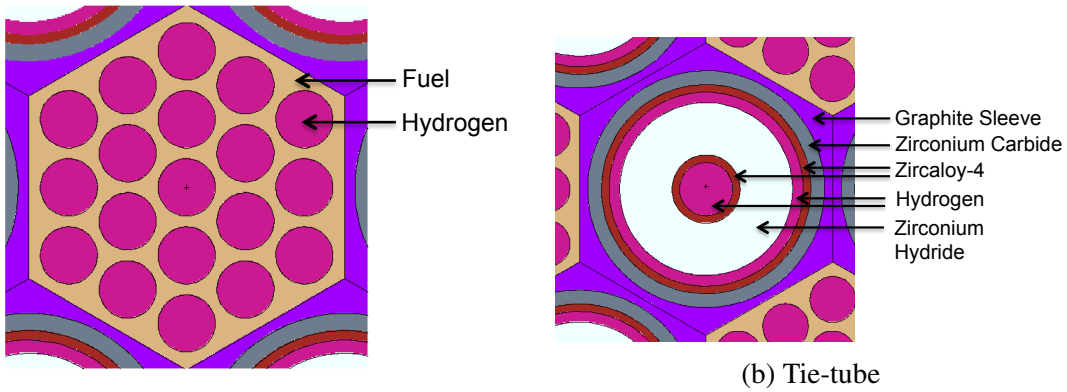

(a) Fuel

(b) Tie-tube

Figure 2.3: Reactor Components

approximately $7.8 billion in 2019 dollars. A total of 22 nuclear reactors were designed, built, and tested during the program. The NTP was to be the upper stage of the Saturn V rocket, allowing for much more payload to orbit than a chemical upper stage. Figure 2.4 shows a timeline of major reactor concepts. Kiwi (flightless bird) was used to test reactor kinetics and control and was not meant to be flight hardware. Phoebus was an evolution that was higher power and longer duration. PEWEE was a smaller core made to be simpler for un-crewed missions, and NERVA cores were to be flight ready, human capable engines. The program was canceled in the early 1970s due to many political factors.

The main fuel of choice in program were graphite based fuels used with heterogenous moderator elements as seen in Fig 2.5. The fuels and coatings developed had a high technology readiness level. As such, a conceptual core was designed with all lessons learned from the Rover/NERVA program. The Small Nuclear Reactor Engine (SNRE) [6] was this engine. The SNRE unit-cell and dimensions are shown in Fig. 2.6. This reactor is used in analysis studies to represent an HEU system.

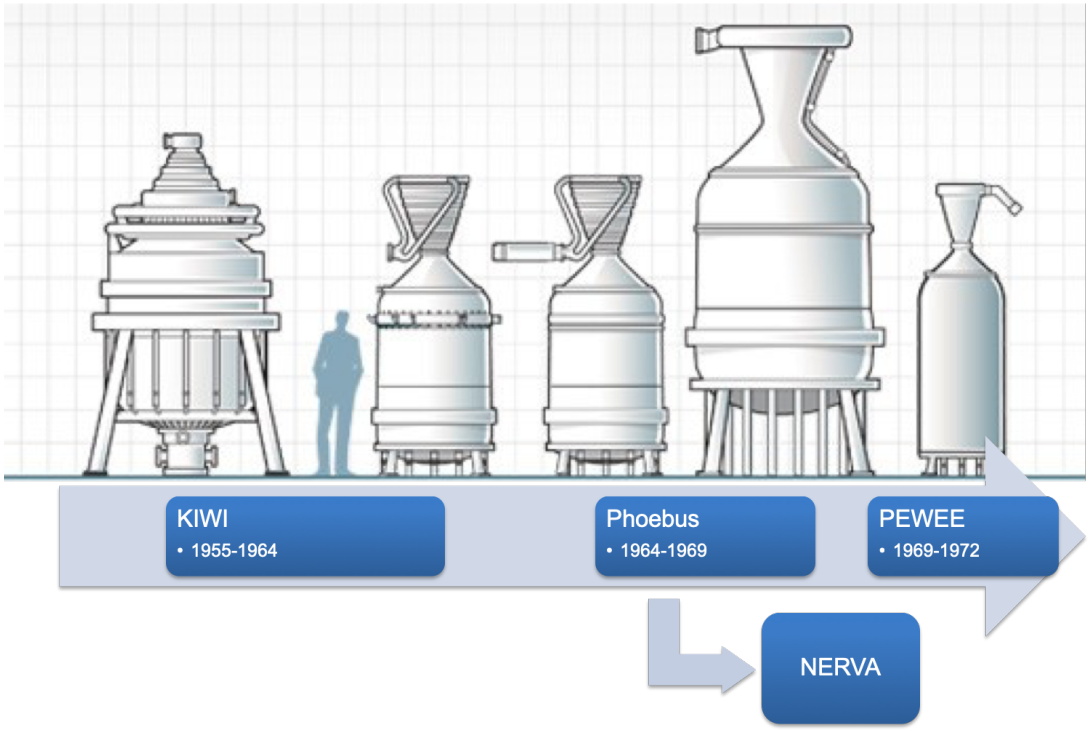

Figure 2.4: Various Historic NTPs Timeline. Reprinted from [2]

2.6.4 Recent Work: SCCTE and Beyond

Recent political trends have lead to the removal of HEU from future and current reactors. As such, any new NTP design must use low enriched uranium. This is often considered counter-intuitive for NTP design because the goal of NTP is to be a light and small as possible, and that tends to necessitate HEU fuel. However, properly moderated LEU systems can have similar performance as HEU systems [45]. This is because after a certain thrust level of a few thousand pounds-force, the system design is thermal heat transfer area limited and not criticality limited. This means the HEU reactor has a minimum size.

The Space Capable Cryogenic Thermal Engine (SCCTE) [46] is an LEU-NTP design that was a main effort of NASA-Marshall to form a small team to re-discover the full NTP design process. This was a tungsten-cermet fueled core with ZrH_x moderator. This

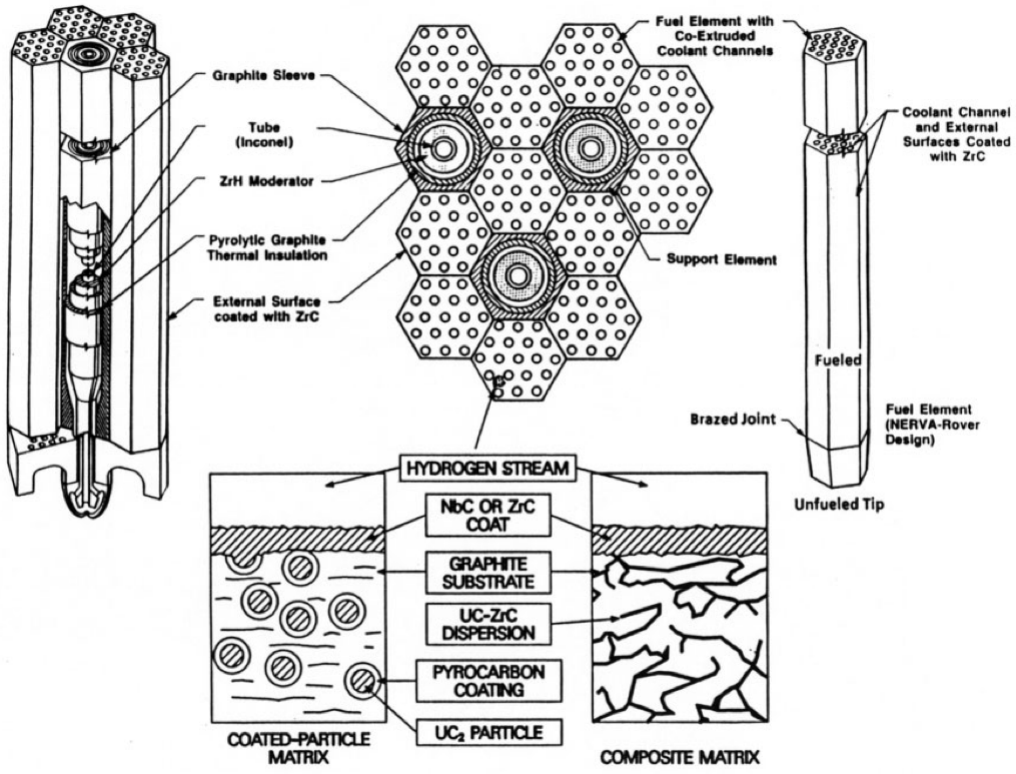

Figure 2.5: Typical NTP Fuel and Moderator Arrangement and Fuel Description. Reprinted from [3]

core used enrichment of ^{184}W to reduce parasitic capture of neutrons in the fuel because this tungsten isotope has the smallest absorption cross-section. The SCCTE unit-cell and dimensions are shown in Fig. 2.7. This reactor is used in analysis studies to represent an LEU system. The unit-cell attempts to capture the 1:1 ratio of the fuel to moderator, however it is not a true unit-cell since one cell does not exist for the core.

Label	Component	Radius (cm)	Material
A	Coolant	0.13000	Hydrogen
B	Clad Thickness	0.10000	ZrC
C	Supply	0.20950	Hydrogen
D	Supply Tube	0.26050	Zircaloy-4
E	ZrH	0.58400	ZrH1.89
F	Return	0.67800	Hydrogen
G	Return Tube	0.70500	Zircaloy-4
H	Insulator	0.80650	ZrC 60%
I	Sleeve Half Flat to Flat	0.95650	Graphite

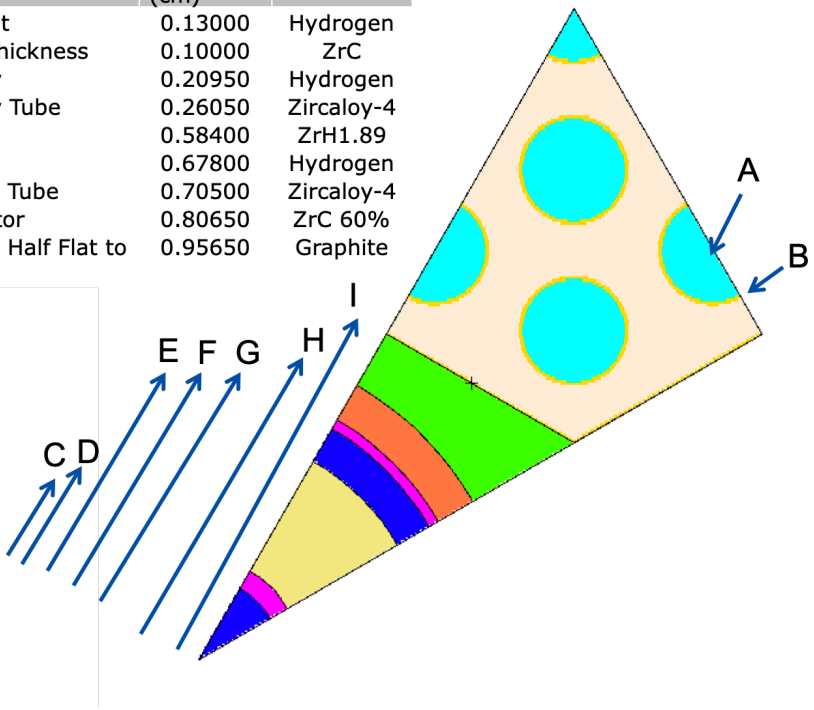

Figure 2.6: SNRE Dimensions

Label	Component	Radius (cm)	Material
A	Coolant	0.14000	Hydrogen
B	Clad Thickness	0.01700	ZrC
C	Supply	0.20000	Hydrogen
D	Supply Tube	0.25700	Zircaloy-4
E	ZrH	1.24940	ZrH1.89
F	Return	1.32940	Hydrogen
G	Return Tube	1.38634	Zircaloy-4
H	Insulator	1.48940	ZrC 60%
I	Sleeve Half Flat to Flat	1.55190	Graphite

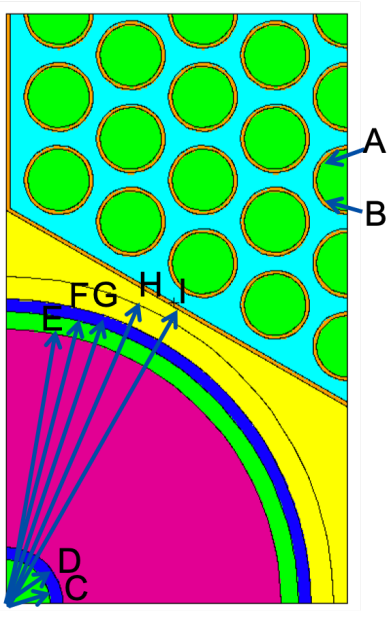

Figure 2.7: SCCTE Dimensions

3.1 MCACE

mcACE is a tool developed to perform UQ using MC methods in this dissertation. It is used to manipulate MCNP input files to create random perturbations based on changing any line given variables to change and distributions to sample from. It also handles data post-processing, data transfer, MCNP/ORIGEN coupling, and performs statistics on relevant results. The typical flow of mcACE is shown in Fig. 3.1. This process is automated within mcACE given the user input that is also shown in the figure. This section describes the details of mcACE.

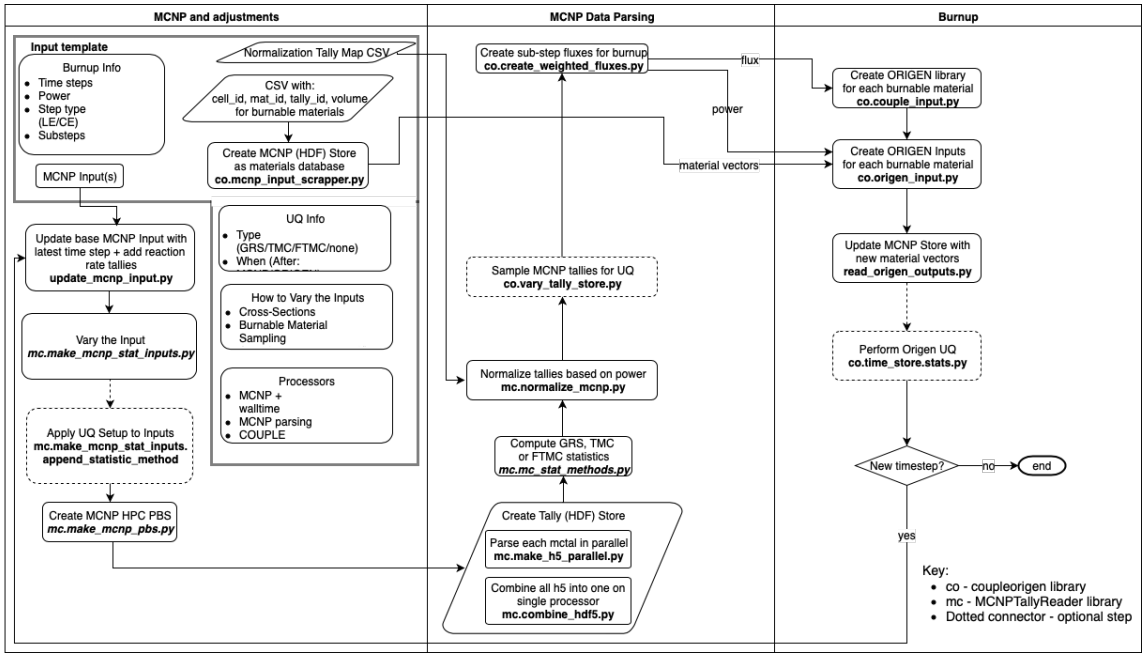

Figure 3.1: mcACE Flow Diagram

3.1.1 MCNP Input Parsing and Sampling

The goal of mcACE was to apply to many reactor designs rather than only work with a single reactor. This goal necessitated writing a program that could understand MCNP syntax. Particularly, MCNP cell lines can be parsed for cell numbers, material numbers, densities, and volumes; MCNP problem lines can be parsed for material numbers and materials. More subtle MCNP features are also handled such as MCNP single line comments (C comment), end of line comments (valid line $ comment), and both types of continuation lines (lines starting with 5 spaces and lines following a &). This allows for reading as well as writing back MCNP files that can be ran with MCNP directly. The whole input file is parsed into a python class that allows access to the MCNP title, cell, surface, and problem blocks. Find and replace functions help sampling procedures vary inputs.

Any parameter in the MCNP input can be sampled using the mcACE input. Given the original line and a properly formatted version of that line, sampling can be performed. An example to vary density is shown in Fig. 3.1, where the first line is the original MCNP line in pseudo-code format, and the second line is the original line with the 'density' number replaced with a python string formatter with index 0. The index 0 corresponds to the position in the 'sampling_scheme' list. The 'sampling_scheme' allows for many sampling functions like uniform, normal, latin-normal, repeating the last sampled value, giving an exact value for a simple find/replace, or a user generated math function. This interface provides good flexibility to sample MCNP files. The mcACE input allows for repeated sampling blocks so sets of parameters can be varied as needed.

3.1.2 MCNP Tally Reader

MCNP prints relevant outputs to '.o' files, and optionally '.mctal' files. The '.o' files contain a wealth of information, particularly about statistics and problem run information as well as relevant outputs like tallies and eigenvalue. The '.mctal' files contain a subset of

Listing 3.1: Sample mcACE MCNP Line Sampling SNippet

```
mcnp_lines=cellnum mat# density surf cards imp:n=1,
lines_to_vary_with=cell# mat# {0:.6f} surf cards imp:n=1,
sampling_scheme=latin ,
sampling_values=0.1 0.05,
```

the information in the '.o' files but the information is very structured, allowing for efficient readers to be created. mcACE implements an '.mctal' reader to read eigenvalues, problem information, and most tallies (i.e., F:anything, FC, E, T, C, FM, DE/DF, and SD), missing is a mesh-tally reader though one could be added. MCNP '.o' files can also be read for information that is not present in a '.mctal' file such as kinetics parameters and sensitivity coefficients.

3.1.3 mcACE Storage

The UQ process implemented generates a large amount of output depending on the relevant output parameters. In a typical run with 500 MCNP in eigenvalue mode, 5 tallies with 100 energy bins would result in 2.5e5 outputs to track. In a burnup calculation that uses a 238-group structure and 100 unique materials, a minimum of 11.9e6 outputs must be tracked. Storing this data in typical text files or csv's is not efficient and error prone. mcACE opts to use the HDF5 storage format along with python pandas dataframes to store data as tables in HDF5 format. After relevant outputs are parsed for each MCNP run, all of the similar results are combined into a dataframe with multiple index as tally info as needed and a run number index, with columns as energy bins or other specific names such as 'keff'. This format also makes it easier to perform statistics on the outputs.

3.1.4 MCNP Coulpling with COUPLE/ORIGEN

In order to propagate uncertainties through time, a burnup scheme must be selected. MCNP contains CINDER90 to perform burnup, however it is not very flexible in terms of specifying what nuclides should be tracked and how the time-integrator works. COUPLE+ORIGEN within SCALE 6.1+ provides a flexible interface to perform burnup calculations. Burnup solvers solve the 0D Bateman equations given a flux or power level and an initial material concentration and time step. COUPLE is used to generate 0D cross-sections for material specific burnup libraries. These COUPLE libraries are used in ORIGEN to integrate the Bateman equations. mcACE creates COUPLE and ORIGEN inputs from MCNP outputs and then reads ORIGEN outputs to update MCNP inputs with new material concentrations.

The time-stepping in most MC neutronic codes are quasi-steady state. The neutron transport equation is solved assuming steady-state concentrations and operations, then the Bateman equations are solved assuming constant cross-sections. This weak operator split scheme has been shown to work well in many applications. The time integration scheme has evolved from simple forward marching techniques to advanced predictor-corrector/higher order methods [47]. An integration method that out-performs all other methods in all cases has not been found, though some integrators are certainly worse than others.

mcACE implements constant-extrapolation (CE) and linear-extrapolation (LE) for predictors and linear-interpolation (LI) and quadratic-interpolation (QI) for correctors. The CE and LE can be used without correctors. The typical combinations are CE/LI, LE/LI, and LE/QI. CE alone is never recommended due to large errors from the method. LE alone can be used but step sizes need to be about half as large as the predictor-corrector methods.

Figure 3.2 shows the reaction rates or fluxes used in the depletion calculations for

the CE/LE/LI methods. Specifically, CE uses the cross-sections predicted at the current timestep, t_n to predict materials at t_{n+1}, LI would then correct this by solving for new cross-sections at t_{n+1}, then averaging the t_n and t_{n+1} cross-sections to perform another depletion with the averaged cross-sections to determine the new concentrations at t_{n+1}. If QI were used instead of LI, the interpolation step would use cross-sections from t_{n-1}, t_{n+1}, and t_{n+1} to create the average cross-section for depletion. LE uses the cross-sections from the previous step and current step to extrapolate to the next time-step and uses this extrapolated cross-section to perform depletion. The LI or QI predictors can then be applied.

Sub-step methods can be used with LE/LI/QI. Sub-step methods break the time-steps down into smaller steps where depletion is solved using cross-sections extrapolated or interpolated to the sub-step time. The stair-cases shown in Fig. 3.2 would be an example of sub-steps. Any number of sub-steps can be used, mcACE allows for as many as the user desires in all cases. A COUPLE library is generated for every sub-step and for every sampled MCNP input file. In cases were the previous time-step is not available like the very first step, CE is used, and for QI when previous 2 steps are not available LI is used.

Burnup tallies are automatically added to relevant materials when the user specifies a material as 'burn'. The first step to using mcACE is to pre-process the MCNP input. mcACE looks for all cells with a volume card and generates a csv to fill in for the user based on the cell having a tracked material, burnup material, or activation material in it. When a material is marked burnup, a 238-group tally as well as specific reaction rate tallies: (n, γ), (n, fission), (n, 2n), (n, 3n) (n, p), (n, α). These reaction rates are important to calculate directly within MCNP such that self-shielding can be accounted for. The user can request any MT numbers to calculate any extra specific reaction tallies. The reaction rates and the 238-group flux is passed to COUPLE to generate material specific ORIGEN libraries. The 238-group flux is used for nuclides where the reaction rate was not calculated such as those not present in the transport problem.

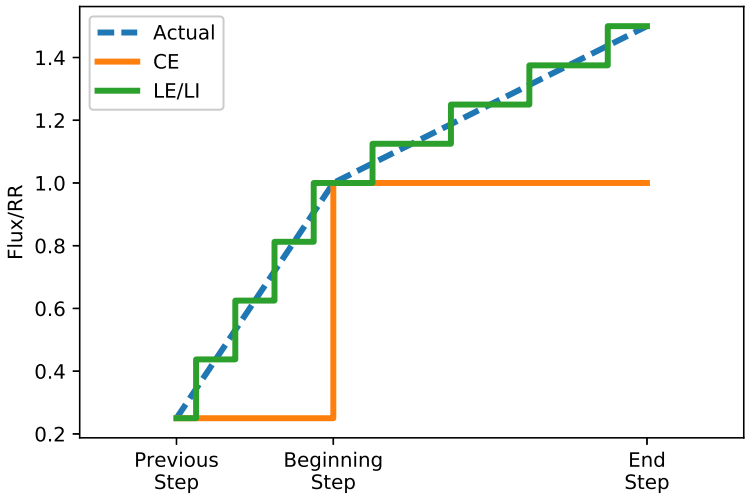

Figure 3.2: Time Steppers

3.1.5 Total Monte Carlo

The Total Monte Carlo method refers to a technique to randomly vary fundamental nuclear data parameters to generate many random nuclear data libraries from theoretical models. These random data are used in many long running MC calculations to determine the effects of nuclear data variations. The statistical method to remove the MC statistics from output calculations can be described by breaking up the observed uncertainty into Monte Carlo and input uncertainties,

$$\sigma_{ob} \approx \overline{\sigma_s^2} + \sigma_i^2 \tag{3.1}$$

$$\overline{\sigma_s^2} = \frac{1}{N} \sum_{j=1}^{N} \sigma_{s,j}^2, \tag{3.2}$$

where σ indicates uncertainties, and the subscripts ob, s, i, indicate observed, statistical, input uncertainties, and N is the total number of observations. If a set of observations

due to varying inputs can be made along with the associated MC uncertainty, the input uncertainty can be determined using Eq. (3.1).

A large (500-1000) set of random inputs are generated to create a large set of outputs. Within an MC calculation, each run should have sufficiently low relative MC uncertainty (e.g., $\overline{\sigma_s} \approx 0.05$) such that the total uncertainty observed from the large set of outputs is predominately from epistemic input uncertainties. This method, though easy to implement for most code frameworks, increases calculation time by 500-1000 times that of a single run. This is an unacceptably large overheard within reactor physics calculations, especially when burnup calculations are involved. A faster version of this method is described in Sec. 3.3.2 using the ideas of the following section.

3.1.6 GRS

The GRS method relies on the statistical distribution of MC outputs in order to determine input uncertainty. By taking two sets of random simulations, two distributions with the same uncertainties are found. The covariance of these distributions is the input uncertainty because statistical errors are the same in both sets and are removed by the covariance operation. In a mathematical sense, given a model, $Y = X(U)$, with input set U that is randomly varied, the average output μ, is,

$$\mu = \mathbf{E}[\mathbf{E}[Y|U]],$$

which given the results of iterated expectations (sometimes called law of total expectation),

$$\mu = \mathbf{E}[Y],$$

with variance, σ^2 as,

$$\sigma^2 = \mathrm{Var}(\mathbf{E}[Y|U]).$$

The square-root of the variance gives the uncertainty of the inputs on the outputs. However, with a single MC run, a very large number of particles would need to be ran (like in TMC) to reduce MC statistics. However, when two sets of MC runs are made with two different random number seeds, two sets of outputs, Y, Y' are created that are conditionally independent and identically distributed, e.g., on average the outputs are the same but comparing individual results will show differences ($\mu = \mathbf{E}[Y] = \mathbf{E}[Y']$). By using this fact and the following form of the expectation of the two outputs multiplied, the variance of the mean output can be related to the covariance between the two output sets. The expectation of the two outputs multiplied is,

$$\begin{aligned}
\mathbf{E}[YY'] &= \mathbf{E}[\mathbf{E}[YY'|U]], \\
&= \mathbf{E}[\mathbf{E}[Y|U] \cdot \mathbf{E}[Y'|U]], \\
&= \mathbf{E}[\mathbf{E}[Y|U] \cdot \mathbf{E}[Y|U]], \\
&= \mathbf{E}[\mathbf{E}[Y|U]^2]. \qquad (3.3)
\end{aligned}$$

Inserting Eq. (3.3) into the definition of covariance,

$$\begin{aligned}
\mathrm{Cov}[Y, Y'] &= \mathbf{E}[YY'] - \mathbf{E}[Y]\mathbf{E}[Y'], \\
&= \mathbf{E}[\mathbf{E}[Y|U]^2] - \mathbf{E}[Y]^2, \\
&= \mathrm{Var}(\mathbf{E}[Y|U|]), \qquad (3.4)
\end{aligned}$$

shows that the covariance between the two output sets is the variance of the desired mean output given input uncertainties U. This formulation cancels out (or averages) the MC uncertainties such that only the input uncertainties remain. This method avoids Eq. (3.1) so criteria for $\overline{\sigma}_s^2$ are not required, though MC uncertainties should be reasonably sized and enough particles ran to ensure source convergence.

3.1.7 Fast Total Monte Carlo

The fast TMC method relies on the principle of the GRS method that all of the statistical uncertainties of similar random runs have the same distribution such that only one long running MC run needs to be performed to get good MC statistics.

This is accomplished by running a single problem run with a typical batch size, b similar to TMC to obtain small σ_s. This uncertainty is used in Eq. (3.2), instead of summing many uncertainties together. Then, instead of running N problems, each with batch size b, N problems with batch size b/N and N unique random number seeds are run to obtain a runtime similar to a single problem with a batch size b. A larger batch might have to be run if input uncertainty is small but important, or a difficult to tally quantity is required. The FTMC method in about twice the time of a single long TMC run, can reach about 15% of the TMC uncertainty with less total runs compared to TMC, about 300 vs 500-1000, depending on the problem. In fact, the FTMC uncertainty will not decrease much with more random inputs because the MC statistics are not decreased with more random inputs, only with more histories per run. The FTMC method can be as fast as running a single long calculation if each run's results are combined to create a pseudo-long running result.

It has been shown that re-running the same calculations with different random number seeds in order to capture the true variance of the MC calculation does not change the results of calculations [20]. This is likely due to the fact that the true variance for the similar calculations are all similar such that they cancel out when input uncertainty is

determined through Eq. (3.1).

3.1.8 Extension of Methods

The UQ methods described have traditionally be used to calculated global reactor quantities like eigenvalues to support nuclear criticality safety and nuclear data adjustment applications. It is observed in this dissertation that he GRS method can, in theory, be used to determine uncertainties on any output quantity. Even more importantly, the GRS method can be applied after the output quantities have been used in other analyses to calculate other outputs. This provides a method of propagating the nuclear uncertainties to other physics domains. It will be established that GRS uncertainties agree with TMC uncertainties even with local quantities by running very long running TMC calculations. The TMC calculations also provide a basis to perform sensitivity analysis. The Fast TMC method will be shown to be found to not work very fast for local quantities needing many more particle histories for uncertainty convergence, however it remains to be extremely fast for eigenvalue uncertainty calculations.

3.1.9 Nuclear Data Sources

TENDL, ENDF/VII, ENDF/VII.1, ENDF/VIII, and SCALE 6.1 nuclear data were used in studies in this dissertation. Cross-sections in ACE format were obtained from MCNP 6.1 and TENDL. Covariance data was calculated from ENDF data files and extracted from SCALE 6.1 data via AMPX.

3.2 A Simple ACE Python IO (ASAPy)

Randomly generated cross-section files available within TENDL are an excellent resource, however not all desirable cross-sections are available and evaluated covariances are not used when sampling data. While the latter is considered a positive feature of TENDL random data, it is not fully accepted that generated data from fundamental parameters

MT	Description	MTs in Sum
1	Incident Neutron Total cross	2, 4, 5, 11, 16-18, 22-26, 28-37, 41-42, 44-45, 102-117
4	Total of neutron levels	50-91
18	Total fission	19-21, 38
103	Total of proton levels	600-649
104	Total of deuteron levels	650-699
105	Total of triton levels	700-749
106	Total of 3He levels	750-799
107	Total of alpha levels	800-849

Table 3.1: ENDF Sum Rules

is the correct method of making nuclear data. The ability to generate random data with SCALE based covariance data is a positive feature to overcome issues when data is not available and to sample data based on evaluated distributions. A deficiency in this method of sampling is that the covariance data must be available for the reaction and nuclide of interest to actually sample data. Furthermore, sampling from ENDF formatted covariances directly has a benefit of sampling from any ENDF based data as well as from covariance data that has not yet made it to official SCALE releases.

ASAPy is a tool that was created in this dissertation to perform data sampling from ACE files using SCALE covariance data or ENDF data via NJOY to address the above issues. This tool is similar to the NUSS tool described in Sec. 2.5.4, except it uses the newest SCALE covariance data or newest ENDF data and written in python. It also features the ability to use any group structure and/or any user flux weighting functions for covariance collapsing. The sampling procedures also uses lognormal sampling along with the ability to use any sampling function as long as the percent point function is available.

3.2.1 ACE Data Manipulations

The A Compact ENDF file (ACE) format is used for nuclear data within MCNP and other monte-carlo codes. It contains all relevant data from ENDF files, support random access of data, and specifies all cross-sections on the same unionized energy grid. The ACE data is a formatted data file and readers are available, though writers tend to only translate ENDF data to ACE, with no general method to manipulate the ACE data directly. The ACE data reader within OpenMC [48] was used to read in ACE files. A writer was created based on the structure of ACE files. All data is represented in contiguous arrays, so that if the original data is known (from reading the ACE data), that data can be searched for within the ACE file and replaced with new values as long as the exact same energy grid is specified. This method of adjusting ACE data is implemented in ASAPy. A few nuances when dealing with different data will be discussed.

Cross-Section Perturbation: Nuclear data sampling occurs using multi-group methods while ACE data is stored in a continuous format. Perturbation factors are generated based on taking a ratio of sampled cross-sections and multi-group average cross-sections. These perturbation factors are then applied to the continuous cross-sections by mapping the multi-group structure on the continuous structure.

ENDF Sum Rules: Many ENDF reactions are subsets of other reactions, so when one cross-section is sampled, others might need to be adjusted for consistency. This is performed within ASAPy by keeping track of all MTs adjusted and comparing against sum rules. Table 3.1 shows the relevant sum rules from the ENDF manual [26].

$\bar{\nu}$ Data: ENDF data allows for inclusion of total, average number delayed, and prompt fission neutrons. MCNP only uses the total values within ACE files, so only these are modified.

Fission χ Spectrum: The distribution of energy of neutrons born from fission depends

on the incident neutron energy. As such, ACE data file stores several tables for a few incident neutron energies. ENDF covariance data does not have covariance data for each incident neutron so the covariance data within the ENDF file is applied to all incident neutron energy distributions. The distributions are also stored as probability and cumulative distribution functions (PDF and CDF). To sample these, the PDF is perturbed then the CDF is adjusted based on the PDF perturbations then the CDF is renormalized by adding up the original PDF and perturbation factors to ensure the CDF sums to 1.

3.2.2 Covariance Data

The most comprehensive resource for covariance data is distributed within SCALE 6.2 [21]. It combines covariance data from several nuclear data sources and experiments. A fine 252-group and coarse 56-group structure is available within SCALE. An older 44-group structure exists but contains old data that is not recommended for use. The covariance data can be converted from the internal SCALE binary format to a ASCII format using the SCALE tool AmpxCOVConverter. The resulting data file contains data for material numbers and their relevant reactions correlated with one another. The standard deviations of the specified reactions are given in the relevant group structure followed by the actual correlation matrix. A covariance parser was created within ASAPy to convert the ASCII file to a more general HDF5 store with a hierarchy based on: '/mat1/mt1/mat2/mt2' corresponding to data correlating mat1 MT1 with mat 2 MT2. Often mat 1 and mat 2 are the same, and MT1 and MT2 are the same, specifying self-correlation. Any group structure can be accommodated by the parser such that new evaluations can be easily used within ASAPy.

Covariance data also exists in ENDF files and these covariances can be used to create any group structure as well as use any weighting flux to create covariance matrices to sample with. The SCALE based data was generated using a typical LWR flux that in-

clude a thermal, epi-thermal, and fast region. ENDF data can be parsed with NJOY [27] to generate covariance data. ASAPy implements NJOY input writers along with ENDF readers to minimize the amount of user input to generate covariance data. The minimum input is a path to an ENDF file and the reaction MT numbers to generate covariance data for. A BOXER format reader was also generated in order to read the BOXER formated covariance files into the previously described HDF5 format.

The covariance data comes in multi-group format which must be mapped to relevant continuous energy bins in ACE data. After sampling data within the multi-group structure, the data is divided by the multi-group mean cross-section to calculate a relative cross-section. These cross-sections are mapped onto the continuous energy group bins then multiplied by the ACE data to generate a sample of data. Two assumptions made are that the group-mean values within the data are very similar to the mean values within the ACE data and that the data within an energy bin are fully-correlated with one another.

3.2.3 Sampling Techniques

A slight deficiency in the ENDF format is the inability for evaluators to convey what type of distribution covariance data should take. Often physical parameters like cross-sections cannot take negative values, but assuming normal distributions are assigned to reported covariances, negative values are possible. An approach often taken is to discard negative data, biasing the sampling scheme. Another method is to assume the distributions are log-normal, which always has positive values. However, without knowing what distributions the covariance data were specified for, errors can occur when large relative errors are present with strong negative correlations [49] due to not transforming the normal-cov to lognormal-cov. In this dissertation, ENDF covariance data is transformed to log-normal covariance data then log-normal sampling is performed ensuring no negative samples are taken.

Nuclear data has strong correlations between energy groups so when sampling data, the full covariance of the data must be taken into account. Multivariate-normal distributions allow for sampling of such data. Given a desired covariance matrix, C, that is semi-positive definite, and mean values, μ, a multi-variate sample, X_i can be generated as follows. First draw uncorrelated values from the mean using a standard-normal distribution, $\mathcal{N}$ and place the means in a diagonal matrix,

$$x_i = \mathcal{N}[\mu = 0, \sigma = 1],$$

then perform a singular value decomposition of the covariance,

$$C = USV, \tag{3.4}$$

where U and V are orthogonal matrices, and S is a diagonal matrix containing the singular values of C. A sample can then be drawn as

$$X_i = \mu + x_i S^{0.5} v$$

This method is implemented in Scipy [50] within np.random.multivariate_normal. One may also use eigen or Cholesky decomposition instead of singular value decomposition with similar results.

ENDF based nuclear data sometimes is published with non-semi-positive-definite covariances. In this case the correlation data R must be manipulated to draw samples. An eigen-decomposition of the correlation matrix is made,

$$R = Q \Lambda Q^{-1},$$

where Q contains the eigenvectors of R, and Λ contains the eigenvalues on the diagonal. The negative eigenvalues are set to a small positive number (1e-8) to form $\tilde{\Lambda}$ then the original eigenvectors are multiplied back in to form an adjusted correlation matrix, $\tilde{R}$,

$$\tilde{R} = Q\tilde{\Lambda}Q^{-1}.$$

The correlation matrix is used due to smaller spreads in eigenvalues, however often the small eigenvalues imposed on the matrix cause numerical difficulties when converting the correlation matrix to a covariance matrix so the above procedure may need to be repeated on the created covariance matrix.

A second method based on a partial Cholesky decomposition [51] that generates a positive semi-definite matrix that equals the original matrix minus an error term was also implemented for correcting non semi-positive definite matrices.

A non-semi positive definite correlation example is the correlation matrix for (n, γ) cross-section of ^{184}W within ENDFB/VIII. The eigen-decomposition and partial Cholesky algorithms were applied to generate 500 samples and the correlation matrices are shown in Fig. 3.3, where it can be seen that both algorithms perform well compared to the original correlation matrix.

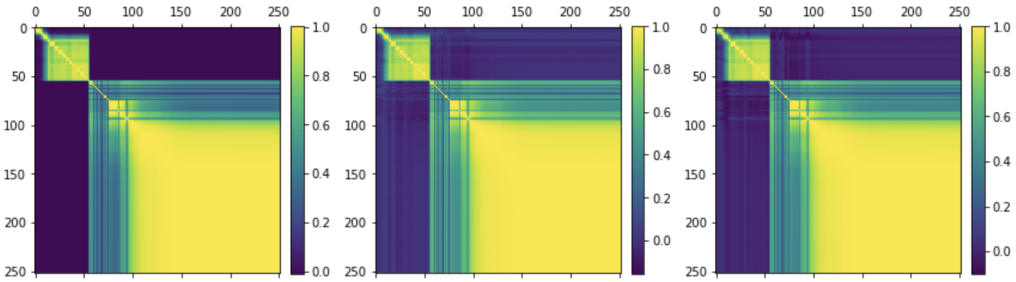

Figure 3.3: Correlation matrices from (left) the evaluated data file (middle) eigen-decomposition sampling (right) partial Cholesky decomposition sampling

3.3 Variance Based Sensitivity Analysis

The goal of sensitivity analysis is to determine what uncertain inputs or combinations of inputs most contribute to output uncertainty. For a linear problem, variance based sensitivity analysis is similar to regression estimators like Pearson Correlation Coefficients. However, variance based sensitivity analysis is applicable to non-linear problems too, unlike linear regression estimator. Two types of variance based sensitivity estimators are usually studied, first order effects (Sobol Indices) and total effects. First order effects are useful in factor prioritization and total effects are useful in factor fixing. Factor prioritization leads to finding out what inputs are most important and may warrant more research, and factor fixing leads to finding out what inputs can be set constant without affecting any results. First order indices also tend to predict affects of correlated inputs whereas total indices predict affects of interactions of variables. A first order sensitivity analysis is performed to determine what inputs are most important.

3.3.1 Interpreting Correlated Sensitivities

The interpretation of global sensitivity indices when correlated model inputs are present is difficult and still in the early stages of being studied, particularly in neutronics. Two different calculations of first order and total sensitivity indices have been compared for simple models [**?**]. The two estimators Kuchernko [52] and ANOCVA [53] agree for uncorrelated inputs do not always agree when inputs are correlated. Particularly, the Kucherenko indices best informs when interaction of correlated inputs are present, and ANCOVA tend to inform based on model structure rather than apparent input interactions.

The Kucherenko indices show influences of variables on total output variance. An issue is that variables that maybe unimportant in the model are predicted to have larger sensitivities if the relevant variables are correlated with actually influential variables. The EASI method described in Sec. 3.3.2 is similar to calculating first order Kucherenko in-

dices in terms of calculated results and as such can be interpreted similarly.

When predicting neutronic results, Kucherenko indices may imply if two highly correlated inputs have similar sensitivities, the interaction is important or simply the variables are highly correlated. In terms of real world applications, reducing input uncertainty in a single neutron energy range with no dependence on other energies is not likely to be measured, so groups with high correlations and high Kucherenko sensitivities may mean that whole range needs to be better understood to reduce output variance.

3.3.2 EASI Sensitivity Analysis

The sampling approach chosen does not have a built-in sensitivity measure like previous work [54], which has used Random Balance Design - Fourier Amplitude Sensitivity Test (RDB-FAST) to perform SA. The RDB method creates a complex input generation requirement and a corresponding input/output relationship that must be accounted for in order to perform SA. This dissertation aims to decoupled the sampling process and the SA process by implementing the EASI [55] method. Another key advantage is that the EASI method has potential for bootstrapping in order to produce uncertainty estimates of predicted sensitivities.

The EASI method calculates first order global sensitivity indices. There has not been work on interpreting global sensitivity indices for nuclear data applications, particularly when data is highly correlated. It has been shown [54] that highly correlated data tend to have the same variance fraction and that in the case of uncorrelated inputs with linear problems, global sensitivities and local sensitive are the same. Though the interpretation of global sensitivities for high correlated inputs is not fully understood, the analysis procedure is still valid. In this dissertation, relevant sensitivity profiles are plotted in terms of variance fraction, which is the amount of variance that is attributed to the output from the input. In uncorrelated cases, the sum of variance fractions equals the total variance. In

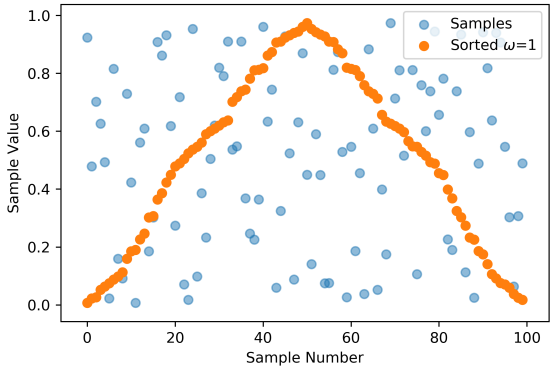

Figure 3.4: EASI Sorting Algorithm

correlated cases this is not the case.

The EASI methods is a Fourier based technique for variance based sensitivity analysis. It is particularly powerful because it can be used on datasets that have already been created, rather than having to redo analysis with a very specific sampling scheme. Inputs are sorted such that they create a periodic signal of frequency one, then outputs are sorted with the same order as the inputs. The power spectrum of the output can than be used to analyze sensitivities using Fourier methods. Higher order sensitivities can be calculated using EASI by using higher order sorting algorithms, however it was shown [55] that only cases with a few inputs can be used before the efficiency of the method degrades severely. First order sensitivity indices are still available when many inputs are present.

During ASAPy data sampling and mcACE MCNP input sampling, the samples taken are stored such that relationships between input and outputs can be maintained. The EASI method starts by sorting the inputs such that there is a periodic frequency of 1. This is done by sorting the inputs in increasing order, saving the index that would sort the inputs. Then each odd input is taken then each even input is appended in reverse order. An example of this sort is shown in Fig 3.4. The sort indices created are also applied to the outputs.

Next, the power spectrum of the sorted outputs is taken. Resonances at the input frequency ($\omega = 1$) and higher harmonics are used to determine sensitivity using Fourier sensitivity analysis. Given the power spectrum densities, P_x the sensitivity, S_i can be found by,

$$S_i = \frac{\sum_{x=1}^{X} P_x}{\sum_{x \neq 1} P_x}, \tag{3.1}$$

with M being the maximum harmonic which is usually 7 in this analysis. Bias correction is then performed according to previous work [56]. The EASI algorithm used in mcACE is within SALIB [57], however it's labeled as RDB-FAST. Analysis of the source code reveals there is no actual dependency on sampling strategy so it is a misnomer.

3.3.3 Bootstrap Estimator

The original EASI method does not specify confidence intervals. However, the bootstrap method can be used to do this. The EASI method imposes no restrictions on the mapping of input to output. This means samples can be re-ordered, or a sub-set of samples can be taken and EASI statistics are still valid. This leads to a straight-forward bootstrap prediction of confidence intervals.

The basic procedure is to take random samples of the random inputs with replacement. The total number of random samples of the original samples to take should be equal to the original number of samples [58]. The EASI method is then applied to the new sampled inputs along with the corresponding outputs to create an estimate of the sensitivity index. This whole procedure is repeated many times to create a vector of sensitivity indices. Confidence intervals can then be calculated by sorting the vector and calculating the lower and upper cutoffs based on a desired confidence interval.

A similar bootstrap estimate can be made for the TMC method. The GRS method requires unique samples so bootstrapping is not valid, however different estimators could

be used such as jack-knifing.

3.4 NTP Design Process

The current method of designing NTP from a coupled neutronic and thermal-hydraulics aspect was pioneered only recently [59]. The process involves largely repeating many of the analyses performed in the NERVA program with the design of the SNRE [6]. This involves solving for a given fuel configuration, the deterministic neutron transport equation for the eigenvalue of the system as well as fission heating rates. Various approximations were used depending on the detail of the study from diffusion to few angle SN discretization. The found heating rates were then used as heat sources in a heat transfer calculation to determine fuel temperatures and flow temperatures. The process would take some time to complete due to slower computers, and did not give very detailed results, though the NERVA program had many experiments to overcome any computational deficiencies. The current method [60] involves performing parametric analysis using one-at-a-time sampling based on expert opinion distributions of various physical parameters such as fuel channel radius or fuel height. Neutronics is performed with MCNP which generate power profiles to be used in an average/hot channel thermal analysis to determine rocket performance. Engineering margins are applied to account for uncertainties and be conservative to handle un-modeled features. Typically a +5000 pcm margin is used to select reactor cores for further analysis.

In order to determine the effects of the uncertain heating profiles, the heating rates should be used in a thermal performance analysis. TRICORDER [61], a thermal-hydraulics software for NTP simulation was used to determine uncertainties in performance by running each random MCNP output as a heat source for a thermal calculation. The outputs of each of these calculations is then used in the relevant MC statistics method, TMC or GRS.

4. VERIFICATION AND VALIDATION STUDIES

Any method implementation needs to be validated by comparing to a known result if possible. In general this is not possible but code-to-code or method-to-method verifications can be made. Validation studies should also be performed to check validity of the code to predict relevant physics. Each physics code used in this study have had extensive V&V studies. However, when the codes are made to communicate with one another, new domains of application are created such that new V&V studies must be performed. The goal of this research is to create a tool to perform UQ and thus verification validation studies are important. This chapter provides verification details of the software developed.

4.1 UQ Calculations

Verification of the GRS and TMC methods compared to one another are performed. The theory behind the two techniques is different, but their results should be similar. The UQ process is reactor agnostic such that other reactors can be analyzed and verifications performed can be applied to NTP systems. Initial results for comparing TMC and GRS were performed on the Idaho National Laboratory Advanced Test Reactor model, and burnup studies used the UAM pincell benchmark model.

4.1.1 Verification of UQ Methods

To verify the GRS implementation the TMC (Total Monte Carlo) method is used as the "true" result. Furthermore, convergence studies are performed to determine how many runs are needed for GRS cases. This study focuses on a large reactor to determine uncertainties of relatively fine group flux tallies.

Each model ran has a unique U-235 data library created from TENDL-12 ENDF files. No other variation is performed for this study. The number of runs is set to 495 for each

case. Number of histories used are reported when appropriate.

In the following comparisons, flux tallies, heating tallies, and reaction-rate tallies are created. Flux and reaction-rate tallies are used to create burnup libraries and heating tallies are used for normalization to power.

Flux tallies in burnup materials use a 238-group structure. Six reaction's are calculated that tend to be relevant for burnup calculations: (n, f), (n, g), (n, a), (n, p), (n, 2n), (n, 3n). If relevant libraries are not available in MCNP, ORIGEN libraries are used within COUPLE along with the MCNP calculated flux. Heating tallies use MCNP's f7 type tallies in order to calculate all heat created by fission.

The relative errors reported are those uncertainties in the output quantities from input uncertainty, and not the typical MCNP related statistical error. The relative errors of each value are compared by plotting the relative error of the GRS method to the TMC method. If the two methods agree, a point will be on the y=x line. Ideally, the GRS relative error will be within 20% of the TMC relative error (e.g, if TMC relative error is 0.4, GRS relative error should be within 0.4 ± 0.08). This is a difference that must be accepted to use GRS. Furthermore, the plots shown generally provide all data for a given run's tally instead of following a specific tally value between runs. This is chosen because a single point between runs can be misleading when comparing relative errors, e.g., some points vary more than others between runs.

4.1.2 Simple Case: UAM Pincell Benchmark

The UAM Pincell Benchmark [62] at hot-zero power was modeled according to the specifications in Fig. 4.1. The TMC cases were ran with 7500 particles / cycle for 15000 active cycles, the GRS cases used 40 cycles (187.5 times less total particles ran because GRS requires twice as many model runs). In Fig. 4.2 it can be seen that in general, GRS agrees well with TMC. The cases that don't agree are due to TMC not being well resolved

enough or the inability of TMC to estimate the uncertainty.

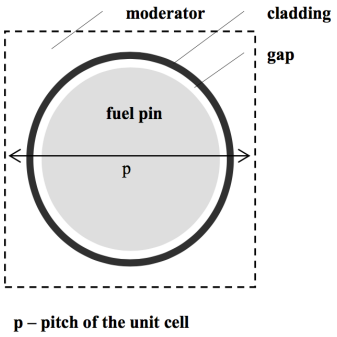

Parameter	Value
Unit cell pitch, [mm]	18.75
Fuel pellet diameter, [mm]	12.1158
Fuel pellet material	UO_2
Fuel density, [g/cm^3]	10.42
Fuel enrichment, [w/o]	2.93
Cladding outside diameter, [mm]	14.3002
Cladding thickness, [mm]	0.9398
Cladding material	Zircaloy-2
Cladding density, [g/cm^3]	6.55
Gap material	He
Moderator material	H_2O

Parameter / Reactor condition	HZP	HFP
Fuel temperature, [K]	552.833	900
Cladding temperature, [K]	552.833	600
Moderator (coolant) temperature, [K]	552.833	557
Moderator (coolant) density, [kg/m^3]	753.978	460.72
Reactor power ,[MWt]	3.293	3 293
Void fraction (%)	-	40

Figure 4.1: UAM Pincell Dimensions

All points that lie on the Y axis are those when TMC show 0 relative error due to statistical variances being larger than observed variances. Furthermore, the rule of thumb when applying TMC is that the ratio of statistical standard deviation to observed standard deviation should be less than 0.05. Removing these cases where TMC probably should not be used shows good agreement with GRS results. An important note is that GRS is able to calculate relative errors due to input uncertainties in cases where TMC is not.

4.1.3 Complex Case: ATR Full Core Model

To further verify the agreement of TMC and GRS, a more complex model was used. The ATR full core model requires many more histories to run than the UAM model. The

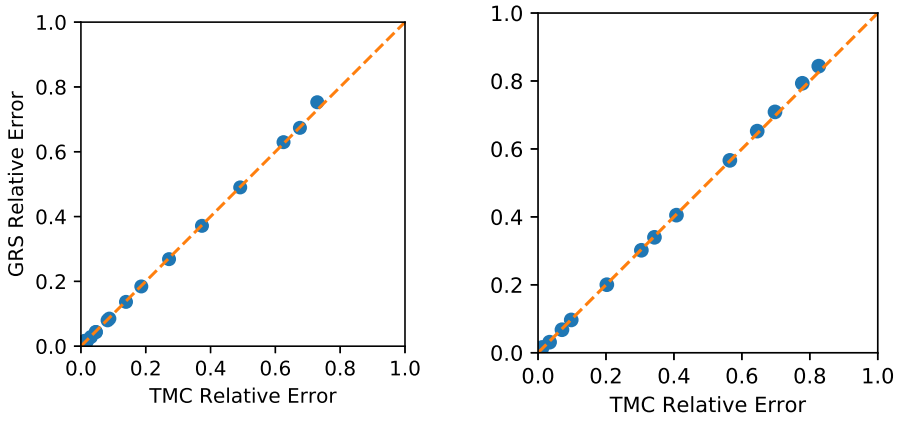

(a) 238-Group Flux

(b) Reaction Rates

Figure 4.2: TMC and GRS Relative Uncertainties

TMC results used 2.142e9 particles. This calculation takes about 4.6 hours per run on 120 cores. With the available hardware, the total run time was about 5 days to run 500 models. This runtime would increase if more fission products are tracked. The kcode parameters for the GRS runs is not known though the general rule of thumb for smaller models is to use the TMC particles divided by the total number of model runs, 500 in this case. This relatively small number of particle histories was expected to not be enough, especially for smaller regions of interest. A range of histories was ran using the GRS method with 595x less particles, 297.5x less particles, 148.75x less particles, 99.17x less particles, 74.38x less particles, 37.19x less particles, and 12.9x less particles than the TMC case. These are numbers for a both random seeds, each seed runs twice as less particles are reported. The well resolved 12.9x less particles case took about 8 hours to complete with each run using 24 cores (e.g., 5 GRS model runs could run during 1 TMC model run). Further increases in speed result from availability of nodes on the computer as well as it being easier to get single nodes (24 processors) than multiple nodes at once.

The flux, heating rates, and reaction rates in fuel elements and the flux in graphite

experiment samples of interest are investigated.

The data given for TMC cases does not follow the rule of thumb that statistical error should be 20x less than the observed variance of outputs. Instead, the condition was relaxed to 4x less than the observed variance. This was found to be a good assumption by checking that MC deviations were small. Small MC deviations with small output variances would lead to rejection of uncertainty predictions, but these values are the best values to use in this study due to low MC errors.

First the mean values for relevant tallies are compared in Fig. 4.3. If the mean values cannot be well predicted, predicting relative error well has no purpose. It can be seen that even when the least number of particles were ran using the GRS method, mean values agreed well with the resolved TMC case. Cases running with more particles have similar trends.

Calculating the energy dependent flux in fuel elements is important because it is used to create COUPLE burnup libraries for ORIGEN. It is also indicative of reaction rates within the fuel elements. Figure 4.4 shows the flux in the fuel can be well resolved even with cases running fewer particles. Most of the 238-group flux values have very small uncertainties ($< 3\%$) due to the varied U-235 cross section.

The energy dependent flux within graphite shown is very important in determining predicted DPA as well as spectral adjustments based on experiment flux wires. The predicted GRS relative errors (shown in Fig. 4.5) for the 148.75x case shows good agreement with the TMC values. It can be seen that the grouping of TMC values near the y-axis that TMC failed to predict the input errors because of relatively large MC standard deviations or large MC variance to observed variance ratios in the calculated values. This shows that the GRS method is able to predict relative output uncertainties where the TMC method fails.

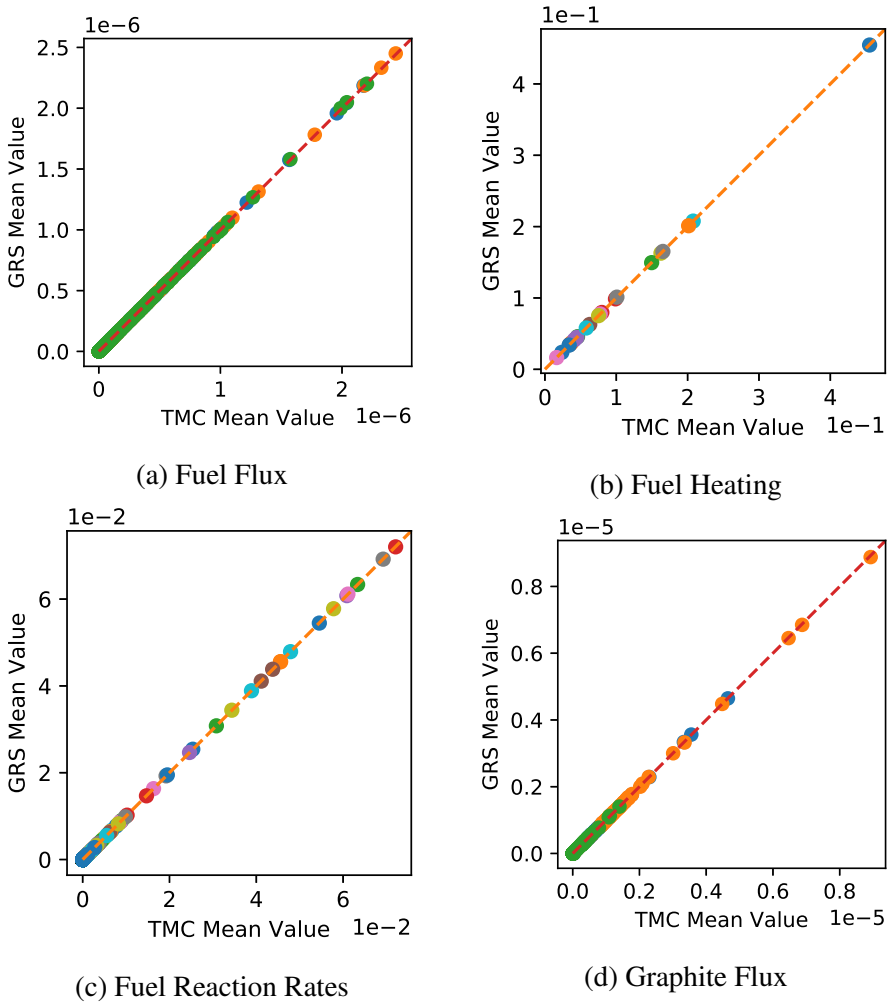

(a) Fuel Flux

(b) Fuel Heating

(c) Fuel Reaction Rates

(d) Graphite Flux

Figure 4.3: Comparing TMC and GRS Mean Values for ATR Fuel and AGC Experiment

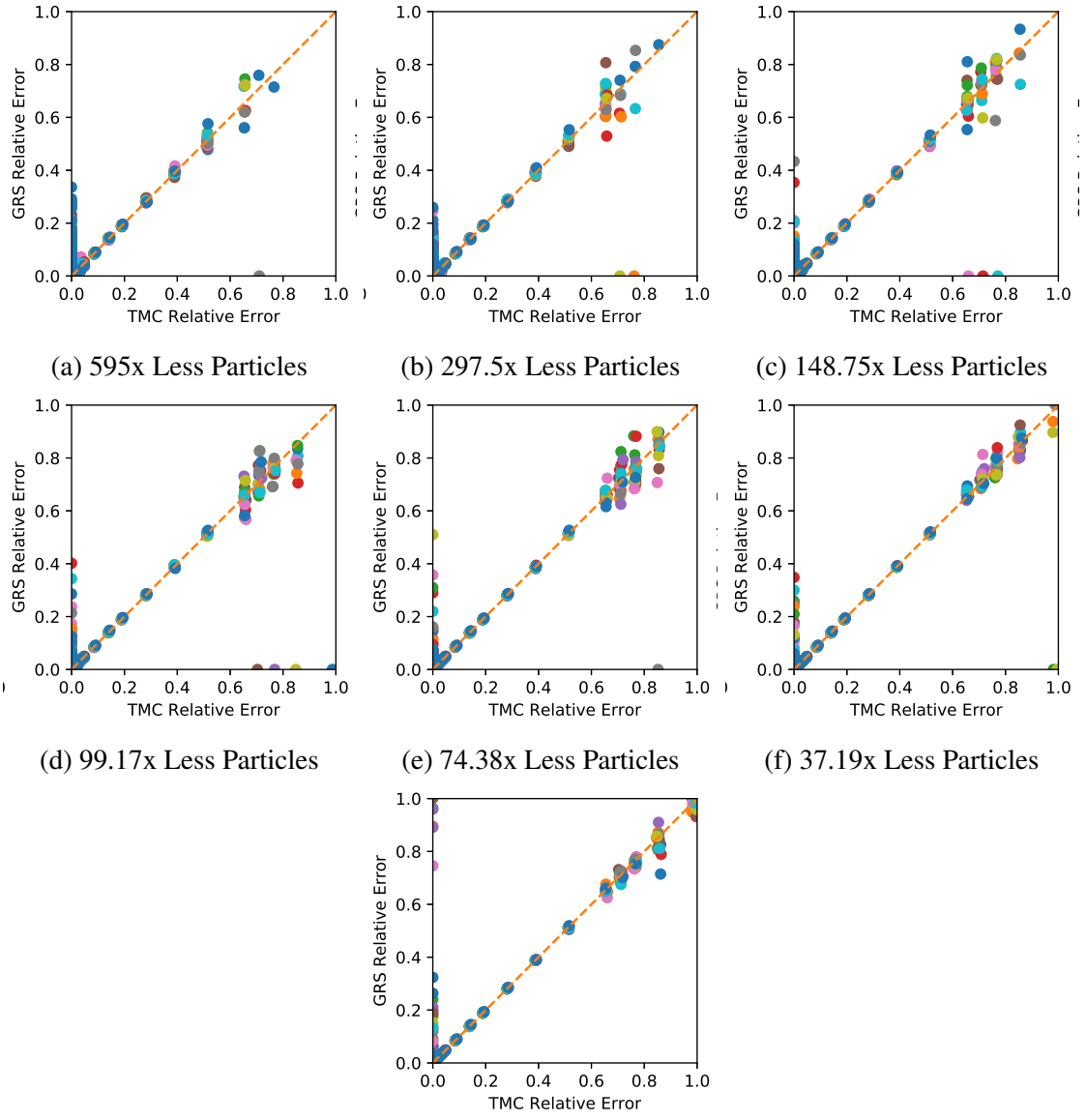

(a) 595x Less Particles

(b) 297.5x Less Particles

(c) 148.75x Less Particles

(d) 99.17x Less Particles

(e) 74.38x Less Particles

(f) 37.19x Less Particles

(g) 12.9x Less Particles

Figure 4.4: Various Runtimes Predicting Fuel Element Flux Using GRS

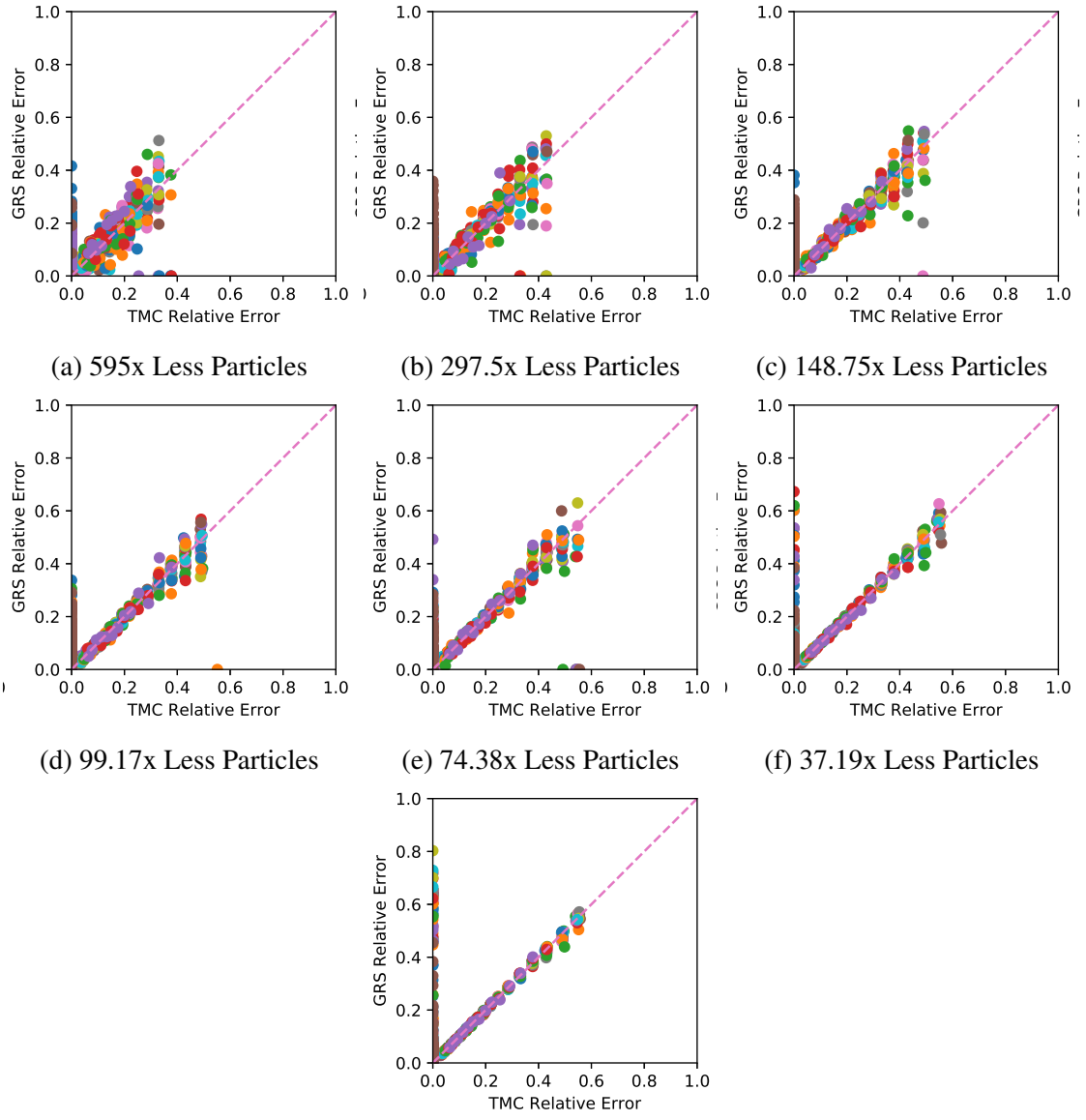

(a) 595x Less Particles

(b) 297.5x Less Particles

(c) 148.75x Less Particles

(d) 99.17x Less Particles

(e) 74.38x Less Particles

(f) 37.19x Less Particles

(g) 12.9x Less Particles

Figure 4.5: Various Runtimes Predicting Graphite Flux Using GRS

4.1.4 Refining Number of Particles

In all of the cases, the long running GRS (12.9x) agreed well with TMC when TMC was able to predict output uncertainties. This shows that the GRS method will converge to the TMC method when enough particles are transported. However, the point of the GRS method is to reduce runtime and a speedup of 12.9x less time is still impressive. Even more speedup is possible if uncertainty in global outputs like eigenvalue or larger spatial regions for flux results were used.

The TMC case was able to resolve the flux rather well for the whole fuel element. Figure 4.4 shows when considering the whole element, more particles (37.19x) must be ran to get good agreement with TMC. When comparing the reaction rates, the flux uncertainties play a little less of a role and GRS cases with 74.38x particles can be used. Furthermore, the cases with not as well predicted output error, or large output error are those nuclides with small reaction rates and thus will not contribute as much to propagated uncertainties. However, the flux is also important in burnup calculations so the 37.19x case should still be used. The center graphite flux compares well with TMC at the 74.38x case shown in Fig. 4.5.

The reaction rate tallies in Fig. 4.6 have similar conclusions as the fuel flux tallies. Increasing the particle histories from 37.19x to 12.9x does not reduce the calculated GRS input uncertainty so this may point to the TMC cases not being well resolved enough to predict the 'actual' input uncertainties.

Mean reaction rates are not easily predicted with fewer particles ran due to energy dependence of reactions. Figure 4.7 shows convergence of reaction rates with increased particles ran.

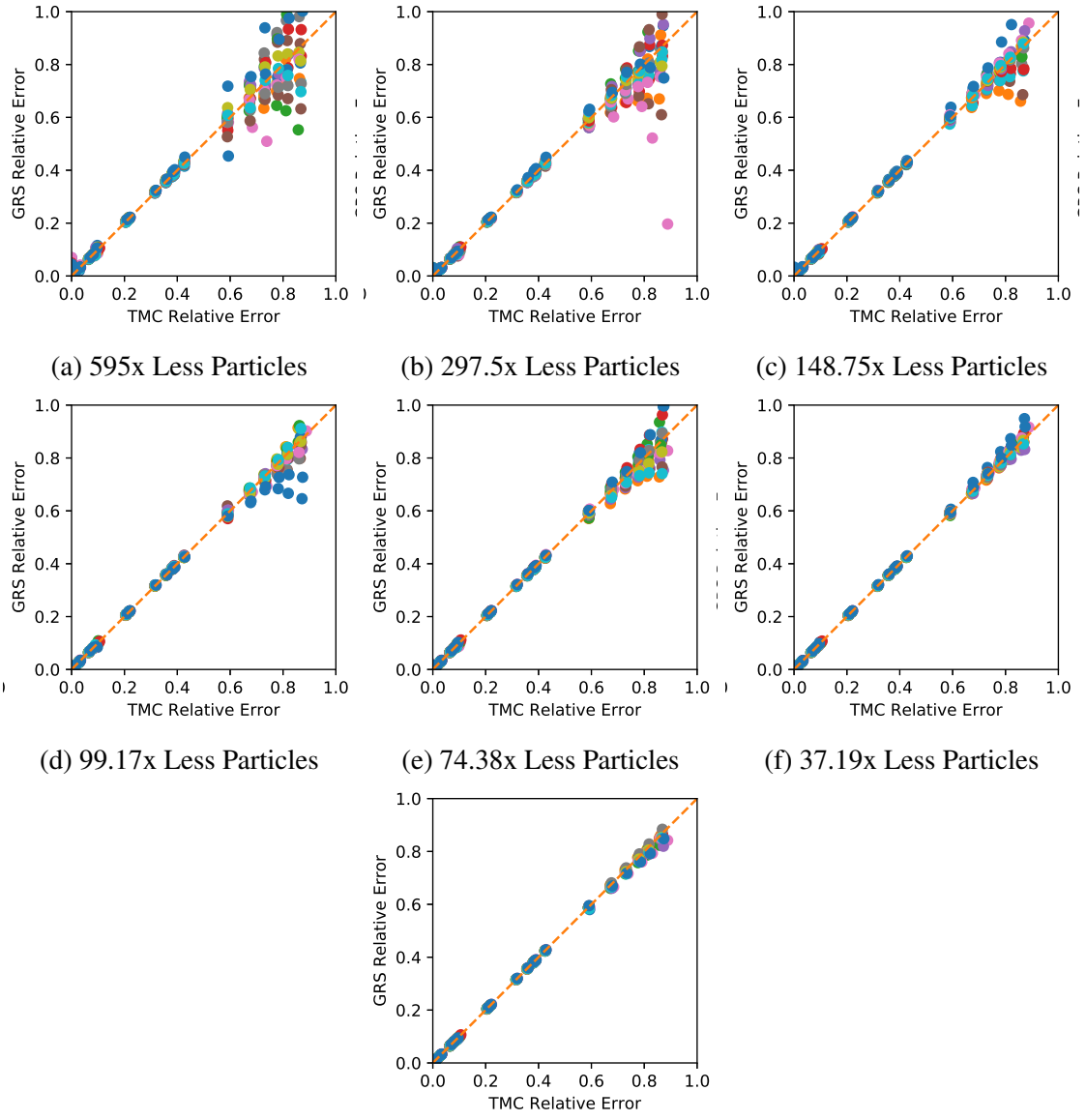

(a) 595x Less Particles

(b) 297.5x Less Particles

(c) 148.75x Less Particles

(d) 99.17x Less Particles

(e) 74.38x Less Particles

(f) 37.19x Less Particles

(g) 12.9x Less Particles

Figure 4.6: Various Runtimes Predicting Fuel Element Reaction Rate Using GRS

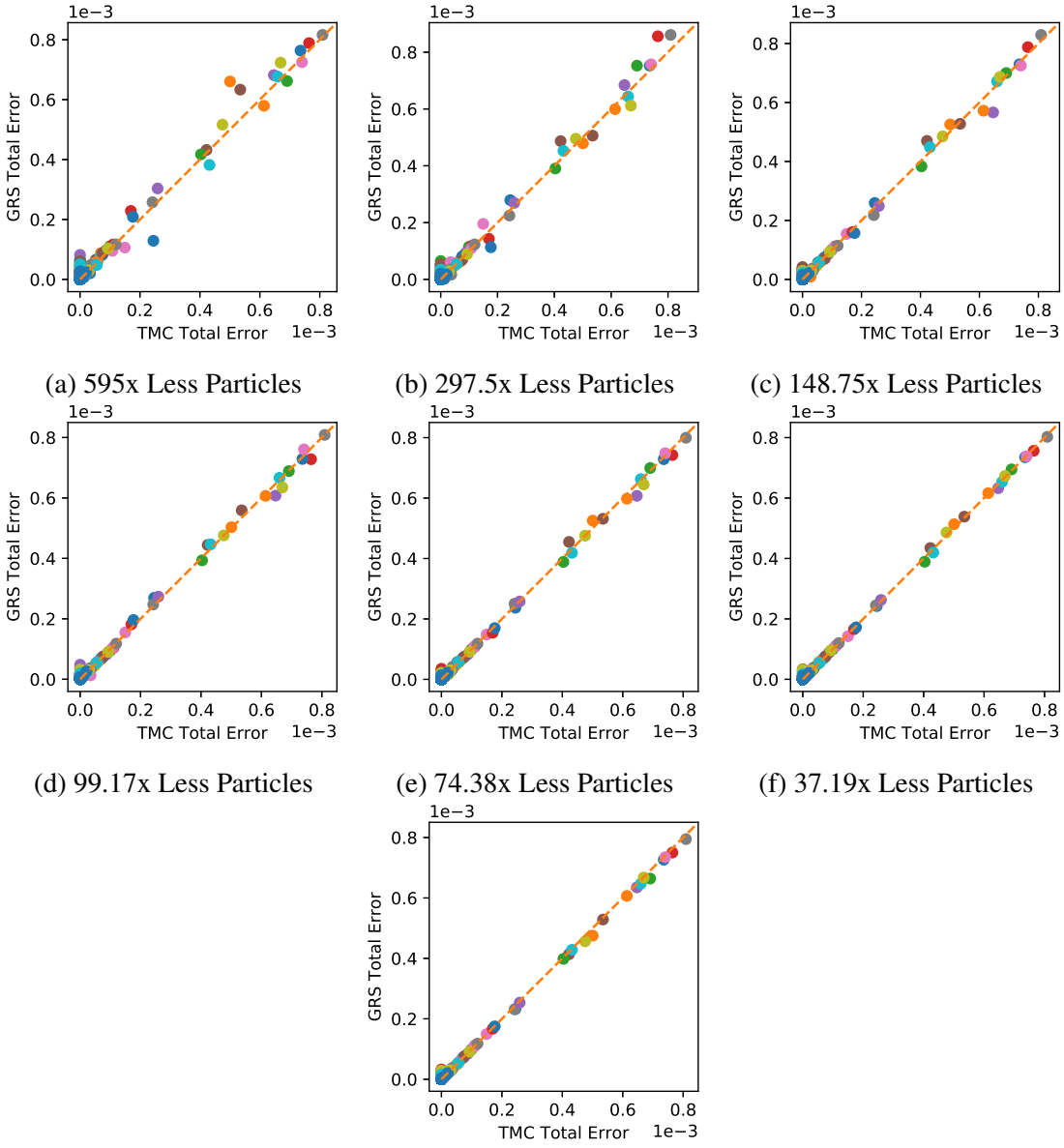

(a) 595x Less Particles

(b) 297.5x Less Particles

(c) 148.75x Less Particles

(d) 99.17x Less Particles

(e) 74.38x Less Particles

(f) 37.19x Less Particles

(g) 12.9x Less Particles

Figure 4.7: Mean Reaction Rate Values in ATR Fuel Element

4.1.5 Output uncertainty is well predicted

The relative error is a measure where small differences in small numbers divided by each other are compared. This can cause numerical difficulties due to the division. The total output uncertainties for reaction rates in a fuel element are shown in Fig 4.8 to show that the actual values are rather well predicted. Less values are also seen on the y-axis. Those values in the relative error plots were cases where the TMC failed to predict output uncertainties. This shows that those cases had small GRS uncertainties since those values are now near the origen. Similar conclusions can be made for the graphite flux.

4.1.6 Sample Size

The rule of thumb in literature is to use between 300-500 samples when performing FTMC or GRS. This is investigated further for the specific ATR model. Figures 4.9, 4.10 and 4.11 shows 300 samples is enough samples such that adding more samples does not decrease the variance of fuel flux, reaction rates, and graphite flux, particularly when considering all values are within 20% of the TMC predicted relative error.

4.1.7 Convergence Rates

Another representation of the sample size is to show how the predicted error changes when more observations are available. In general, it would be expected that predicted errors would converge upon a set of values. Figure 4.12 shows this case for three energy groups in a graphite axial slice. The results do not converge to a single value however they do converge to a range of values. This implies the uncertainty result should have error bars themselves, but the error bars will be small.

4.1.8 Comparing large relative error to observed error uncertainties

When performing TMC, at least 500 samples should be taken and values above a predicted statistical error to observed error ratio should be rejected. Removing all input uncer-

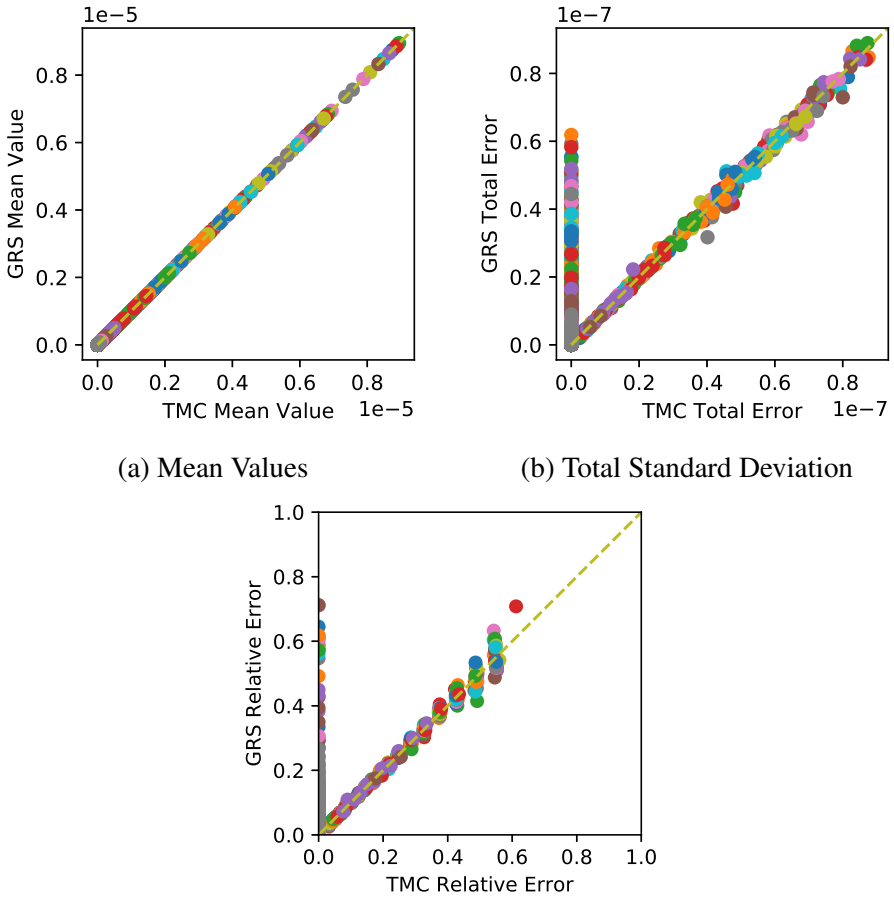

(a) Mean Values

(b) Total Standard Deviation

(c) Relative Error

Figure 4.8: Comparing Mean Values, Standard Deviations, and Relative Errors in ATR Fuel Element (37.19x less)

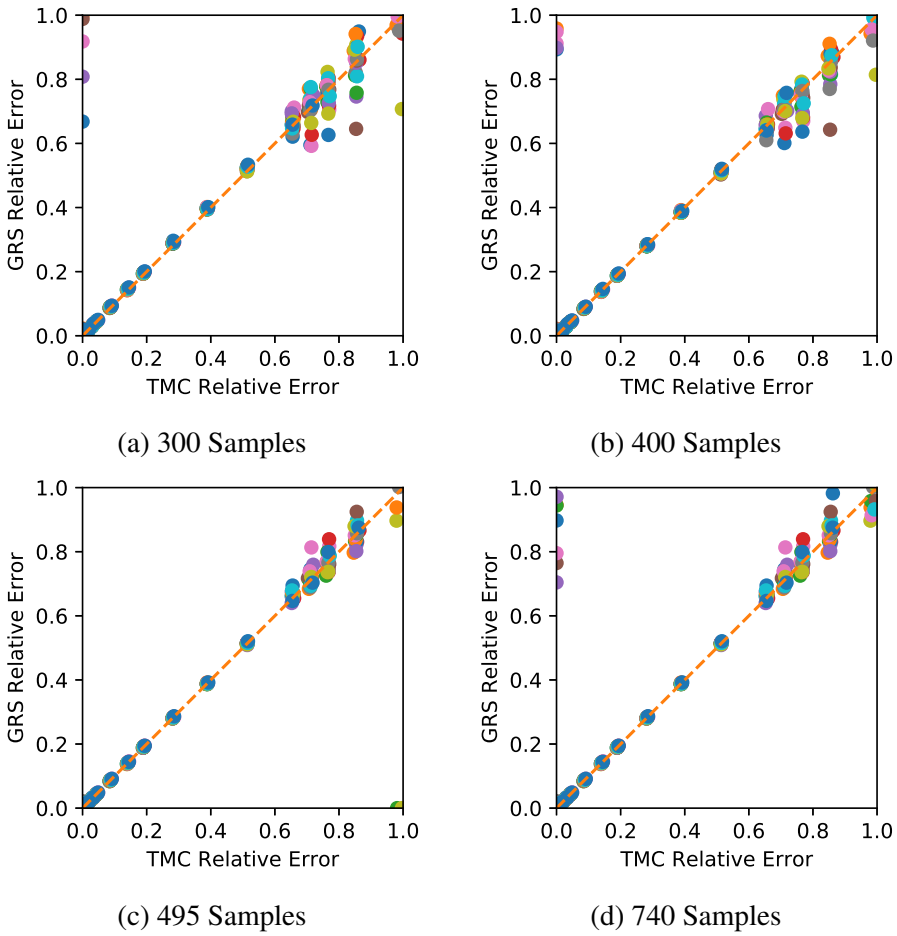

(a) 300 Samples

(b) 400 Samples

(c) 495 Samples

(d) 740 Samples

Figure 4.9: Varying Random Nuclear Data Sample Size for ATR Fuel Element Flux

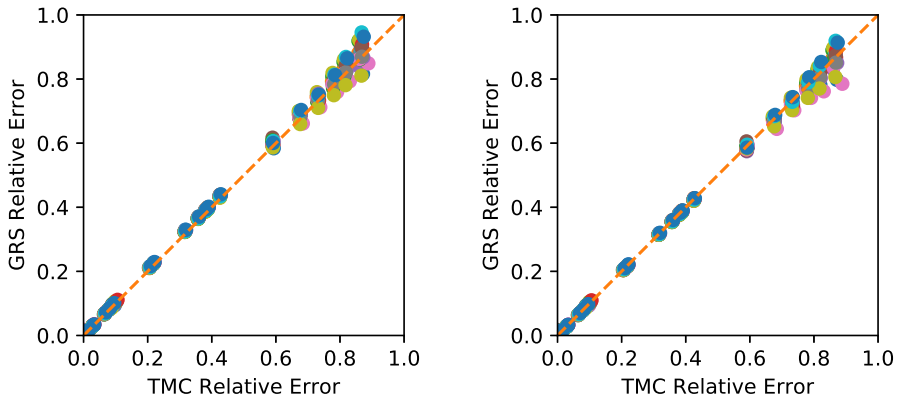

(a) 300 Samples

(b) 400 Samples

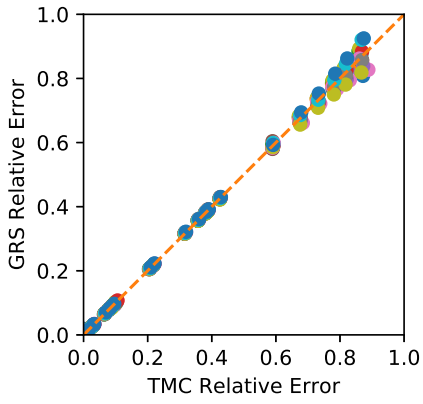

(c) 495 Samples

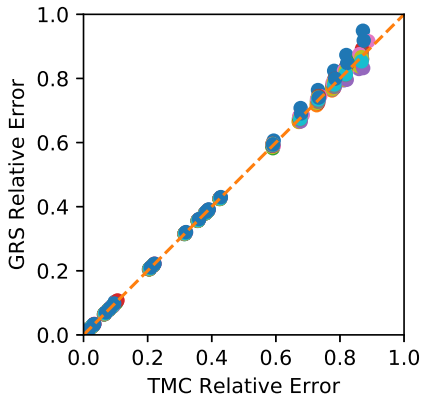

(d) 740 Samples

Figure 4.10: Varying Random Nuclear Data Sample Size for ATR Fuel Element Reaction Rate

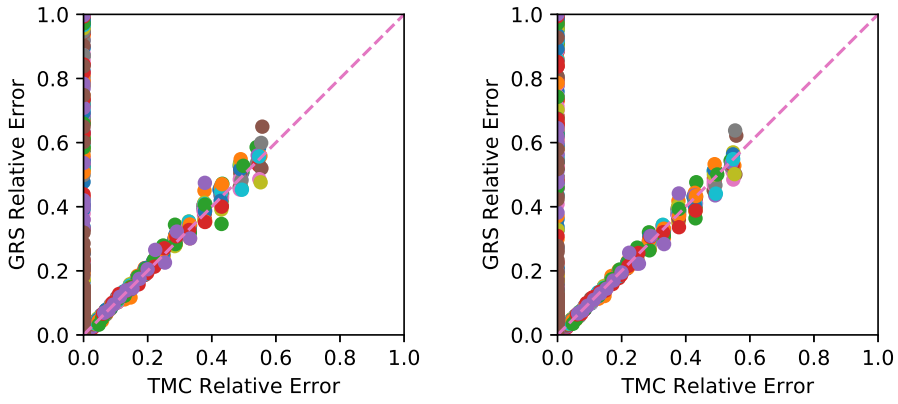

(a) 300 Samples

(b) 400 Samples

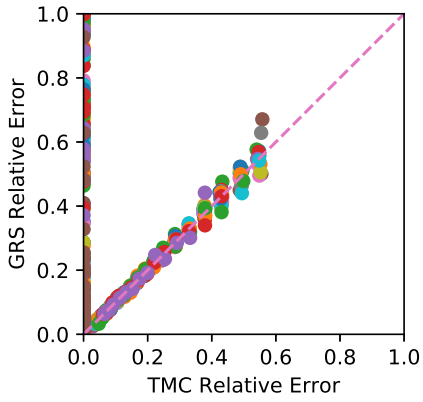

(c) 495 Samples

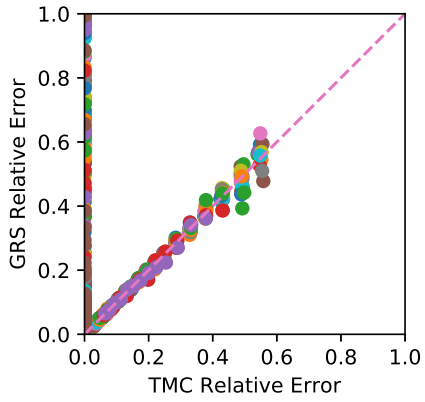

(d) 740 Samples

Figure 4.11: Varying Random Nuclear Data Sample Size for ATR Graphite Flux

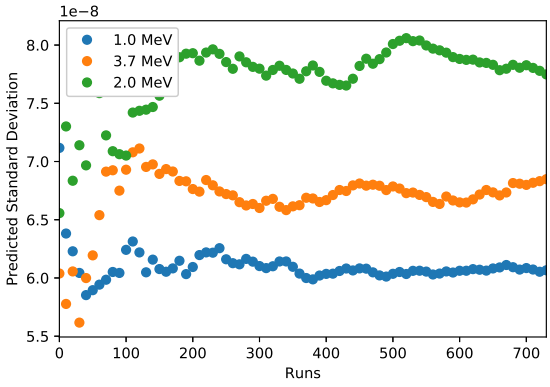

Figure 4.12: Convergence of Three Energy Bins within Graphite

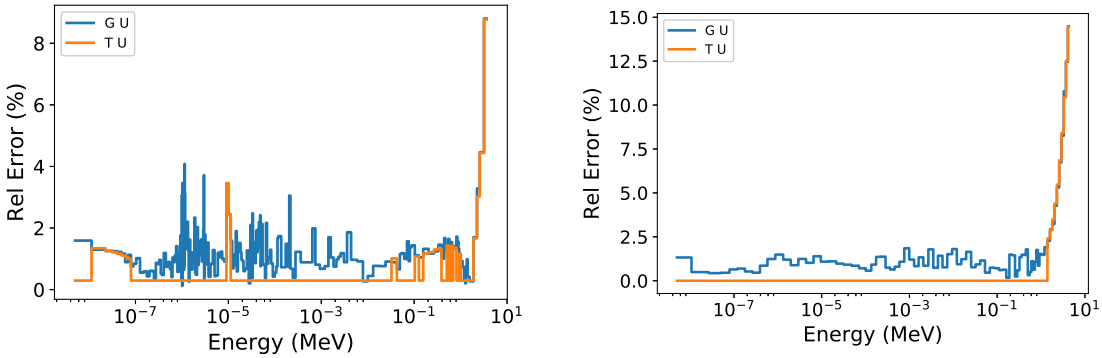

(a) Fuel

(b) Graphite

Figure 4.13: Relative Error in Flux Comparisons

tainty calculations that have $\sigma_{mc}/\sigma_{obs} > 0.20$ creates uncertainties with higher confidence, however many uncertainties must be set to zero since they are rejected. Figure 4.13a shows that when TMC is able to predict output uncertainty, GRS agrees well with it. A similar spectrum is shown for GRS cases in Fig. 4.13b. In general, even the lower number of particles ran cases predict some deviations. Uncertainties do not strictly converge onto a value, though they are very close to each other.

4.2 Coupled MCNP / ORIGEN Time-Stepping Verification

The burnup propagation described in Sec. 3.1.4 allows for propagation of uncertainties through time by providing coupling between the neutronics solver and a burnup equation solver. The implementation requires a lot of data processing, input generation, and error checking. For each burned material in each sampled MCNP input:

- 238-group flux calculations need to be added in the MCNP input
- Dummy materials must be added for each nuclide in materials burned such that reaction rates can be calculated using the dummy materials in the MCNP input.
- All calculated cross-sections must be provided to COUPLE along with 238-group

fluxes.

- All material vectors must be provided to ORIGEN with a linking of the COUPLE library generated.
- For sub-stepping, relevant cross-sections and fluxes must be interpolated.
- For predictor steps, relevant cross-sections and fluxes must be averaged.
- All ORIGEN outputs must be read such that the next steps MCNP files can be generated to continue time-stepping.

This is not a trivial task such that verification of the implementation is required. The time-stepping in Serpent was used to verify the mcACE version. MCNP and Serpent models of the UAM pin-cell described in Sec. 4.1.2 was prepared. A full cycle depletion was ran using 5 sub-steps and LE time-stepping. Figure 4.14 shows the eigenvalue during burnup for mcAE and Serpent along with the differences in PCM between the two solutions. Serpent and MCNP models results tend to be slightly different due to different numerical solvers. Serpent options were added to include unresolved resonance probability table sampling for U. Even for the fresh fuel case there was a 25 PCM difference between the Serpent and MCNP. The overall solutions are still expected to be similar through burnup if mcACE implemented burnup calculations correctly. It can be seen that the two core-lifetime predictions are very similar, generally within 250 PCM or lower of one-another, such that the LE time-stepper can be considered verified.

4.3 Sensitivity Verification

The EASI method described in Sec. 3.3.2 and the bootstrap confidence intervals are verified by comparing to similar studies in literature where analytic solutions or other method's predictions are present. An important feature to test is the ability to handle

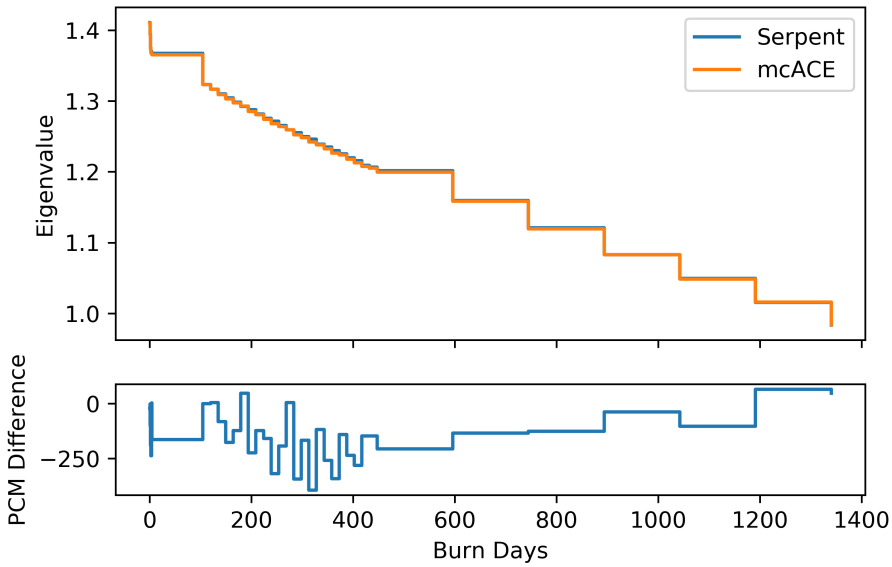

Figure 4.14: Verifying Time-Stepper using UAM Pincell to Compare mcACE and Serpent

correlated inputs, which is not well studied in literature. Two models are tested here, one with analytic solution and another without, both with correlated inputs. Results from literature [52] are compared to, though there is no reference for the confidence interval approach.

4.3.1 Portfolio Model

Mathematically, the portfolio model is,

$$f(x_1, x_2, x_3, x_4) = x_1x_3 + x_2x_4,$$

where the x_i's are normally distributed with mean, and covariance matrix as

$$\begin{bmatrix} \sigma_1^2 & \sigma_{12} & 0 & 0 \\ \sigma_{21} & \sigma_2^2 & 0 & 0 \\ 0 & 0 & \sigma_3^2 & \sigma_{34} \\ 0 & 0 & \sigma_{43} & \sigma_4^2 \end{bmatrix},$$

where each σ_i is the standard deviation and σij is the cross-correlation. First order sensitivties can be calculated as,

$$\begin{aligned} S_1 &= \frac{\sigma_1^2 \left(\mu_3 + \mu_4 \frac{\sigma_{12}}{\sigma_1 \sigma_2} \frac{\sigma_2}{\sigma_1}\right)^2}{D}, \\ S_2 &= \frac{\sigma_2^2 \left(\mu_4 + \mu_3 \frac{\sigma_{12}}{\sigma_1 \sigma_2} \frac{\sigma_2}{\sigma_1}\right)^2}{D}, \\ S_3 &= 0, \\ S_4 &= 0, \\ D &= \sigma_1^2 \left(\sigma_3^2 + \mu_3^2\right) + \sigma_2^2 \left(\sigma_4^2 + \mu_4^2\right) + 2\frac{\sigma_{12}}{\sigma_1 \sigma_2} \left(\frac{\sigma_{34}}{\sigma_3 \sigma_4} + \mu_3 \mu_4\right). \end{aligned}$$

Table 4.1 shows input parameters used in this verification. 5000 samples were taken using correlated normal sampling, and 500 bootstrap samples were taken to estimate 95% confidence intervals. Figure 4.15 shows good agreement between EASI and analytic results along with confident intervals. Rerunning the whole analysis shows sometimes the calculated value is not as close to the actual value as shown here, though it is within the confidence interval.

Parameter	Value
μ_1	0
μ_2	0
μ_3	250
μ_4	400
σ_1	4
σ_2	2
σ_3	200
σ_4	300
σ_{12}	2.4
σ_{34}	-1.8e4

Table 4.1: Parameters Used in Portfolio Verification Problem

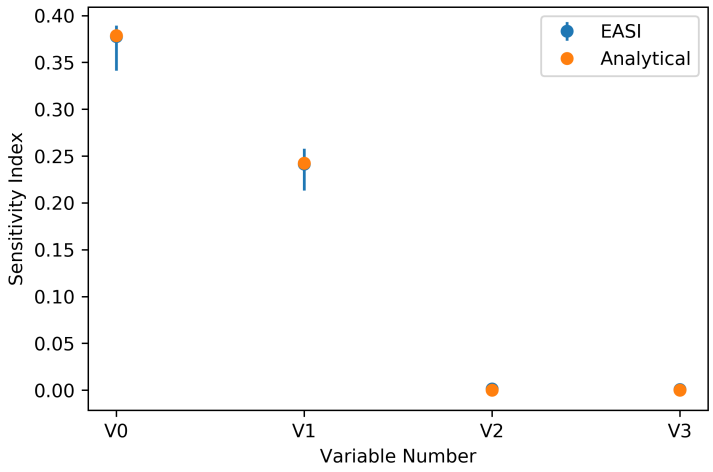

Figure 4.15: Portfolio Model with Correlated Inputs

4.3.2 Ishigami Function

The Ishigami Function is a typical function used for testing UQ/SA methods because the function is nonlinear and non-monotonic. It is defined to be,

$$f(x) = \sin(x_1) + a\sin^2(x_2) + bx_3^4\sin(x_1), \tag{4.-7}$$

where a, b are constants, originally and in this work as $a = 7, b = 0.1$, and x_1, x_2, and x_3 are uniformly sampled from $[-\pi, \pi]$. The inputs are generally left uncorrelated to perform global sensitivity analysis without correlations, however this example adds correlations to test EASI implementation.

The inputs to the Ishigami function are made to have a correlation between the 1st and 3rd variables, with the other correlation combinations assumed to be uncorrelated. The correlation is varied from -0.9 to 0.9. Figure 4.16 shows results of simulating the Ishigami function and compares results to digitized literature results [52]. The first order sensitivity indices agree well for all values of correlations within 95% confidence intervals. This result allows for some interpretation on the correlated sensitivity calculated as described in Sec. 3.3.1. This example agrees with the the Kucherenko first order sensitivity coefficient. This means highly correlated inputs will tend to have similar first order sensitivities.

4.3.3 UAM Pincell

The UAM Pincell described in Sec. 4.1.2 was simulated with randomly varied ^{238}U absorption cross-sections using the SCALE 252 group structure. Eigenvalue sensitivities with respect to the varied cross-sections were determined with the EASI method. These are first order (correlated) sensitivities sensitivities as opposed to local sensitivities, which is what MCNP-IFP calculates. These local sensitivities do not agree with first order sensitivities as described previously.

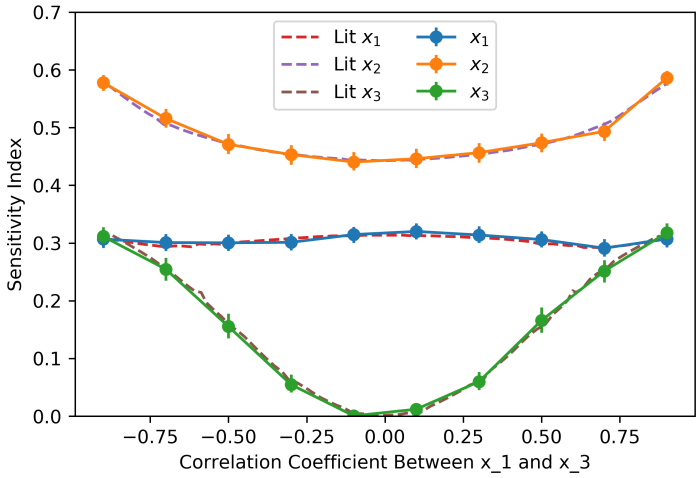

Figure 4.16: Ishigami Model with Correlated Inputs Compared with Kucherenko Sensitivity

Figure 4.17 shows the EASI sensitivity estimates of the UAM pin-cell eigenvalue with respect to uncertain cross-sections. These results were compared to literature results [63] to determine the correctness of the first order Sobol sensitivity indices for eigenvalues given correlated inputs. The results agreed well even though different neutronics software and energy group structures were used. This agreement gives further confidence on the applicability of EASI on correlated inputs to determine first order sensitivity indices.

4.4 ASAPy Nuclear Data Sampling

4.4.1 Visual Comparison of Sampled Correlations

In order to verify sampling procedures, plots are made and compared with original data if applicable. Figure 4.18 shows correlated log-normal samples of ^{235}U scattering cross-section. Figure 4.18a shows the base cross-section with relative error, Fig. 4.18b shows a few samples that are used in transport calculations, and Fig. 4.18c compares the ENDF correlation with the correlation of 500 samples generated.

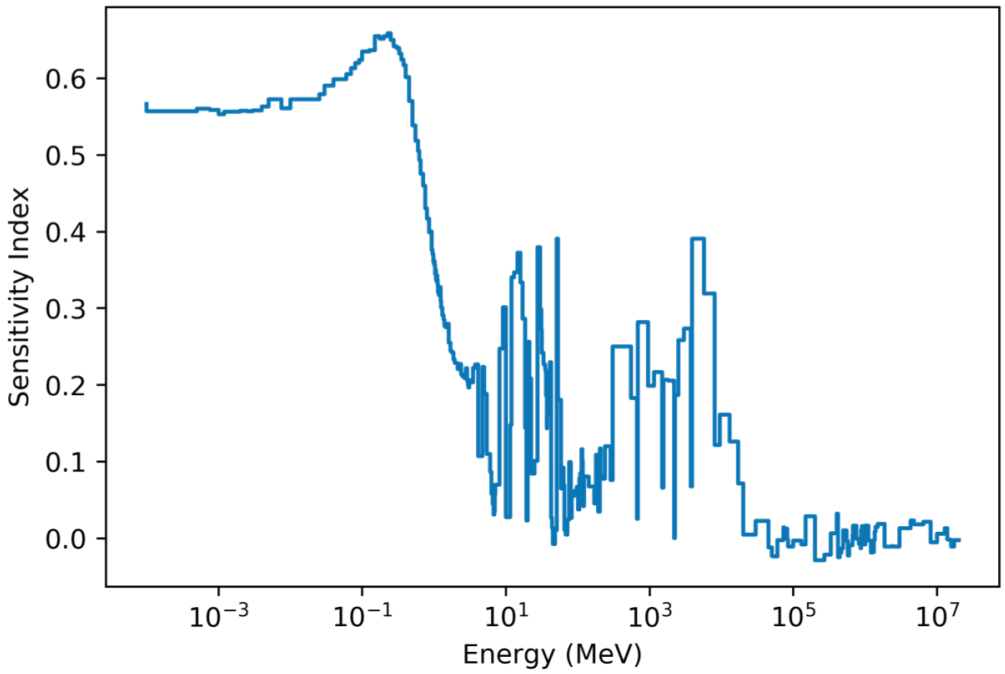

Figure 4.17: EASI Sensitivity Results for UAM Pincell

4.4.2 Godiva Eigenvalue

The Godiva core is a well known benchmark model / experimental validation core. It is a spherical mass of HEU that has a well quantified uranium material vector and critical dimensions. It's also a simple reactor core to analyze due to it's fast spectrum. The MCNP-IFP method was used to calculate sensitivities for several reaction MTs. Covariances were provided by ASAPy to calculate the total uncertainty on eigenvalue from reaction rates. The mcACE UQ process using TMC and ASAPy generated cross-sections was performed using 1000 runs. Table 4.2 shows good agreement for all studied reaction MTs, all values agree within uncertainty. MCNP-IFP uncertainty was not propagated. This result shows that the TMC/GRS method agrees well with the IFP theory in terms of eigenvalue uncertainties.

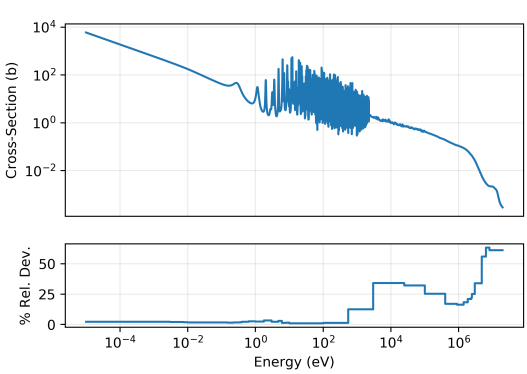

(a) Base Cross-Section

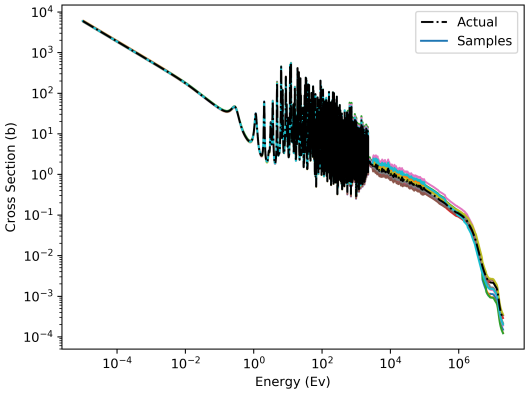

(b) A few sampled cross-sections

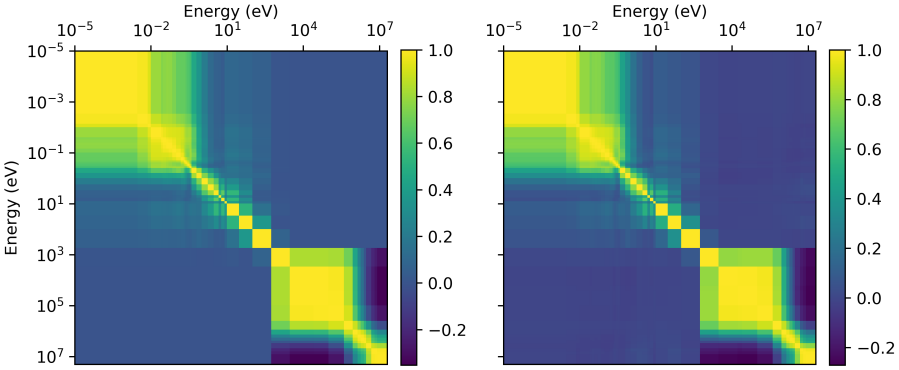

(c) Sampled Correlation

Figure 4.18: Samples of ^{235}U Scattering Cross-section (MT=102)

Correlation	Reaction	Unc. (pcm)	95% σ	MCNP-IFP
Uncorrelated	(n,γ)	479.4	13.3	482.3
	(n,f) + (n,γ)	493.5	13.3	-
	(n,f)	121.2	3.3	119.8
	$\bar{\nu}$	221.1	5.5	218.5
	Fission χ	167.4	5.0	169.3
Correlated	(n,γ)	838.8	24.4	848.9
	(n,f) + (n,γ)	883.3	25.1	-
	(n,f)	269.5	6.8	269.4
	$\bar{\nu}$	546.0	13.9	544.1
	Fission χ	269.0	12.7	276.2

Table 4.2: Comparing Godiva Uncertainties using ASAPy to MCNP-IFP

5. APPLICATION TO NUCLEAR THERMAL PROPULSION REACTOR DESIGNS

Important outputs to consider when designing NTP reactors are eigenvalue, power profile, and reaction rates. Eigenvalue uncertainties affect the design through the ability to become critical and the ability to determine exact critical control drum positions. NTP reactors coolant flow is tailored to expected heat distributions which are different depending on drum position. Power profile uncertainties directly affect fuel and moderator temperatures which impact performance via uncertainties in coolant outlet temperature. Reaction rate uncertainties can directly impact core lifetime and operational characteristics like drum movement. All of these uncertainties are calculated for SNRE and SCCTE.

5.1 SNRE: A Carbide Heritage Design

The SNRE was described in Sec. 2.6.3. The sources of uncertainty considered in this section are ^{235}U cross-sections and $ZrH_{1.6}$ density. The SNRE is an HEU reactor so the fuel is mostly ^{235}U, to enable a compact system moderating material is included which is the ZrH. This analysis showcases the ability to perform TMC and GRS statistics for eigenvalue, spectrum and heating rate results given nuclear data and engineering manufacturing uncertainties.

5.1.1 Further Verification for a Harder Spectrum

The TMC and GRS verification study from Sec. 4.1.1 was applied to the ATR which is a thermal reactor. SNRE unit-cell is much harder spectrum reactor than ATR, in theory the TMC/GRS methods will apply well to the SNRE and all previous results are applicable. To further motivate this, the fuel spectrum in the SNRE unit-cell was calculating using GRS and TMC. Figure 5.1 shows these results and that TMC and GRS agree well in this unit-cell and are applicable.

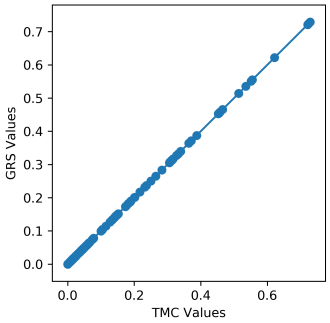

(a) Values

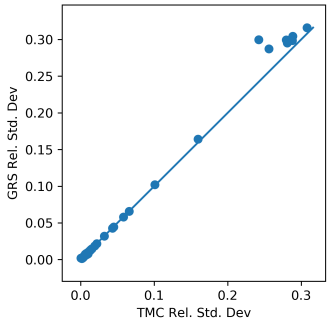

(b) Relative Errors

Figure 5.1: TMC and GRS Relative Uncertainties Compared in SNRE unit-cell

Correlation	Reaction	Unc. (pcm)	95% σ	MCNP-IFP
Uncorrelated	(n,γ)	349	9	351
	(n,f) + (n,γ)	355	9	-
	(n,f)	63	1	64
	$\bar{\nu}$	*363*	9	152
	Fission χ	12	1	12
Correlated	(n,γ)	671	20	677
	(n,f) + (n,γ)	677	20	-
	(n,f)	86	2	87
	$\bar{\nu}$	585	15	591
	Fission χ	20	2	22
Density 5%	Fuel	11	2	-
	ZrH	140	5	-

Table 5.1: Uncertainties of SNRE Unit-Cell From Various Input Sources

5.1.2 Unit-cell Uncertainties from Various Inputs

Eigenvalue are important in initial core designs and criticality safety. Enough margin must be kept to to account for engineering uncertainties as well as future design decisions. Often arbitrarily high margins are made because failure to predict eigenvalue correctly can invalidate an otherwise well performing core. Table 5.1 shows results to a similar study as Sec. 4.4.2, where the SNRE unit-cell is compared with MCNP-IFP method. Fuel and moderator density effects are also added. Again, similar results from the IFP method and the TMC/ASAPy/mcACE method are shown. An exception is the uncorrelated $\bar{\nu}$ results where the IFP method predicts about twice as small uncertainty as TMC/ASAPy/mcACE. This inconsistency will be neglected because only the correlated results are actually important and those agree well. A probable cause to this difference is a dependence on the group structure for $\bar{\nu}$ when sampling is uncorrelated and the reactor has a fast spectrum. The IFP method cannot create sensitivities for multiple cross-sections at the same time, however assuming independence, the two results could be combined. The MCNP-IFP method does not have any ability to perform density perturbations. Other MCNP methods such as the kpert can address this but these were not investigated further. These results show the TMC method is well applicable to the cores of interest.

During core design phases, the flux spectrum is important to calculate to determine peripheral and structure core materials. For example, high thermal absorbers are acceptable if the spectrum is sufficiently fast and neutron poisons to control reactivity should be designed to the spectrum calculated. Figure 5.2 shows uncertainty in reactor flux using the SNRE unit-cell due to various cross-section uncertainties. MCNP-IFP currently cannot perform this analysis so there is no comparison to be made. It can be seen that absorption and fission χ cause large uncertainties in the spectrum. Interestingly, fuel density does not have much effect on the spectrum however moderator density can cause large uncertain-

ties. The individual cross-section uncertainties when all applied at the same time show a sum of uncertainties effect such that there is not a large covariance between uncertain parameters. This also shows that typical perturbation theory results are valid for this unit cell since the inputs do not interact via correlations.

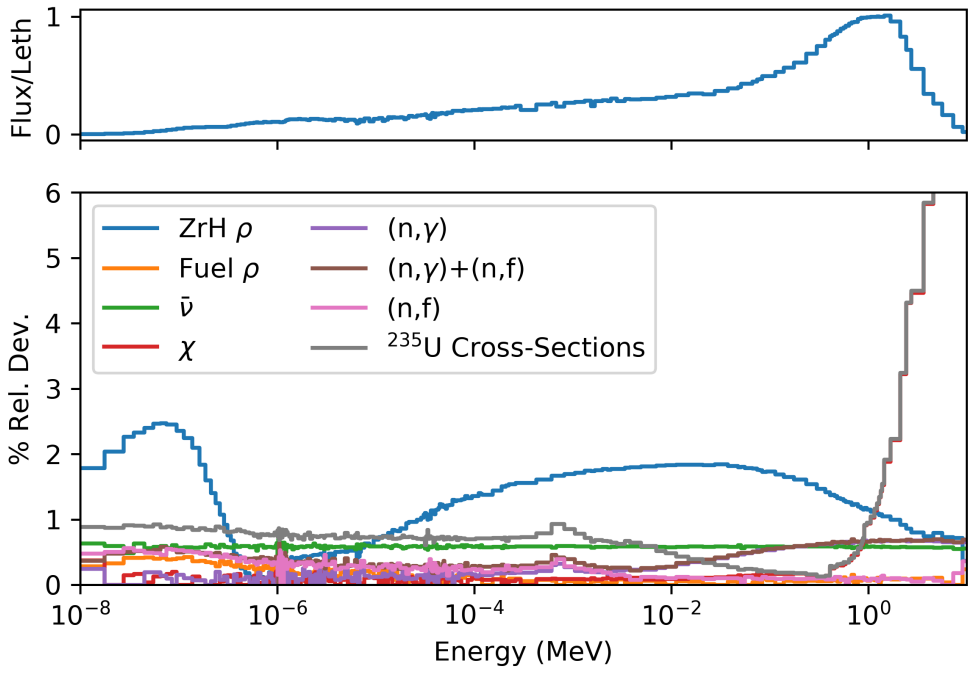

Figure 5.2: SNRE Unit-Cell Spectrum Uncertainties from Various Inputs

5.1.3 Full Core Uncertainties from Various Inputs

Unit-cell results are a good starting point for reactor analysis, however full core results are needed to ensure power and core size requirements can be met. Unit-cell results can also be misleading, particularly when reflectors are present and cores have high leakage. The full SNRE core was modeled in MCNP [64] and mcACE was used to perturb cross-

Reaction	Unc. (pcm)	95% σ	Full Core	95% σ
(n,γ)	671	20	515	17
(n,f) + (n,γ)	677	20	521	18
(n,f)	86	2	102	6
$\bar{\nu}$	585	15	596	19
Fission χ	20	2	**426**	13

Table 5.2: SNRE unit-cell vs Full Core

sections to compare differences between unit-cell and full core calculations. Table 5.2 shows eigenvalue uncertainties from several cross-sections. Cross-section samples were all fully correlated. It can be seen that full core results tend to have similar uncertainties as the unit-cell results, except in the case of Fission χ, where the full core result is a factor of 21 larger than the unit-cell result. Fission χ describes the energy distribution of neutrons born from fission. The increase in eigenvalue uncertainty from fission χ is likely from core-edge effects where the neutron spectrum is much different than the unit-cell spectrum.

The TMC and GRS methods can be used to predict heating spectrum uncertainties as well as eigenvalue uncertainties. Heating spectrum results with TMC and GRS in an axial layer of the SNRE is shown in Fig. 5.3. It can be seen that the faster running (16x faster) GRS predicts the uncertainties well. Figure 5.4 shows heating spectrum uncertainties of all axial layers of the SNRE. Notably, all the layers have similar relative uncertainties. This is because the spectrum is similar through the axial height in the modeled case. It implies a computational savings could be made by combining all layers into one tally for energy results then adjusting magnitudes with another axial dependent tally that only calculates flux magnitudes.

Reactor flux spectrums are used to calculate reaction rates, particularly for heat source calculations and burn-up. Figure 5.5 shows uncertainties in axial power distributions in

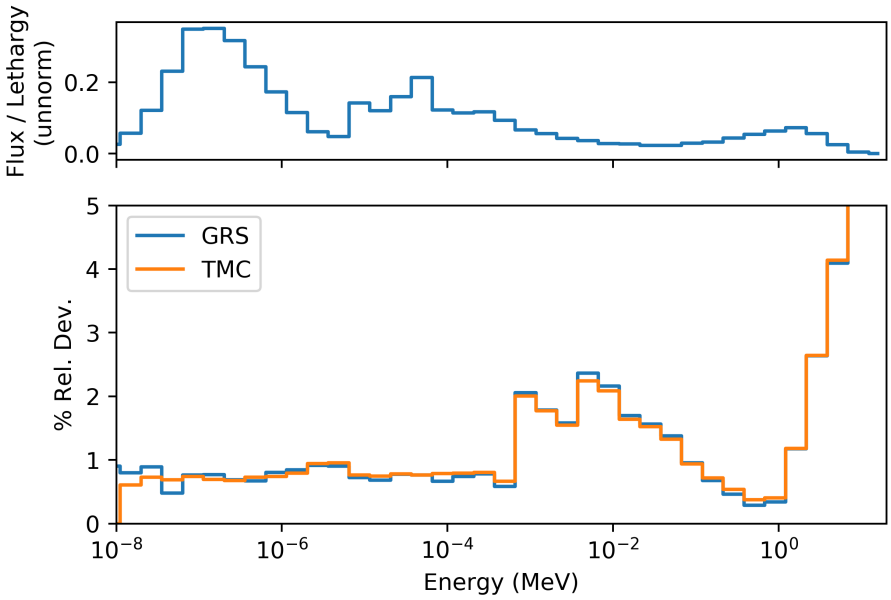

Figure 5.3: Full SNRE Heating Spectrum with TMC and GRS

the full core due to absorption and fission only, fission χ only, and the previous with $\bar{\nu}$. The total predicted uncertainty at the bottom of the core is less than the uncertainty from χ alone implying correlated effects (error-canceling) if not all uncertainties are taken into account at once. The power distributions calculated could be used in system thermal analysis to propagate uncertainties to the thermal domain. An example of this will be discussed in Sec. 5.2.11.

TMC with boot-strap estimate of statistics was also performed to best check if GRS and TMC are equal within statistical uncertainty. Figure 5.6 shows good agreement between the two methods. The TMC run took had 15 times as many particles as the GRS run and thus would take 15 times longer to run.

5.2 SCCTE: A Tungsten Cermet Design

SCCTE was described in Sec. 2.6.4. It differs from SNRE in that it has a slightly softer neutron spectrum, a different geometrical arrangement of fuel and moderator, different

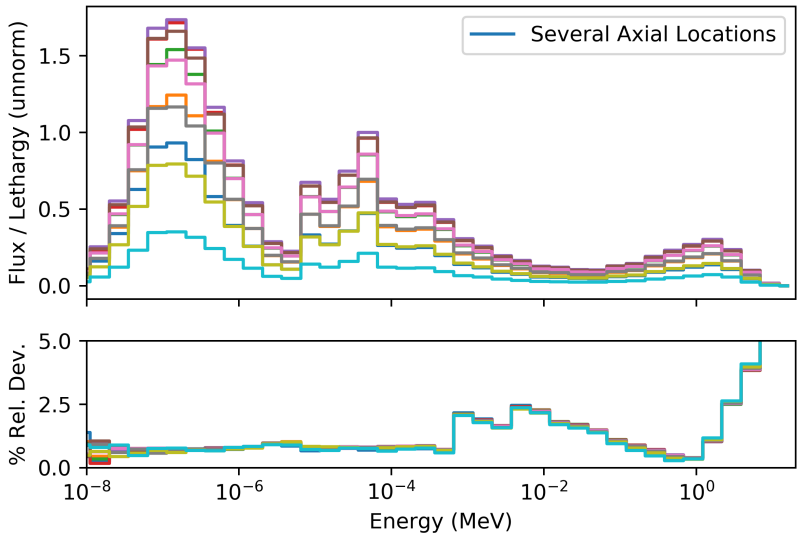

Figure 5.4: All SNRE Axial Levels Heating Spectrums Compared

fuel type, and SCCTE uses LEU. The spectra of the two reactors in the ZrH material are compared in Fig. 5.7. The SNRE unit-cell, even with moderating material has an epithermal spectrum, whereas SCCTE is more thermal. The full core spectra are slightly more thermal due to small core size and reflectors. The sources of uncertainty considered in this core are ^{184}W and ^{235}U cross-section uncertainties. ^{184}W enables the reactor to become critical by removing highly absorbing naturally occurring W isotopes from the system. This analysis showcases the ability to perform GRS statistics for eigenvalue, spectrum and heating rate results given nuclear data in a regime often not explored: high assay LEU and non-U enriched isotopes.

5.2.1 GRS vs TMC For SCCTE

GRS and TMC were shown to agree well in Sec. 4.1.1. However those runs did not use the ASAPy generated cross-sections so the study was re-ran using the SCCTE unit-cell. Figure 5.8 shows the convergence rates when performing GRS and TMC using randomly

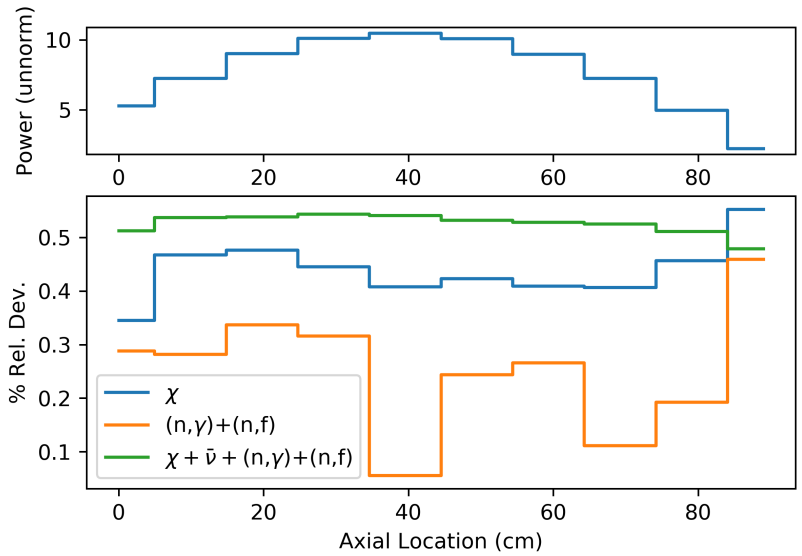

Figure 5.5: Heating Rate Uncertainties from Nuclear Data Sources

varied ^{235}U cross-sections. It can be seen that both methods converge to a similar value with a similar number of runs.

5.2.2 Group Structure Dependence

When performing any multi-group based analysis, even when just projecting continuous solutions onto a grouped domain, there is a dependence on results based on group structure used. There is no one group structure that is good for all reactor types, and similarly no one good structure for all NTP. For instance, the SNRE unit-cell has a faster spectrum than SCCTE. The full SNRE and SCCTE are slightly more thermal than their unit-cells. Four group structures (44, 56, 238, 252) are compared for 4 reaction types (fission, absorption, $\bar{\nu}$, χ) in Fig. 5.9. The results were made using MCNP-IFP. Sensitivities follow similar patterns, though resonances can clearly be seen as more groups are used. The dependence of uncertainties on group structure can be seen by convolving the results with calculated covariance matrices in Tab. 5.3. The largest discrepancy is a 10% differ-

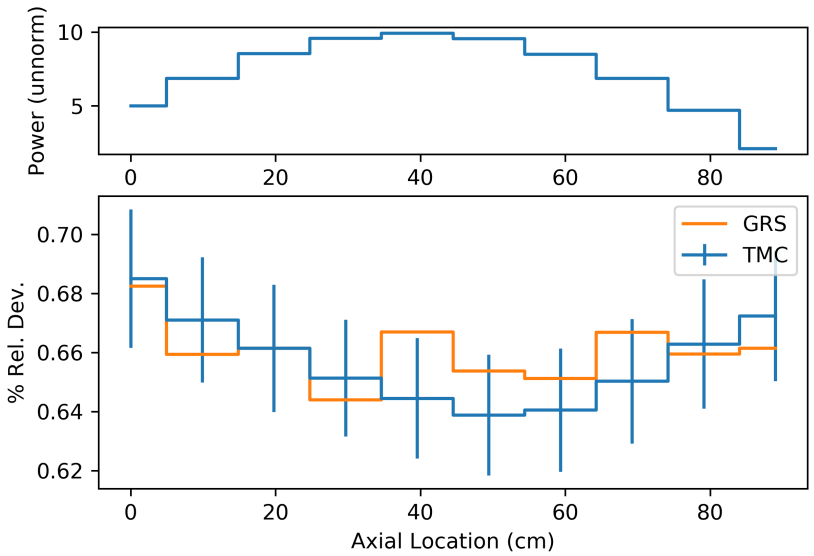

Figure 5.6: SNRE Axial Power Profile with TMC and GRS

ence between using 44 groups and 252 groups when analyzing the correlated results. The uncorrelated results show larger differences, however the uncorrelated uncertainty should not be used in uncertainty quantification.

Table 5.4 shows a study using ASAPy generated cross-sections with 44 and 252 group structures. The two group structures showed similar trends as the MCNP-IFP results. It is still recommended to use a group structure that well captures the problems spectrum.

5.2.3 Temperature Dependence

Table 5.5 shows the eigenvalue uncertainties fow two different temperatures. It can be seen that uncertainty does not change between temperatures so neglecting temperature variations for uncertainty analysis is a good approximation. However mean values will change due to typical temperature dependencies. Figure 5.10 shows relative spectrum uncertainties between the two temperatures. Again the differences are small over most of the spectrum range.

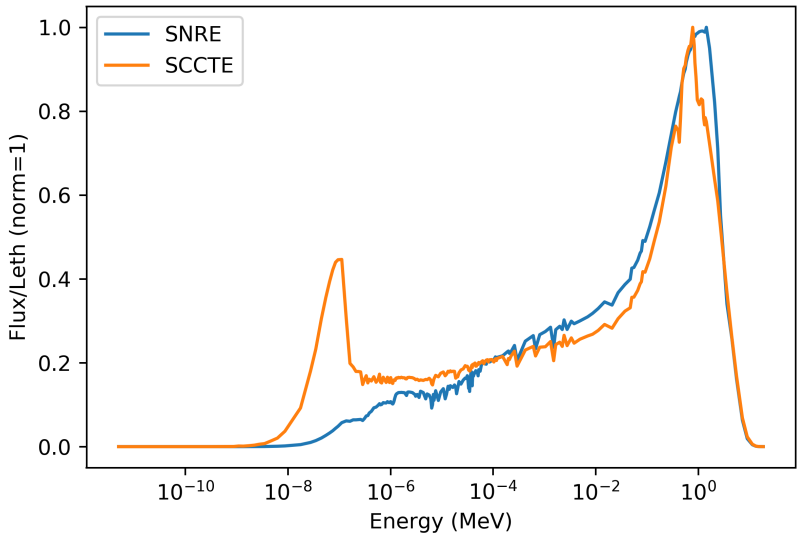

Figure 5.7: SCCTE Spectrum in ZrH Compared with SNRE

5.2.4 Unit-cell Uncertainties from Various Inputs

Table 5.6 shows SCCTE unit-cell uncertainties from various cross-section uncertainties. The SCCTE reactor is an LEU reactor with 19.75% enrichment. As such, uncertainties from ^{235}U are expected to be lower than the SNRE. However, results show the fission cross-section and $\bar{\nu}$ have similar uncertainties to the SNRE unit-cell. The (n,γ) reaction is about 3 times lower in uncertainty. The fuel is enriched to 95% ^{184}W to reduce parasitic absorption, however the absorption cross-section is still high such that it contributes a large uncertainty. Uncertainties from ^{238}U likely will increase the fuel absorption uncertainties. MCNP-IFP results shown as '-' are because MCNP-IFP cannot directly calculate these results unless the reactions are assumed to be completely independent.

The SCCTE reactor has a more thermal spectrum than the SNRE, as such it is expected to have a slightly different spectrum uncertainty but not by much. Figure 5.11 shows the SCCTE spectrum uncertainty from various uncertain inputs. The results are similar

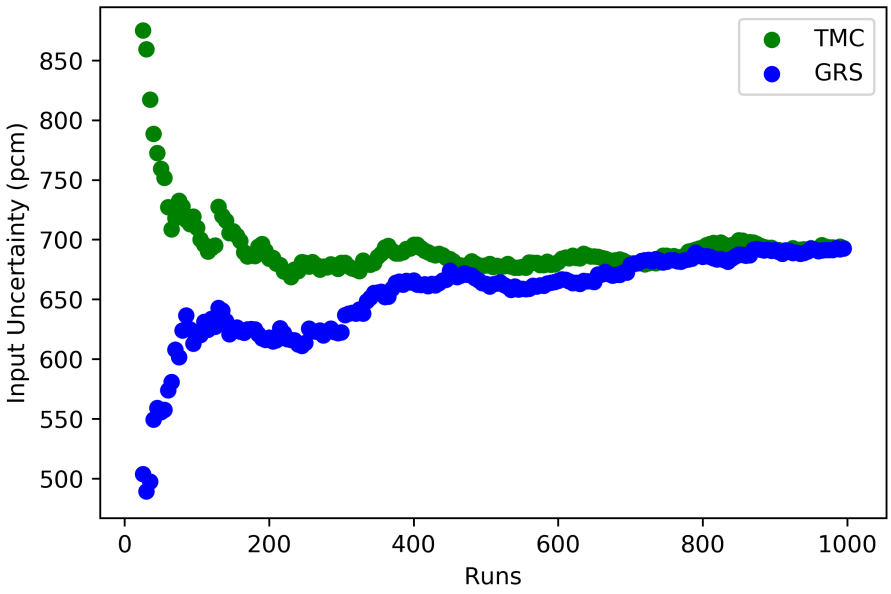

Figure 5.8: SCCTE GRS vs TMC Convergence Rates

to SNRE. It can also be seen that tungsten absorption uncertainties do not increase the spectrum uncertainty appreciably.

5.2.5 Full Core Eigenvalue Uncertainties

For the full core case, only the all ^{235}U and all ^{235}U + ^{184}W cases were used in results. Furthermore, ^{238}U cross-sections (same as ^{235}U) were varied along with $ZrH_{1.8}$ manufactured densities. Table 5.7 shows eigenvalue uncertainties from cross-sections. Each additional cross-section increases eigenvalue uncertainty. Varying the $ZrH_{1.8}$ density by 5% increases uncertainties by a similar amount as all varied cross-sections. This is an upper-bound estimate on moderator uncertainty since manufacturing tolerances should be lower than 5%.

Figure 5.12 calculates the full core heating spectrum uncertainties at 10 axial layers in SCCTE using random nuclear data. The full core heating spectrum is similar to the SNRE and as such similar uncertainties are calculated for each axial layer. Figure 5.13 compares

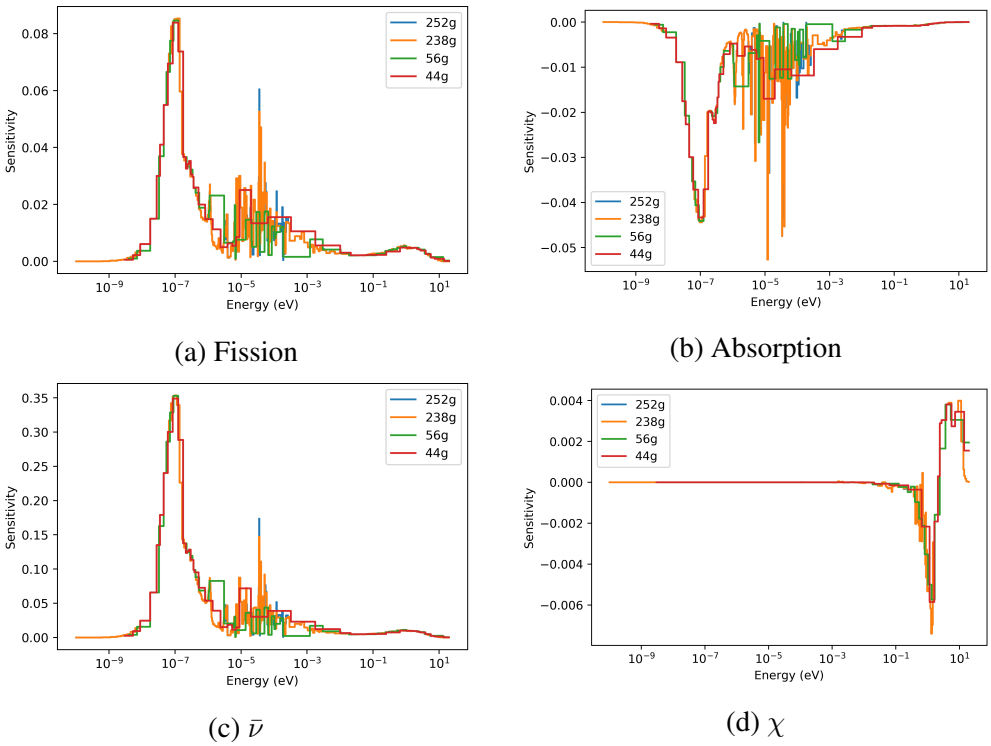

(a) Fission

(b) Absorption

(c) $\bar{\nu}$

(d) χ

Figure 5.9: Comparing Group Structure in SCCTE through Sensitivities

the total power profiles for the varied cases. Results show that even though ^{184}W and ^{238}U uncertainties increase eigenvalue uncertainties, the heating spectrum uncertainties do not change appreciably. Moderator density changes do change uncertainties based on spectrum. The top end of the core is more thermalized due to the presence of an axial reflector.

5.2.6 Full Core Spectrum Uncertainties

Flux spectrum uncertainties are of interest because spectrum calculations are used in lifetime calculations as well as all reaction rates. Figure 5.14 shows spectra uncertainties from various sources. Nuclear data only sources have similar uncertainties at around 1% except in the region at higher energies where fission χ effects dominate. Even with the high uncertainties in this range, most heating happens due to thermal neutron fissions so

MT	Groups	Uncorrelated (pcm)	Correlated (pcm)
102	44	61	245
	56	60	245
	238	131	260
	252	126	278
18	44	23	83
	56	23	82
	238	82	116
	252	43	91
452	44	124	612
	56	124	612
	238	165	612
	252	174	612
1018	44	37	95
	56	37	95
	238	46	74
	252	49	86

Table 5.3: Comparing Group Structure in SCCTE through Uncertainties

Groups	Input Uncertainty (pcm)
44	692.5
252	683.6

Table 5.4: Comparing Group Structure in SCCTE from ASAPy Generated Cross-Sections

the heating profile uncertainties remain relatively low.

5.2.7 Full Core Reaction Rate Uncertainties

In burnup and material damage calculations, nuclear reaction rates important. Uncertainties tend to increase as burnup increases though only fresh fuel is used in these simulations. mcACE is capable of automatically adding reaction relevant burn-up cross-sections for all materials that are marked as burnup. This produces a very large amount of

	Eigenvalue	Uncertainty	Relative %
300 K	1.325047	0.009052	0.683145
1200 K	1.295989	0.008974	0.692439

Table 5.5: Eigenvalue Temperature Dependence

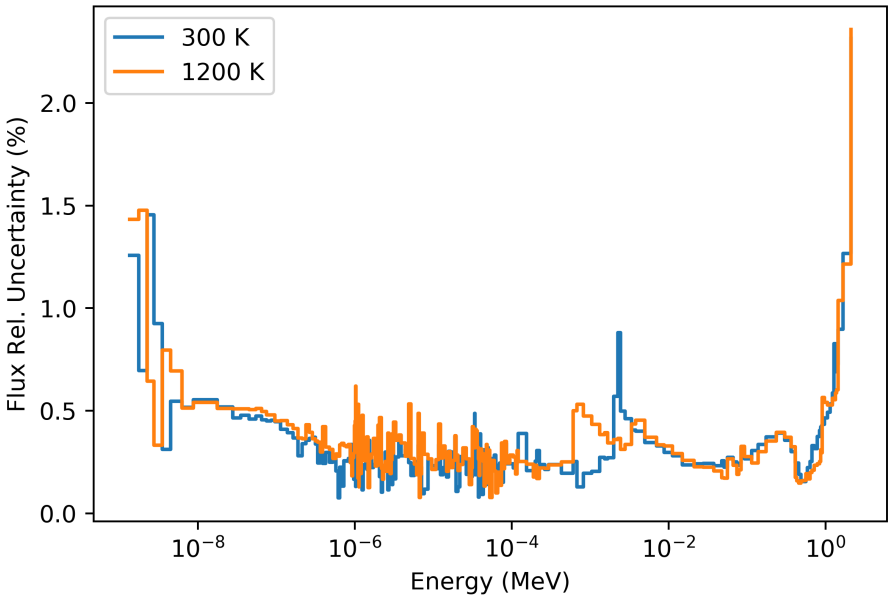

Figure 5.10: Spectrum Uncertainty Temperature Dependence

data so only a subset is shown. Figure 5.15 shows microscopic reaction rate calculations that would be used in burn-up calculations. Percent relative uncertainties are shown above the bar plots. Twenty-one fuel elements locations were chosen to show that reaction rates and uncertainties are similar through the core.

5.2.8 Full Core Flux and Heating Uncertainties from Manufacturing Uncertainties

Manufacturing uncertainties can also be propagated to the full core models. Understanding where uncertainties are the largest can help determine tolerances needed for manufacturing. The moderator density was varied by 5% in this simulation. Figure 5.16 shows

Correlation	Reaction	Unc. (pcm)	95% σ	MCNP-IFP
Uncorrelated	(n,γ)	125	3	126
	(n,f) + (n,γ)	132	3	-
	(n,f)	44	1	43
	$\bar{\nu}$	453	11	*174*
	Fission χ	52	2	50
Correlated	(n,γ)	278	7	279
	(n,f) + (n,γ)	292	7	-
	(n,f)	91	2	92
	$\bar{\nu}$	604	15	612
	Fission χ	87	3	86
	All ^{235}U	693	29	-
	All ^{235}U + ^{184}W	861	38	-

Table 5.6: Uncertainties of SCCTE Unit-Cell From Various Input Sources

Reaction	Input Uncertainty (pcm)
All ^{235}U	710.0
All ^{235}U + ^{184}W	807.5
All ^{235}U + ^{184}W + All ^{238}U	849.0
All ^{235}U + ^{184}W + All ^{238}U + $ZrH_{1.8}$ ρ	1621.9

Table 5.7: Full Core Eigenvalue Uncertainties from Cross-Sections in SCCTE

axial heating and spectrum relative uncertainties. The moderator density effects both axial heating and spectrum results by increasing uncertainties. These uncertainties would change thermal calculations as well as burn-up results.

5.2.9 Sensitivities Analysis with Correlated Input Uncertainty

Given a well resolved TMC calculation, sensitivities can be determined using the variance based indicator described in Sec. 3.3.2. In Monte-Carlo neutronics calculations, typically only the eigenvalue sensitivity is calculated due to the lack of methodology for other parameters of interest. This dissertation allows for determining relative sensitivities of any

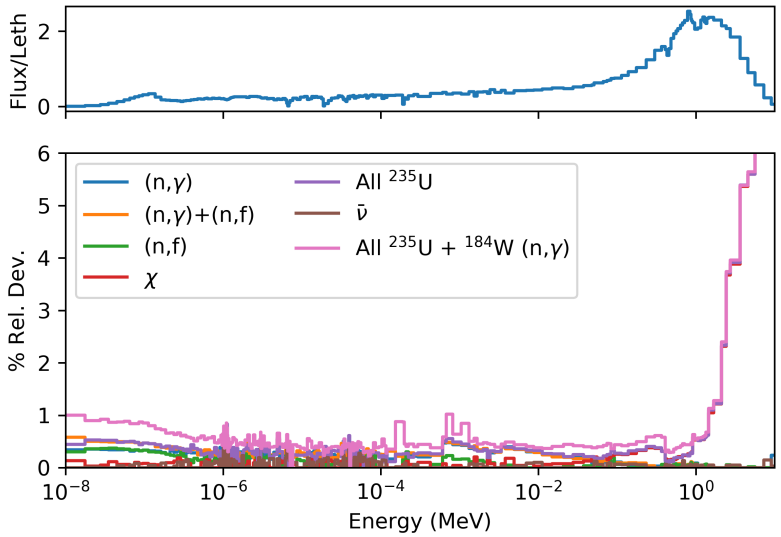

Figure 5.11: SCCTE Fuel Flux Uncertainties

output parameter based on any input parameter. The full core SCCTE is used in these simulations. The sensitivities presented are all from a single TMC simulation where relevant outputs were tallied.

First a more traditional analysis with eigenvalue sensitivities with respect to varied cross-sections is shown in Figure 5.17a. The result implies $\bar{\nu}$ causes the largest uncertainties in eigenvalue. Table 5.3 shows that this is indeed true. All sensitivities less than zero are largely due to Monte-Carlo statistics. It is known that the absorption cross-section is the next most important, however the plot does not reveal this easily.

Figure 5.17b shows sensitivities of the capture cross-section based on the four cross-sections varied. The capture cross-section is most sensitivity to the capture-section changing. The result is seemingly obvious but the sensitivity ranking confirms this.

Figure 5.17c shows sensitivities of the fission cross-section based on the four cross-sections varied. The fission cross-section is actually most sensitivity to the fission χ dis-

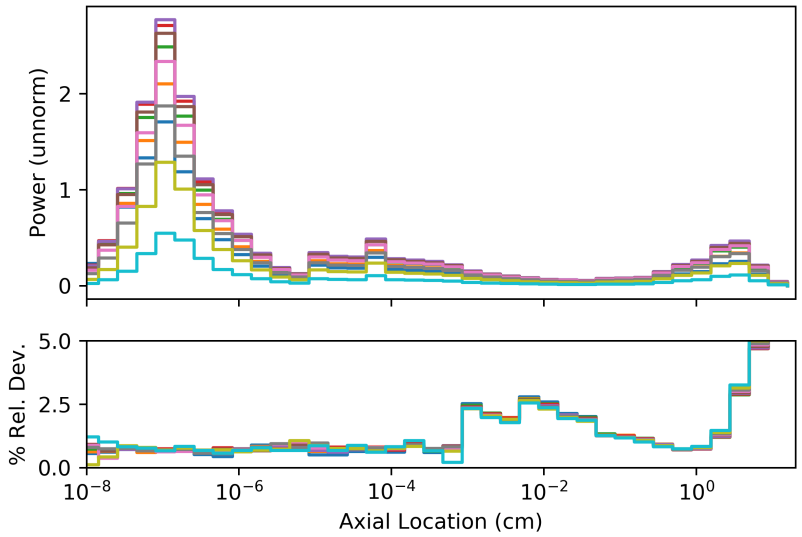

Figure 5.12: SCCTE Full Core Heating Spectrum at All Axial Levels

tribution and not simply the fission cross-section. The varied fission cross-section does not change the eigenvalue much either so it makes sense that the calculated fission cross-section is not changed much either by the varied cross-section. This is a result that could not be performed with current MC based sensitivity methods in MCNP.

Figure 5.17d shows the sensitivity of various cross-sections based on varied ^{184}W capture cross-section. The calculated W cross-section is most sensitive to the varied W cross-section. The ^{235}U calcualted capture cross-section also has an appreciable sensitivity to the varied W cross-section. This is likely from the change in fission rates based on changing W resonance capture.

A practical application of the calculated sensitivities is to determine rankings which are the most important parameter effecting a specific output. Figure 5.18a shows the variance based sensitivities of an axial heating rate with respect to varied cross-sections. The main contributor appears to be the ^{184}W absorption cross-section. In order to verify this predic-

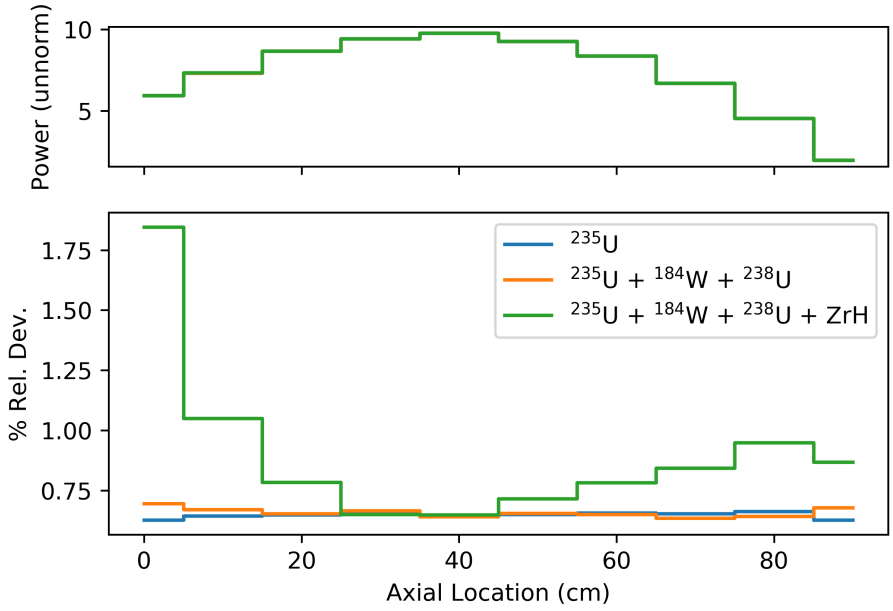

Figure 5.13: SCCTE Axial Heating Profile Uncertainties

tion, a second set of cases was ran without any W variations with the expected outcome of reduced axial heating rate uncertainties. Figure 5.18b shows the axial heating rates with and without W variations showing axial heating rate uncertainties do decrease without any W variations. However, the relative magnitude of the decrease in uncertainty does not reflect the prediction of W sensitivities dominating the axial heating uncertainties. This is likely due to a relatively small covariance term associated with the sensitivity. The sensitivity analysis did predict the expected change in heating uncertainties. If samples were taken in an uncorrelated manner, MCNP-IFP like sensitivities could be calculated for any output parameter, though MCNP-IFP could not calculate these values. These results are useful in code verification studies for future IFP-like sensitivities to non eigenvalue parameters.

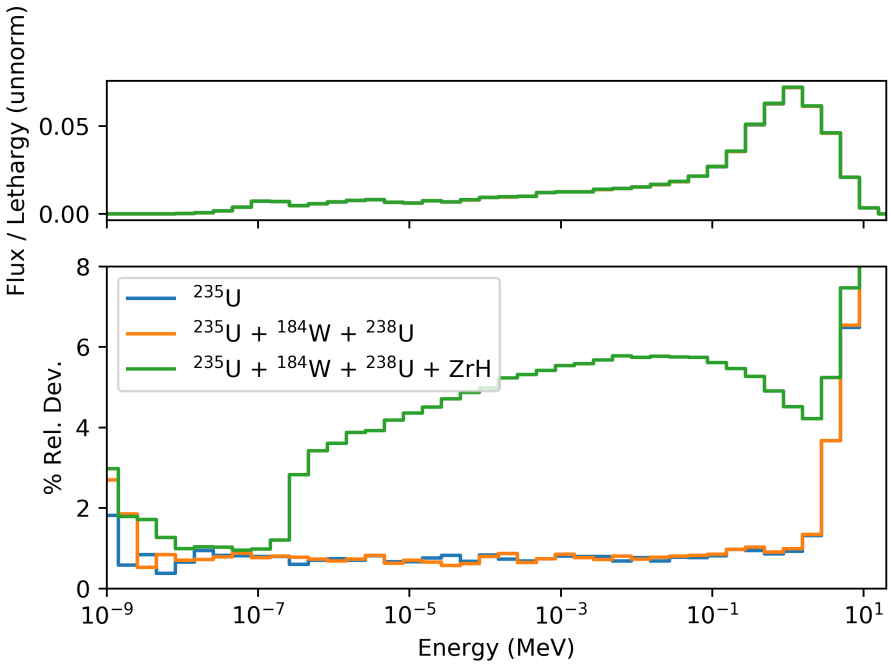

Figure 5.14: SCCTE Spectrum Uncertainties from Various Inputs

5.2.10 False Convergence of FTMC

The Fast Total Monte Carlo method works very well for determining eigenvalue uncertainty, however using it for other parameters such as reaction rates or energy flux can lead to false convergence. The rule of thumb is to maintain relative uncertainties of individual calculations at less than 0.5. A SCCTE unit cell and full core calculation was performed with various number of particles ran for each run to compare results with a GRS run which is considered the expected value. Figure. 5.19 shows a positive result of eigenvalue converging for the unit cell, but the full core 25x less particles case does not converge to the value the other cases predict. This deviation is not large, though it is apparent. Figure. 5.20 shows a similar scenario in the unit cell where two energy bins are compared. The 6.343 MeV bin is well converged, however the 0.013 MeV bin exhibits similar false convergence for the 25x less particles case. It is important to note that increasing the number of runs

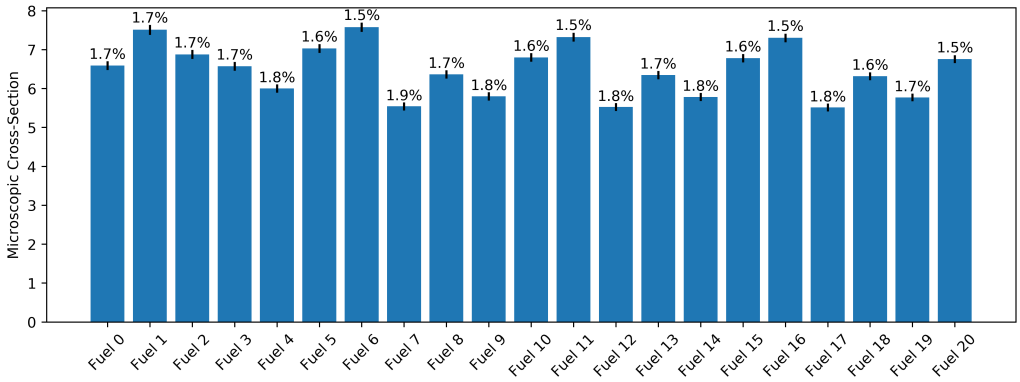

(a) ^{235}U (n,f)

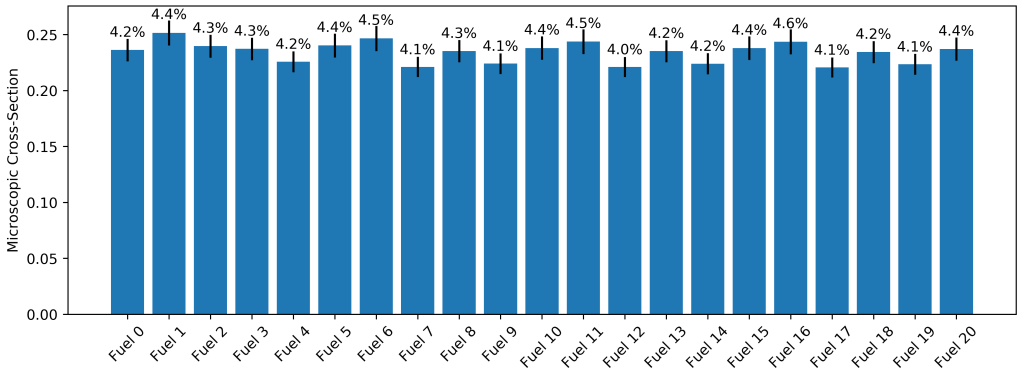

(b) ^{184}W (n,γ)

Figure 5.15: Some Microscopic Reaction Cross-Sections in SCCTE

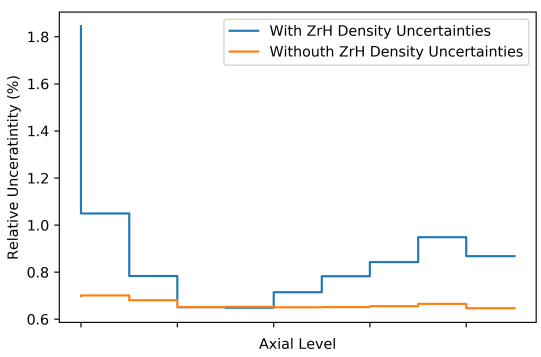

(a) Axial Heating

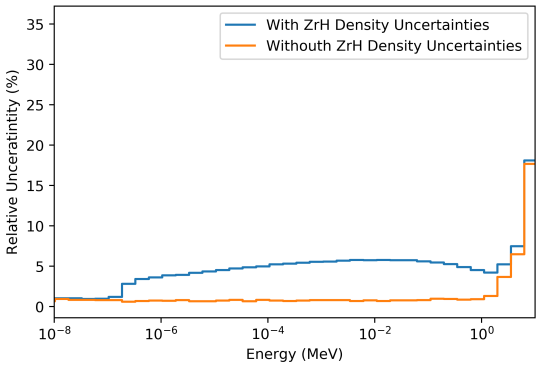

(b) Spectrum

Figure 5.16: Full Core SCCTE Uncertainties from Moderator Density Variations

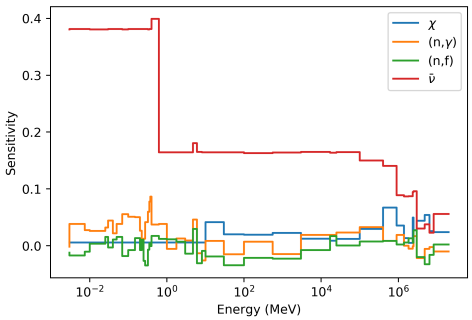

(a) Eigenvalue from Various ^{235}U

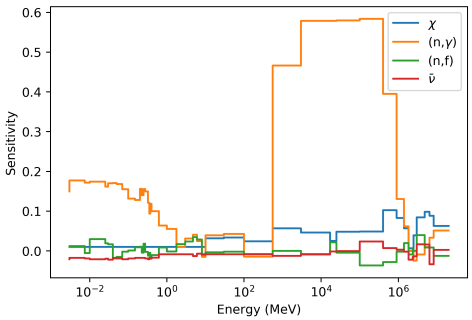

(b) ^{235}U (n,γ) from Various ^{235}U

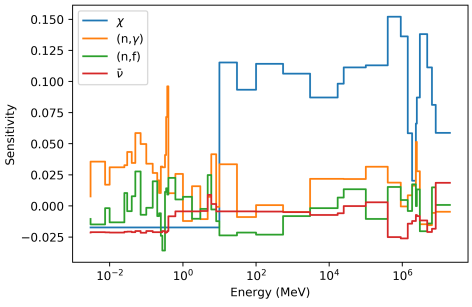

(c) ^{235}U (n,f) from Various ^{235}U

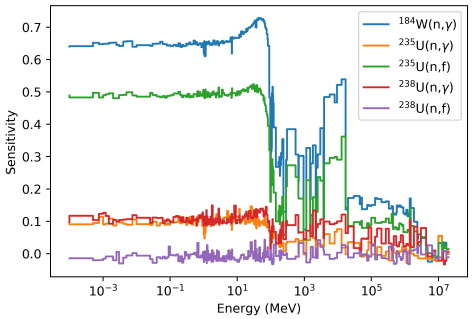

(d) Various σ from ^{184}W (n,γ)

Figure 5.17: Various Sensitivities in SCCTE Full Core

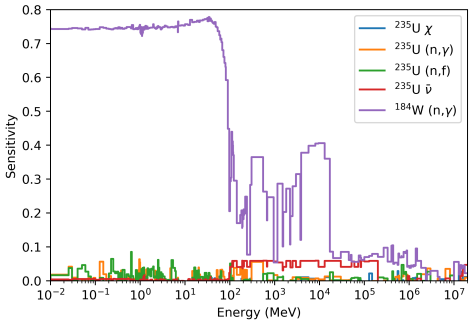

(a) Axial Heating Spectrum EASI Sensitivities

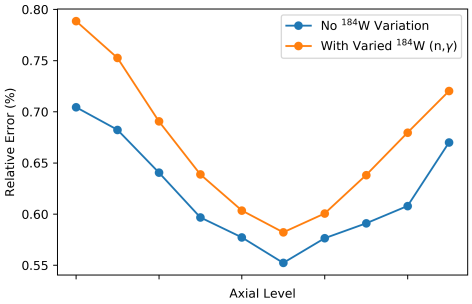

(b) Reduction of Uncertainties

Figure 5.18: ^{184}W Impact on Axial Heating

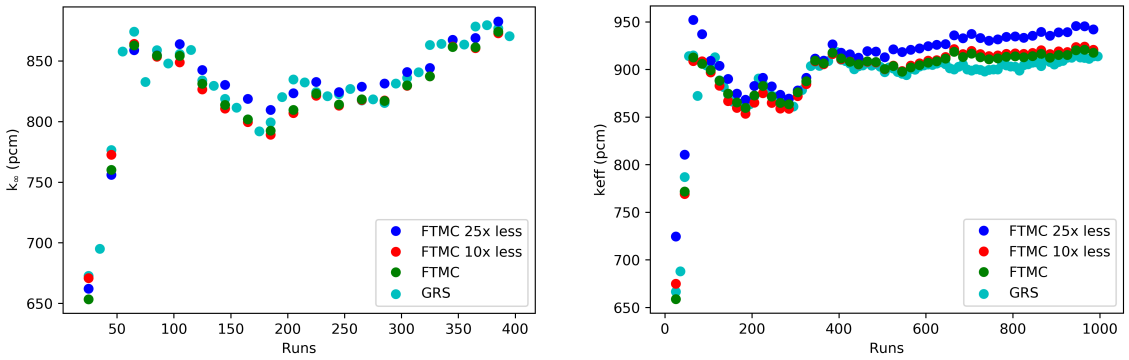

(a) Unit Cell

(b) Full Core

Figure 5.19: FTMC Eigenvalue Uncertainty Convergence in SCCTE

does not reduce uncertainties. Figure. 5.21 shows full core axial heating values. The total flux is not well converged in the 25x case again, though the others agree very well. Taking a single axial level out of a total of 10 axial bins shows a much larger discrepancy between number of particles ran. The full axial heating profiles are also compared to GRS along with TMC to see if similar behavior is observed, though for the 25x particle case TMC is not applicable due to the large uncertainties in each run. FTMC again predicts higher uncertainties than the longer running cases do. GRS and TMC are used in other calculations in this dissertation.

5.2.11 Reactor Performance Uncertainties

TRICORDER [61] is a multi-physics software to compute coupled solid fuel temperatures and 1D fluid states, with coupling through friction factor and heat transfer correlations. Uncertain heat profiles calculated were used as heating profiles to determine performance uncertainties. Each uncertain profile was used in a unique TRICORDER calculation. The power profiles were normalized similarly to the average power and mass flow-rates were kept the same as the nominal condition. This analysis' goal is to determine how different nominal predicted operating conditions are given uncertain heating profiles.

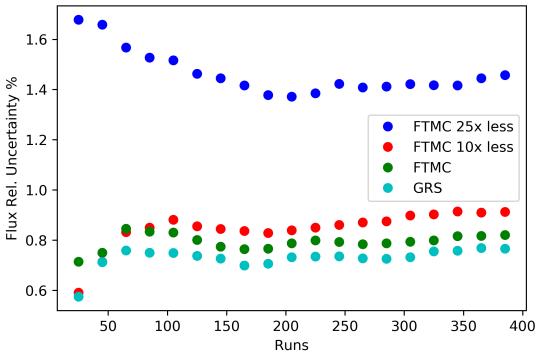

(a) 0.1 - 0.013 MeV

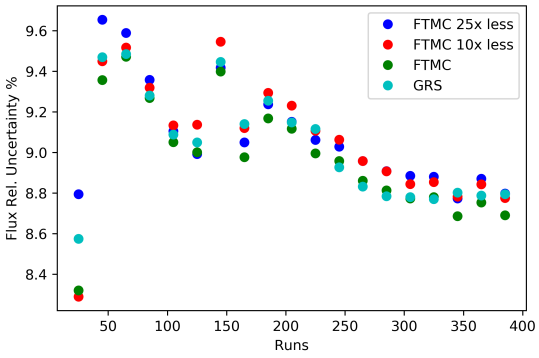

(b) 4.8 - 6.434 MeV

Figure 5.20: FTMC Spectrum Uncertainty Convergence in SCCTE Unit Cell

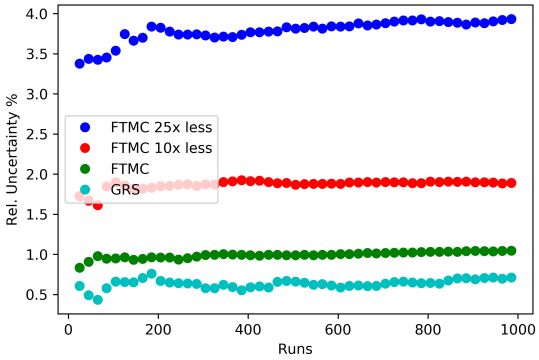

(a) Top Axial Level

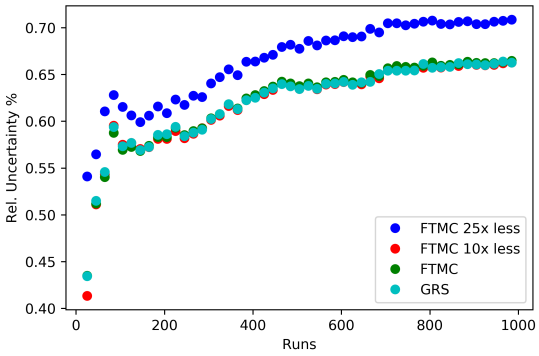

(b) Total Axial Value

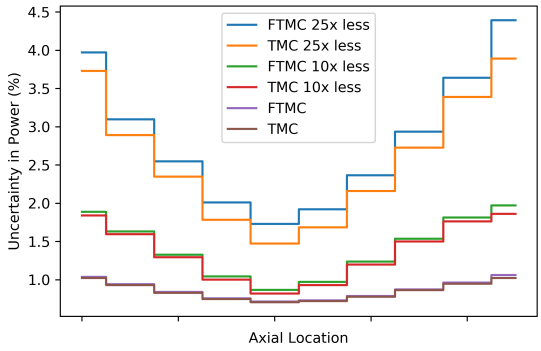

(c) Full Axial Shape

Figure 5.21: FTMC Axial Heating Uncertainty Convergence in SCCTE Full Core

In reality, the system would attempt to compensate based on observed conditions. The system control algorithms can be tuned based on the expected bandwidth of conditions to expect. Faster acting controls can be used if uncertainties of outputs can be determined.

Performance convergence rates are important, similarly to neutronic eigenvalue and tally value convergence rates. Figures 5.22 shows convergence rates of a few performance parameters. They have similar convergence rates as neutronic parameters and are shown to be well converged.

MCNP was ran on the full SCCTE core using varied ^{235}U, ^{238}U, and ^{184}W cross-section data to calculate heating profiles. Given many uncertain heating profiles, TRICORDER was ran for each case. Postprocessing was performed to calculate relevant metrics. Uncertainties were calculated using the GRS method after all thermal calculations were performed. Table 5.8 shows uncertainties in performance metrics due to neutronic uncertainties. The less than 0.75% relative uncertainty in power profiles shows even smaller relative uncertainties in performance metrics. Relative uncertainties are not good metric because the actual magnitude is also important. Small changes in pressure drop and thrust can be compensated for using small course correction maneuvers. Changes in specific impulse are more difficult to quantify but can also be adjusted for. Extra propellant must be taken to compensate for thrust and impulse changes. Maximum temperatures are more difficult to measure and compensate for other than including large margins of safety. The uncertainty predicted can be used to guide how large the margin of safety needs to be such that performance can be optimized.

5.2.12 Burnup Transient

NTP operates for a very short time compared to typical power reactors, however the power density is much higher. As such, burn-up uncertainty propagation is potentially importance due to relatively large fission product build-up for the operating times. There are

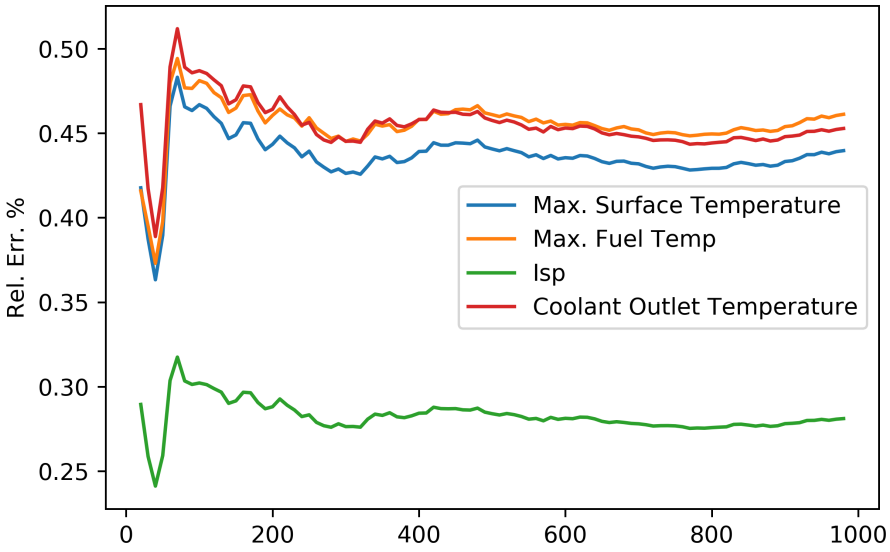

Figure 5.22: Full Core SCCTE Performance Metric Convergence

also short periods of shut-down between propulsive burns due to mission requirements. This means large fission-product build-up also occurs between burns. This analysis considers burn-up propagation of uranium fission and absorption cross-sections, as well as $\bar{\nu}$, and χ distributions.

The SCCTE burnup parameters [65] were described previously and repeated in Tab. 5.9. The various on/off periods are based on mission requirements of two burns to leave Earth, a coast time to Mars, then a burn to slow down at Mars, a long stay at Mars, then a burn to leave from Mars. Earth capture should also be planned for but was not reported.

The GRS method was used with 500 random samples to perform a burn-up analysis in MCNP coupled with COUPLE/ORIGEN. A 238-group flux was calculated for each run as well as relevant burn-up cross-sections to create unique COUPLE libraries for ORIGEN runs. GRS statistics were performed after the full burn-up cycle was completed. Figure 5.23 shows the burn-up for the first two burns. Burn-up uncertainties do not increase with time due to the initial random inputs. This means for a one time use NTP system

Metric	Result	Std. Dev.	Rel Err. %
Outlet Temperature (K)	2595.13	11.75	0.45
Maximum Surface Temperature (K)	2711.24	11.92	0.44
Maximum Clad/Fuel Temperature (K)	2722.46	12.03	0.44
Maximum Fuel Temperature (K)	2789.95	12.87	0.46
Specific impulse	906.501	2.548	0.28
Pressure Drop (Pa)	647281	3527	0.54
Thrust (lbs-f)	35002	98	0.28

Table 5.8: Full Core SCCTE Performance Metric Uncertainties

Parameter	Value
Fuel Meat Average Power Density	13.4 (MW/L)
Full Power	25 Minutes
Shutdown	5 Hours
Full Power	25 Minutes
Shutdown	200 Days
Full Power	12 Minutes
Shutdown	500 Days
Full Power	9 Minutes
Shutdown	200 Days

Table 5.9: SCCTE Mission Profile

burn-up error propagation is not needed. This should be confirmed with a full-core burn-up and the addition of more uncertain cross-sections of relevant nuclides that are generated during burnup. Another large takeaway is that the uncertainty of total reactivity at each calculation time is far greater than the amount of reactivity lost during the actual burn. This suggests decreasing reactivity margins for design can be acceptable without a loss in lifetime. It also means that reducing cross-section uncertainty will not change lifetime estimates.

Uncertainties in tracked nuclides can also be determined by using GRS statistics on

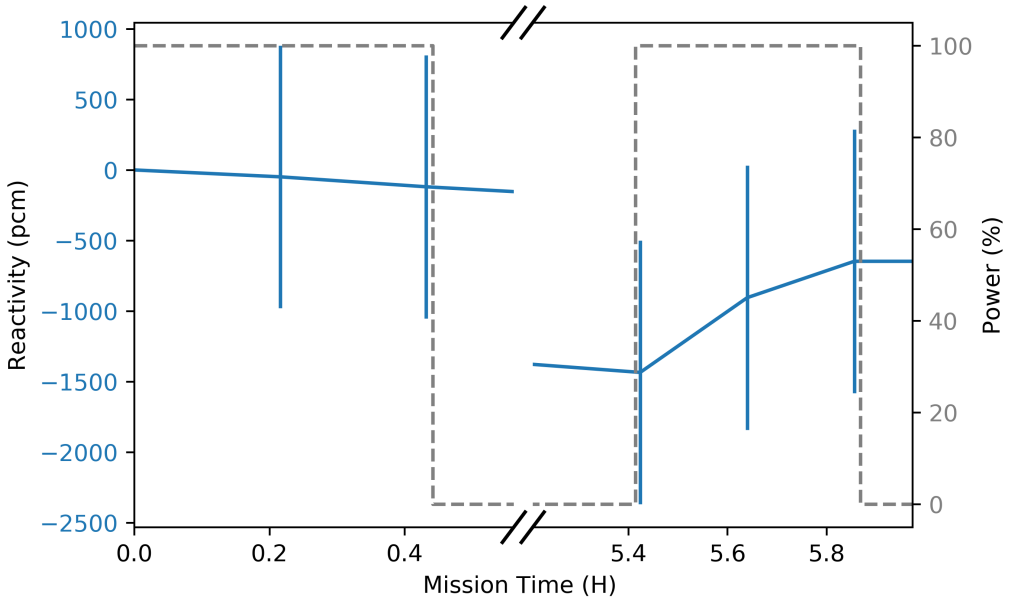

Figure 5.23: SCCTE Burnup Reactivity

the uncertain outputs. Figure 5.24 shows macroscopic cross-sections of three relevant isotopes. Although trends can be visualized in the relative error of the cross-sections, the change from beginning of life to the end of the second burn is not very large. Again, uncertainties do not increase in time, particularly for the nuclides that have varied nuclide cross-sections.

5.2.13 ^{135m}Xe Transient

^{135m}Xe has been identified having a large impact on the reactivity of NTP systems during operation [66]. NTP systems operate at a very high power density and for periods less than an hour at a time. In this operational regime, the impact of ^{135m}Xe is much greater than the operational space of a traditional reactor. This is due to the isotope's 15.29 minute half-life, being produced as 69.4% of prompt Xe fission yield, and absorption cross-section similar in magnitude to ^{135}Xe. To demonstrate the effect of ^{135m}Xe, Fig 5.25 [66] shows that in the representative SCCTE system, the predicted reactivity loss during operation

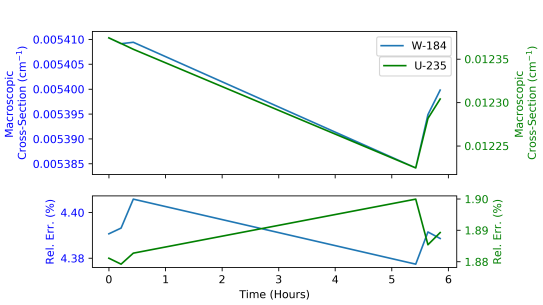

(a) ^{184}W and ^{235}U Absorption

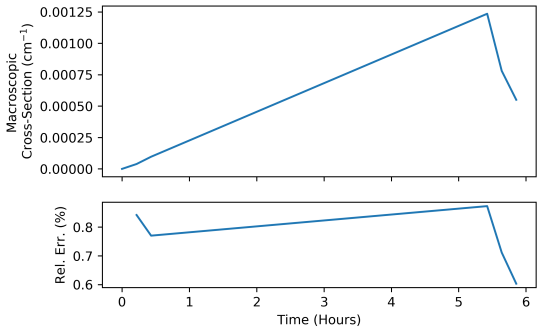

(b) ^{135}Xe Absorption

Figure 5.24: SCCTE Macroscopic Cross-Sections During Burn

increases by a factor of up to 1.93 when ^{135m}Xe is included in burnup models.

Experimental nuclear data cross-sections do not exist for ^{135m}Xe. As such, computational frameworks are used to generate data when gaps exist. The TENDL library[7] contains several evaluated cross-sections for ^{135m}Xe as well as covariance information. The capture cross-section along with group uncertainties is shown in Fig. 5.26. Large relative uncertainties (100-500%) exist in the resonance region, with smaller uncertainty in the thermal region (10%). The resonance region is largely negligible due to the small cross-section.

The covariance of ^{135m}Xe sampled data from the TENDL covariance file and computed from 500 log-normal samples is compared in Fig. 5.27. It can be seen that the covariances agree well.

The samples were ran in Serpent on an NTP infinite lattice unit-cell with 1 to 2 fuel to moderator ratio as shown in Fig. 5.28. One power cycle with two burn-steps of 15 minutes each were used because that is enough to quantify operational uncertainty as shown earlier in Fig. 5.25. Table 5.10 shows the output eigenvalue uncertainty contribution of the input uncertainty based on the GRS statistical method. It can be seen that the cross-section uncertainty has very little effect on the eigenvalue, though compared to a case where ^{135m}Xe

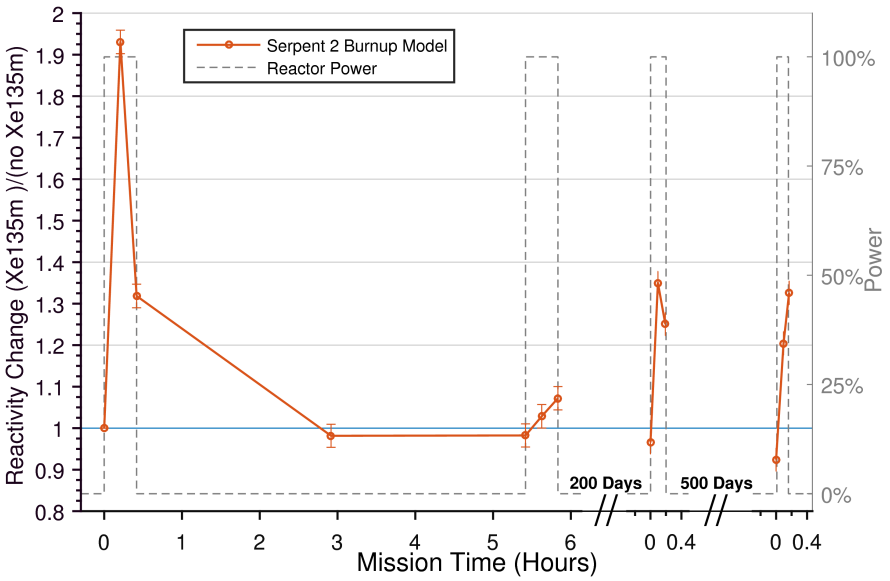

Figure 5.25: Effects of ^{135m}Xe Durning Burnup

is neglected, the Xe makes a large difference. Comparing several years of TENDL cross-sections in Fig. 5.29 shows a large difference between evaluation years. The uncertainty from years shown in Tab. 5.10 is much larger than the uncertainty predicted in a single year's evaluation. The UQ calculation resulted practically in the null hypodissertation, however further investigation into the magnitude of the true ^{135m}Xe is warranted.

UQ Method	Eigenvalue	Uncertainty (PCM)
ENDF-B/VII	1.16105	6.3E-05
GRS	1.15848	5.67088
TENDL Year (Range/Diff.)	1.1591-1.16004	94.0 ± 16.0

Table 5.10: Uncertainty in Eigenvalue from ^{135m}Xe Absorption

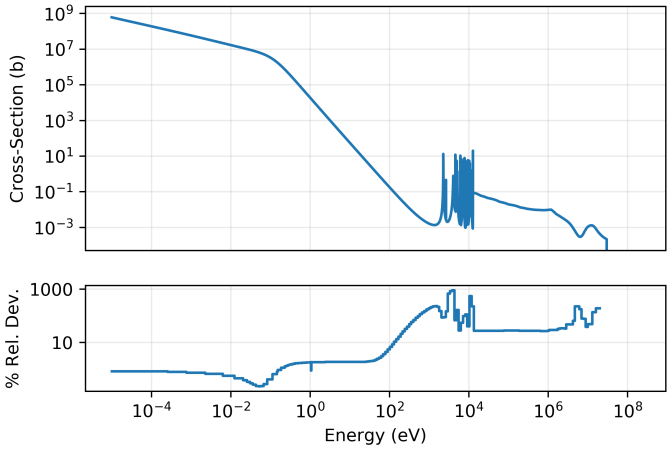

Figure 5.26: ^{135m}Xe Absorption Cross-Section (TENDL 2015)

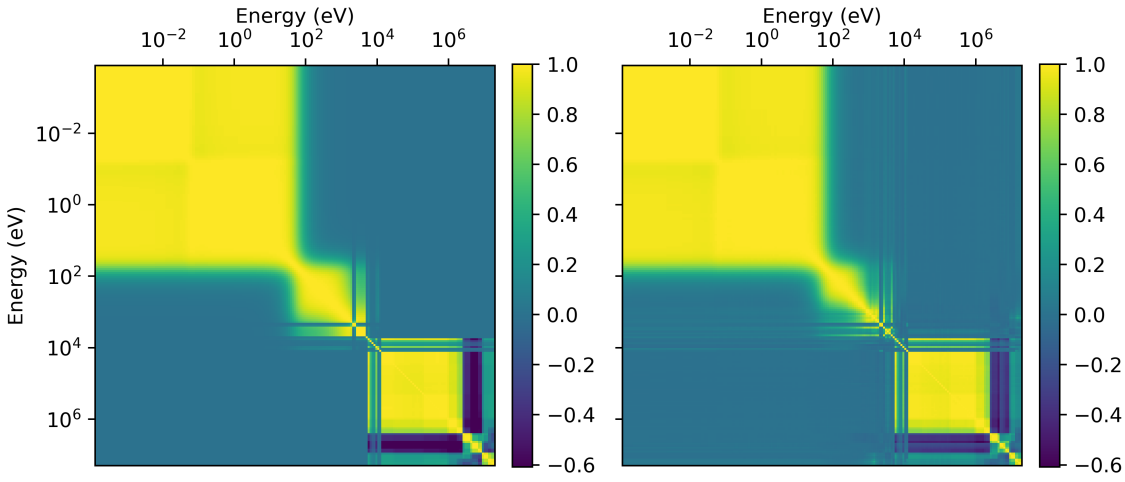

Figure 5.27: Correlation Matrix From ASAPy Calculation. (left: TENDL Actual, Right: lognormal samples)

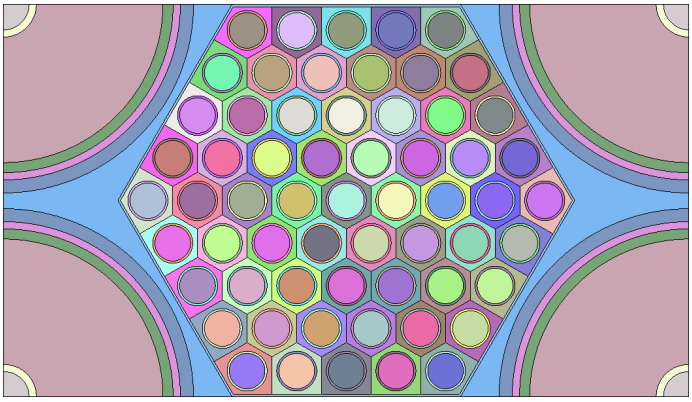

Figure 5.28: Unit-cell Used for Calculations

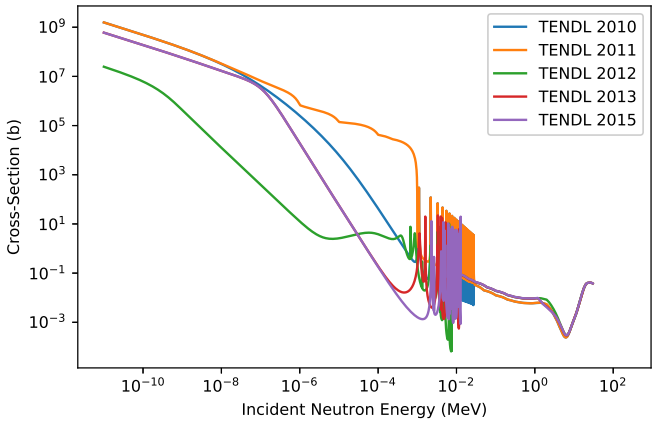

Figure 5.29: Absorption of ^{135m}Xe in Different TENDL Evaluation Years

6. CONCLUSIONS

6.1 Novel UQ Analysis Developed and Performed with Newly Developed Tools

This dissertation developed and performed Monte-Carlo based uncertainty quantification to better understand effects of uncertain inputs on nuclear reactor calculations such as eigenvalue, flux spectrum, and heating rates. A process was developed to quantify uncertainty of any output with an established monte-carlo neutronic code without any source code modification and built into a new code called mcACE. mcACE can now be used in detail design phases of reactor design to calculation uncertainties or used to model experiments in as-run fashion to better incorporate experimental and computational results.

A review of relevant method was performed and a combination of sampling techniques and statistical methods were identified to perform uncertainty quantification on nuclear thermal propulsion reactors. These methods are fast running to allow for UQ of any relevant output of monte-carlo based neutronic software. Comparisons of the selected statistical methods were made to confirm their ability to predict similar outputs. Two NTP reactors, the SNRE and SCCTE were analyzed on the unit-cell and full core scales.

New contributions of this dissertation are as follows:

- Showed GRS UQ method is equivalent but 10+ times faster compared to brute force sampling methods for calculating eigenvalues, heating rates, and reaction cross-sections.
- Developed sensitivity analysis to calculate first order Kucherenko indices using MC neutronics with any input sampling scheme by combined EASI sensitivity method with TMC UQ.
- Performed design analysis of two NTP reactors with UQ of eigenvalues, heating

rates, and reaction cross-sections calculations based on uncertain cross-sections and manufacturing tolerances.

- mcACE code developed to automate UQ processes for MCNP such that any MCNP input can be used and any MCNP input parameter can be sampled from relevant distributions from a single mcACE input file.

- Created a coupling of MCNP6 and ORIGEN within SCALE 6.1+ to perform burnup analysis to support industry accepted tool chains along with implemented MC UQ methods.

- ASAPy code developed to sample ACE based nuclear data from ENDF formatted covariances using any distribution that is equipped with an inverse cumulative distribution function, specifically log-normal was used in this dissertation.

6.2 Capabilities of mcACE and ASAPy

mcACE was created to adjust MCNP inputs via sampling methods, parse MCNP results, create ORIGEN coupling, and setup and perform GRS, TMC, and FTMC statistics. mcACE was verified by comparing to an MCNP method for eigenvalue sensitivity analysis. GRS, TMC, and FTMC were compared for desired MC outputs. GRS was found to agree well with TMC with less computational resources needed. FTMC was found to work well for eigenvalue uncertainties but over-predicted other detailed metrics like heating profiles unless more computational time was used making it similar to TMC. The Advanced Test Reactor was used for these comparisons which further shows that the methods implemented are reactor agnostic. Burnup with MCNP coupled to ORIGEN with various time-stepping techniques were demonstrated with the UAM pincell.

ASAPy was created to sample ACE data based on ENDF and SCALE covariances using normal and log-normal distributions. ASAPy can generate covariance from ENDF

data for any group structure and any spectrum weight. Data is generated as ACE files and methods were developed to update MCNP data tables so that the ACE Files can be used. Generated cross-sections were verified to produce similar uncertainties in the Godiva reactor as adjoint based methods. Variance profiles using TMC and EASI were created to compare with adjoint methods. Variance profiles were well predicted, but sensitivities could not be accurately recovered. Interpretation of correlated sensitivities in neutronic analysis were also made.

6.3 Uncertainties in Nuclear Thermal Propulsion Reactors

Many uncertainties exist in NTP reactors, the effects of these uncertainties can now be calculated. The ability to calculate these uncertainties can help guide reactor design when actual experiments are not available in a timely or cost-efficient manner. More uncertainties exist including more isotopic cross-sections and manufacturing tolerances. Further detail can also be explored by modeling further temperature dependence and core radial spectrum dependencies. This dissertation explored two NTP reactors using Monte-Carlo methods given various input uncertainties.

SNRE unit-cell has a very different spectrum than the full core version, and the SCCTE unit-cell has a slightly different spectrum than the full core version. Each unit-cell tends to have a similar spectrum than the full core even though the full cores are small and have large reflectors. Eigenvalue uncertainties were shown to have similar dependencies but full-core versions hard larger uncertainties showing the need to perform full-core analysis to best quantify uncertainties. Heating profiles could not be determined from unit-cells due to the lack of axial dependence. Spectrum uncertainties for both cores were similar to each other and their unit-cells. Reaction rate uncertainties were calculated for SCCTE and it was found that reaction rates uncertainness were similar throughout the core.

Manufacturing uncertainties through $ZrH_1.6$ moderator density in the SNRE were cal-

culated and found to have a relatively large impact compared to cross-section uncertainties. High assay LEU and non-U material enrichment cross-sections were also explored in the SCCTE design where the LEU had similar uncertainties as HEU and ^{184}W cross-sections added an appreciable amount of uncertainty to calculations. $ZrH_{1}.8$ densities were varied in the SCCTE full core with similar results as the SNRE unit-cell.

Heating profiles calculated using uncertain nuclear data were used in a hot channel analysis to calculate NTP performance uncertainties. Results from this analysis can be useful in guiding how much extra coolant is needed to satisfy the mission or reduce margins on maximum temperatures.

The SCCTE unit-cell was also used in a transient analysis to determine effects of ^{135m}Xe on eigenvalue. It was found that uncertainties in the Xe cross-section evaluation had very little effect on the eigenvalue, but the total cross-section is highly variable depending on the evaluation year so experimental evaluations are recommended.

REFERENCES

[1] MenteMagica, "Thrust to weight ratio vs isp," 2011.

[2] "LANL nss post on project rover." `https://www.lanl.gov/science/NSS/issue1_2011/story4a.shtml`. Accessed: 2010-09-30.

[3] S. Borowski, R. Corban, M. McGuire, and E. Beke, "Nuclear thermal rocket/vehicle design options for future nasa missions to the moon and mars," in *Space Programs and Technologies Conference and Exhibit*, p. 4170, 1995.

[4] NASA Johnson Space Center, *Human Exploration of Mars: Design Reference Architecture 5.0*. NASA, 2009.

[5] J. Finseth, "Overview of rover engine tests (final report)," Tech. Rep. NASA-CR-LD4270, National Aeronautics and Space Administration, 1991.

[6] F. Durham, ed., *Nuclear Engine Definition Study Preliminary Report - Volume II*. LA-5044-MS, Los Alamos, NV, 1972.

[7] A. J. Koning and D. Rochman, "Modern nuclear data evaluation with the talys code system," *Nuclear data sheets*, vol. 113, no. 12, pp. 2841–2934, 2012.

[8] D. Cacuci, *Sensitivity & Uncertainty Analysis, Volume 1: Theory*. CRC Press, 2003.

[9] E. P. Wigner, "Effect of small perturbations on pile period," in *Nuclear Energy*, pp. 540–552, Springer, 1992.

[10] F. B. Brown, *Monte Carlo Techniques for Nuclear Systems - Theory Lectures*. Los Alamos National Laboratory, Nov 2016.

[11] H. Rief, "Generalized monte carlo perturbation algorithms for correlated sampling and a second-order taylor series approach," *Annals of Nuclear Energy*, vol. 11, no. 9, pp. 455 – 476, 1984.

[12] Y. NAGAYA and T. MORI, "Impact of perturbed fission source on the effective multiplication factor in monte carlo perturbation calculations," *Journal of Nuclear Science and Technology*, vol. 42, no. 5, pp. 428–441, 2005.

[13] *Comparison of the Monte Carlo adjoint-weighted and differential operator perturbation methods*, (Tokyo, Japan), 2010.

[14] B. C. Kiedrowski, F. B. Brown, and P. Wilson, "Calculating kinetics parameters and reactivity changes with continuous-energy monte carlo," tech. rep., Los Alamos National Laboratory (LANL), 2009.

[15] H. J. SHIM and C. H. KIM, "Adjoint sensitivity and uncertainty analyses in monte carlo forward calculations," *Journal of Nuclear Science and Technology*, vol. 48, no. 12, pp. 1453–1461, 2011.

[16] C. M. Perfetti, B. T. Rearden, and W. R. Martin, "Scale continuous-energy eigenvalue sensitivity coefficient calculations," *Nuclear Science and Engineering*, vol. 182, no. 3, pp. 332–353, 2016.

[17] J. C. Helton, J. D. Johnson, C. J. Sallaberry, and C. B. Storlie, "Survey of sampling-based methods for uncertainty and sensitivity analysis," *Reliability Engineering & System Safety*, vol. 91, no. 10, pp. 1175–1209, 2006.

[18] A. Koning and D. Rochman, "Towards sustainable nuclear energy: Putting nuclear physics to work," *Annals of Nuclear Energy*, vol. 35, no. 11, pp. 2024 – 2030, 2008.

[19] W. Zwermann, B. Krzykacz-Hausmann, L. Gallner, M. Klein, A. Pautz, and K. Velkov, "Aleatoric and epistemic uncertainties in sampling based nuclear data

uncertainty and sensitivity analyses," tech. rep., American Nuclear Society, Inc., 555 N. Kensington Avenue, La Grange Park, Illinois 60526 (United States), 2012.

[20] D. Rochman, W. Zwermann, S. C. van der Marck, A. J. Koning, H. Sjöstrand, P. Helgesson, and B. Krzykacz-Hausmann, "Efficient use of monte carlo: Uncertainty propagation," *Nuclear Science and Engineering*, vol. 177, no. 3, pp. 337–349, 2014.

[21] B. Rearden and M. Jessee, "Scale code system," Tech. Rep. ORNL/TM-2005/39, Oak Ridge National Laboratory, 2016.

[22] J. T. Goorley, M. R. James, T. E. Booth, F. B. Brown, J. S. Bull, L. J. Cox, J. W. J. Durkee, J. S. Elson, M. L. Fensin, R. A. I. Forster, J. S. Hendricks, H. G. I. Hughes, R. C. Johns, B. C. Kiedrowski, R. L. Martz, S. G. Mashnik, G. W. McKinney, D. B. Pelowitz, R. E. Prael, J. E. Sweezy, L. S. Waters, T. Wilcox, and A. J. Zukaitis, *Initial MCNP6 Release Overview - MCNP6 version 1.0.* Los Alamos National Laboratory, April 2013.

[23] B. C. Kiedrowski, F. B. Brown, J. L. Conlin, J. A. Favorite, A. C. Kahler, A. R. Kersting, D. K. Parsons, and J. L. Walker, "Whisper: Sensitivity/uncertainty-based computational methods and software for determining baseline upper subcritical limits," *Nuclear Science and Engineering*, vol. 181, no. 1, pp. 17–47, 2015.

[24] F. B. Brown, J. E. Sweezy, and R. Hayes, "Monte carlo parameter studies and uncertainty analyses with mcnp5," in *PHYSOR-2004, American Nuclear Society Reactor Physics Topical Meeting*, 2004.

[25] N. Otuka *et al.*, "Towards a more complete and accurate experimental nuclear reaction data library (exfor): International collaboration between nuclear reaction data centres (nrdc)," *Nuclear Data Sheets*, vol. 120, pp. 272 – 276, 2014.

[26] M. Herman and A. Trkov, "Endf-6 formats manual," *National Nuclear Data Centre, BNL, Upton, New York*, 2005.

[27] D. Muir, R. Boicourt, and A. Kahler, "The njoy nuclear data processing system, version 2012," tech. rep., LA-UR-12-27079, 2012.

[28] D. E. Cullen, "Prepro 2015 2015 endf/b pre-processing codes," tech. rep., IAEA-NDS-39, 2015.

[29] D. Wiarda, M. L. Williams, C. Celik, and M. E. Dunn, "Ampx: A modern cross section processing system for generating nuclear data libraries," tech. rep., Oak Ridge National Laboratory, 2015.

[30] C. Mattoon, B. Beck, N. Patel, N. Summers, G. Hedstrom, and D. Brown, "Generalized nuclear data: a new structure (with supporting infrastructure) for handling nuclear data," *Nuclear Data Sheets*, vol. 113, no. 12, pp. 3145–3171, 2012.

[31] S. C. van der Marck, A. J. Koning, and D. A. Rochman, "Benchmarking tendl-2012," *Nuclear Data Sheets*, vol. 118, pp. 446–449, 2014.

[32] O. Buss, A. Hoefer, and J.-C. Neuber, "Nuduna: "nuclear data uncertainty analysis"," in *Meeting on uncertainty propagations in the nuclear fuel cycle Uppsala University*, 2013.

[33] J. Pruet, "Kiwi: An evaluated library of uncertainties in nuclear data and package for nuclear sensitivity studies," tech. rep., Lawrence Livermore National Laboratory (LLNL), Livermore, CA, 2007.

[34] W. ZWERMANN, A. AURES, L. GALLNER, V. HANNSTEIN, B. KRZYKACZ-HAUSMANN, K. VELKOV, and J. MARTINEZ, "Nuclear data uncertainty and sensitivity analysis with xsusa for fuel assembly depletion calculations," *Nuclear Engineering and Technology*, vol. 46, no. 3, pp. 343 – 352, 2014.

[35] T. Zhu, *Sampling-Based Nuclear Data Uncertainty Quantification for Continuous Energy Monte Carlo Codes*. PhD thesis, EPFL, 2015.

[36] D. Rochman, A. Vasiliev, H. Ferroukhi, T. Zhu, S. van der Marck, and A. J. Koning, "Nuclear data uncertainty for criticality-safety: Monte carlo vs. linear perturbation," *Annals of Nuclear Energy*, vol. 92, pp. 150–160, 2016.

[37] M. Behler, M. Bock, F. Rowold, and M. Stuke, "Suncistt - a generic code interface for uncertainty and sensitivity analysis," in *Proc. Probabilistic Safety Assessment and Management PSAM12*, (Honolulu, Hawaii, USA), 2012.

[38] D. Rochman and C. Sciolla, "Nuclear data uncertainty propagation for a typical pwr fuel assembly with burnup," *Nuclear Engineering and Technology*, vol. 46, no. 3, pp. 353–362, 2014.

[39] D. Rochman, A. J. Koning, and S. C. van der Marck, "Uncertainties for criticality-safety benchmarks and keff distributions," *Annals of Nuclear Energy*, vol. 36, no. 6, pp. 810–831, 2009.

[40] D. Rochman, S. van der Marck, and A. Hogenbirk, "Nuclear data uncertainty propagation (adjustment procedure)," *Nuclear Research and Consultancy Group NRG letter to WPEC/sub-group 33*, 2010.

[41] A. Koning and D. Rochman, "Modern nuclear data evaluation: Straight from nuclear physics to applications," *Journal of the Korean Physical Society*, vol. 59, no. 2, pp. 773–778, 2011.

[42] D. Rochman and A. J. Koning, "How to randomly evaluate nuclear data: A new data adjustment method applied to pu-239," *Nuclear Science and Engineering*, vol. 169, no. 1, pp. 68–80, 2011.

[43] D. Rochman and A. Koning, "Random adjustment of the h in H2O neutron thermal scattering data," *Nuclear science and engineering*, vol. 172, no. 3, pp. 287–299, 2012.

[44] S. C. van der Marck and D. A. Rochman, "Nuclear data uncertainties for local power densities in the martin-hoogenboom benchmark," in *SNA+ MC 2013-Joint International Conference on Supercomputing in Nuclear Applications+ Monte Carlo*, p. 02410, EDP Sciences, 2014.

[45] V. Patel, M. Eades, P. Venneri, and C. R. J. II, "Comparing low enriched fuel to highly enriched fuel for use in nuclear thermal propulsion systems," in *American Institute Of Aeronautics And Astronautics: Propulsion and Energy*, July 2016. Submitted for review.

[46] M. Eades, W. Deason, and V. Patel, "Sccte: An leu ntp concept with tungsten cermet fuel," in *Winter American Nuclear Society Meeting*, November 2015.

[47] A. E. Isotalo and P. A. Aarnio, "Higher order methods for burnup calculations with Bateman solutions," *Annals of Nuclear Energy*, vol. 38, no. 11, pp. 1987–1995, 2011.

[48] P. K. Romano, N. E. Horelik, B. R. Herman, A. G. Nelson, B. Forget, and K. Smith, "Openmc: A state-of-the-art monte carlo code for research and development," *Annals of Nuclear Energy*, vol. 82, pp. 90 – 97, 2015. Joint International Conference on Supercomputing in Nuclear Applications and Monte Carlo 2013, SNA + MC 2013. Pluri- and Trans-disciplinarity, Towards New Modeling and Numerical Simulation Paradigms.

[49] G. Žerovnik, A. Trkov, D. L. Smith, and R. Capote, "Transformation of correlation coefficients between normal and lognormal distribution and implications for nuclear applications," *Nuclear Instruments and Methods in Physics Research Section A: Ac-*

celerators, Spectrometers, Detectors and Associated Equipment, vol. 727, pp. 33–39, 2013.

[50] E. Jones, T. Oliphant, P. Peterson, *et al.*, "SciPy: Open source scientific tools for Python," 2001–. [Online].

[51] J. Nocedal and S. J. Wright, eds., *Numerical Optimization*. Springer-Verlag, 1999.

[52] S. Kucherenko, S. Tarantola, and P. Annoni, "Estimation of global sensitivity indices for models with dependent variables," *Computer Physics Communications*, vol. 183, no. 4, pp. 937 – 946, 2012.

[53] Y. Caniou, *Global sensitivity analysis for nested and multiscale modelling*. PhD thesis, Université Blaise Pascal-Clermont-Ferrand II, 2012.

[54] T. Zhu, A. Vasiliev, H. Ferroukhi, and A. Pautz, "Nuss: A tool for propagating multigroup nuclear data covariances in pointwise ace-formatted nuclear data using stochastic sampling method," *Annals of Nuclear Energy*, vol. 75, pp. 713–722, 2015.

[55] E. Plischke, "An effective algorithm for computing global sensitivity indices (easi)," *Reliability Engineering & System Safety*, vol. 95, no. 4, pp. 354–360, 2010.

[56] J.-Y. Tissot and C. Prieur, "Bias correction for the estimation of sensitivity indices based on random balance designs," *Reliability Engineering & System Safety*, vol. 107, pp. 205 – 213, 2012. SAMO 2010.

[57] J. Herman and W. Usher, "SALib: An open-source python library for sensitivity analysis," *The Journal of Open Source Software*, vol. 2, Jan 2017.

[58] M. Kuhn and K. Johnson, *Applied predictive modeling*, vol. 26. Springer, 2013.

[59] V. Patel, M. Eades, and W. Deason, *Center for Space Nuclear Research (CSNR) NTP Design Team Report*. No. EXT-15-36810 in INL, Idaho National Laboratory, 2015.

[60] P. Husemeyer, V. Patel, P. Venneri, W. Deason, M. Eades, and S. Howe, "Csnr space propulsion optimization code: SPOC," in *Nuclear and Emerging Technologies for Space*, February 2015.

[61] L. B. Carasik, V. Patel, S. Judd, and P. Venneri, "Development and implementation of a 1-d fem compressible flow module in tricorder - a moose-based multi-physics code," in *Proc. 18th International Topical Meeting on Nuclear Reactor Thermal Hydraulics (NURETH'18), Portland, USA*, 2019.

[62] K. Ivanov, M. Avramova, S. Kamerow, I. Kodeli, E. Sartori, E. Ivanov, and O. Cabellos, "Benchmarks for uncertainty analysis in modelling (uam) for the design, operation and safety analysis of lwrs-volume i: Specification and support data for neutronics cases (phase i)," tech. rep., Organisation for Economic Co-Operation and Development, 2013.

[63] M. Hursin, D. Siefman, G. Perret, D. Rochman, A. Vasiliev, and H. Ferroukhi, "Determination of sobol sensitivity indices for correlated inputs with shark-x," in *PHYSOR 2018: Reactors Physics paving the way towards more efficient systems. Cancun, Mexico*, ANS, 04 2018.

[64] V. Patel, M. Eades, and C. R. J. II, "Space propulsion optimization code benchmark case: SNRE model," in *Nuclear and Emerging Technologies for Space*, February 2016.

[65] M. Eades, *135Xe in LEU Cermet Nuclear Thermal Propulsion Systems*. PhD thesis, The Ohio State University, 2016.

[66] M. Eades and P. Venneri, "Initial investigation of in- element power peaking in leu cermet ntp fuel elements," in *NETS*, Febuary 2017.